SEPARATION OF SULPHIDES FROM MILL TAILINGS - FIELD

NEW APPROACHES TO THE PREVENTION OF ACID MINE DRAINAGE

MEND ASSOCIATE PROJECT 2.45.2

This work was done on behalf of MEND and sponsored by
INCO Limited, as well as
The Ontario Ministry of Northern Development and Mines and
The Canada Centre for Mineral and Energy Technology (CANMET)
through the CANADA/Northern Ontario Development Agreement (NODA)

September 1997

MEND 2.45.2

NEW APPROACHES TO THE PREVENTION OF ACID MINE DRAINAGE

Contract Report: 23440-4-1111/01-SQ

Prepared for:

O. Dinardo
Scientific Authority
CANMET
555 Booth Street
Ottawa, Ontario
K1A-OG1

Prepared by:

D.W. Blowes
Department of Earth Sciences
University of Waterloo
Waterloo, Ontario
N2L-3G1

Coinvestigators:

R.A. Stuparyk
Hill Station
INCO Limited
Copper Cliff, ON
P0M-1N0

C.J. Hanton-Fong
Department of Earth Sciences
University of Waterloo
Waterloo, ON
N2L-3G1

September 1, 1997

ABSTRACT

The separation of sulphide minerals and the disposal of low sulphur tailings is a promising strategy for the prevention of acid mine drainage. A detailed hydrogeochemical study is underway at the INCO Ltd. Copper Cliff Tailings Area comparing the geochemical evolution of pore waters derived from low sulphur tailings with that derived from higher sulphide tailings. In June, 1993, three 10 m x 15 m field lysimeters were constructed containing low sulphur tailings (0.35 wt.% S), main tailings (0.98 wt.% S), and total tailings (2.3 wt.% S), respectively. The lysimeters were monitored semi-annually to determine the pore-water composition, the pore-gas composition, and the bulk physical properties of the tailings. Geochemical modelling was conducted to interpret mineral phases that limit concentrations of dissolved constituents. Pore-gas oxygen levels are depleted within the upper 20 cm of the main tailings and total tailings lysimeters, indicating the zone of active oxidation. Complete gas-phase oxygen depletion is not observed in the low sulphur tailings lysimeter. Oxidation in the main and total tailings lysimeters has resulted in the development of acidic conditions, whereas pore-water pH in the low sulphur tailings has remained near neutral. Substantial increases in the concentrations of dissolved constituents in the pore water began within the first year in the total and main tailings lysimeters, but has yet to be observed in the low sulphur lysimeter. Maximum pore-water concentrations, measured in October, 1995, exceed 13 g/L SO_4, 1,500 mg/L Fe, and 1,500 mg/L Ni in the total tailings lysimeter, whereas the low sulphur lysimeter exhibited lower dissolved concentrations (< 2 g/L SO_4, < 5 mg/L Fe, and < 40 mg/L Ni). The initial results of this study suggest that

pore-water acidification and metal loading to the environment could be substantially decreased through the production of low sulphur tailings.

In conjunction with the field lysimeter experiments, laboratory experiments are underway to evaluate acid neutralization reactions in unoxidized tailings. A series of saturated column experiments are being conducted, using an acidic input solution and tailings samples from the three lysimeters, to study the migration of low-pH conditions through unreacted tailings.

Résumé

La séparation des minéraux sulphureux et l'entreposage des résidus miniers appauvris en soufre est une approche prometteuse pour la prévention d'effluents acides provenant de l'exploitation de dépots miniers. Une étude hydrogéochimique détaillée au site 'Copper Cliff Tailings Area' de la compagnie INCO Ltd. compare l'évolution géochimique de l'eau de porosité d'un bassin de sédimentation riche et d'un pauvre en soufre. En Juin 1993, trois lysimètres de 10 m x 15 m ont été construits pour contenir soit des boues de décantation à faible teneur en soufre (0.35 %S par poids), des boues principales (0.98% S par poids), ou des boues complètes (2.3% S par poids). Les lysimètres ont été échantillonnés deux fois par année pour la composition de l'eau de porosité, les gazs de porosité, et les propriétés physiques des boues de décantation. La modélisation géochimique a été utilisée pour déterminer quelles sont les phases minérales susceptibles de controler la concentration des éléments dissouts. Le taux d'oxygène dans la phase gazeuse était bas dans la porosité des premiers 20 cm des boues principales et complètes, ce qui indique la zone d'oxydation active. L'oxygène dans la phase gazeuse était toujours présent dans les boues appauvries en soufre. L'oxydation des boues principales et complètes a engendré des conditions acides, alors que le pH de l'eau de porosité est demeuré neutre dans les boues appauvries en soufre. Une hausse de la concentration des éléments dissouts a été observée dès la première année dans les boues principales et complètes. Les concentrations sont demeurées basses jusqu'à maintenant dans les boues appauvries en soufre. Les concentrations maximales dans l'eau de porosité ont été mesurées en Octobre 1995, excédant 13 g/L SO_4, 1,500 mg/L Fe, et 1,500 mg/L Ni dans le lysimètre contenant des boues complètes,

alors que dans le lysimètre avec boues appauvries en soufre les concentration sont demeurées moins élevées (< 2 g/L SO_4, < 5 mg/L Fe, et < 40 mg/L Ni). Les résultats préliminaires de cette étude suggèrent que l'acidification de l'eau de porosité et la décharge de métaux lourds dans l'environment peuvent être réduites substantiellement par la production de boues de décantation à faible teneur en soufre.

En parallèle aux expériences avec lysimètres sur le terrain, des expériences en laboratoire sont en cours pour évaluer les réactions de neutralisation des acides dans les boues de décantation non-oxydées. Une solution acide est circulée au travers de colonnes saturées et remplies de chaque type de boue pour étudier la migration des conditions de bas pH.

TABLE OF CONTENTS

LIST OF TABLES

LIST OF FIGURES

LIST OF FIGURES (continued)

LIST OF FIGURES (continued)

1. INTRODUCTION

Acid mine drainage is the most important environmental problem facing the mining industry today. It is estimated that more than 10% of all tailings generated in Canada are stored in the INCO Ltd. Copper Cliff Tailings Area near Sudbury, Ontario (Puro *et al.*, 1995). This is the largest tailings storage area in Canada (22 km^2, 500,000,000 tons) and contains reactive sulphide minerals such as pyrrhotite [$Fe_{(1-x)}S$] (Stuparyk *et al.*, 1995).

Sulphide minerals are thermodynamically unstable when exposed to air. Oxidation of pyrrhotite, the principal sulphide mineral in the INCO Ltd. Copper Cliff Tailings Area (McGregor, 1990; Coggans, 1992; Jambor, 1994; Coggans *et al.*, 1996), can be described via the reaction:

$$Fe_{(1-x)}S_{(s)} + (2 - \frac{x}{2})\, O_{2(g)} + x\, H_2O \rightarrow (1 - x)\, Fe^{2+} + SO_4^{2-} + 2x\, H^+ \qquad (1)$$

The Fe^{2+} produced may be oxidized to Fe^{3+}:

$$Fe^{2+} + \frac{1}{4}\, O_{2(g)} + H^+ \rightleftharpoons Fe^{3+} + \frac{1}{2}\, H_2O \qquad (2)$$

which in turn may act to oxidize additional sulphides through a reaction such as:

$$Fe_{(1-x)}S_{(s)} + (8-2x)\, Fe^{3+} + 4\, H_2O \rightarrow (9-3x)\, Fe^{2+} + SO_4^{2-} + 8\, H^+ \qquad (3)$$

The above sequence of reactions produces Fe^{2+}, SO_4 and H^+, increases the total dissolved solids concentration, and decreases pore-water pH. In addition, heavy metals such as Ni, Co and Cu are also released to the tailings pore-water during sulphide oxidation. Because the dissolved

constituents are present in the pore water, rather than in an immobile solid state, there is concern about migration toward unaltered tailings zones, and eventually off site.

In an attempt to reduce the reactivity of the tailings material that it generates, INCO Ltd. conducted a pilot scale test at the INCO Clarabelle Mill, Copper Cliff, Ontario to produce a tailings of lower sulphide content (McLaughlin and Stuparyk, 1994; Stuparyk *et al.*, 1995). The plant test was based on previous laboratory experiments with froth flotation (McLaughlin and Stuparyk, 1994). Sulphides were separated from a 1 wt.% S feed, producing 94 wt.% recovery of low sulphur tailings at < 0.5 wt.% S and a sulphide concentrate of 11 wt.% S.

The reactivity of low-sulphur tailings was evaluated through a series of laboratory and field experiments. Details of the laboratory static and column experiments, including acid-base accounting (ABA) tests, and preliminary field results are described elsewhere (McLaughlin and Stuparyk, 1994; Stuparyk *et al.*, 1995). Three types of tailings produced at the Clarabelle Mill were studied and include low sulphur tailings, LST (0.35 wt.% S, Net Neutralization Potential (NNP) = 3.60 kg $CaCO_3$ equivalent / tonne material), main rock tailings, MT (0.98 wt.% S, NNP = -17.8 kg $CaCO_3$ eq/t), and total tailings, TT (2.3 wt.% S, NNP = -46.8 kg $CaCO_3$ eq/t). Each tailings type has similar mineralogy and differs in pyrrhotite content (Shaw, 1996). The total tailings material is a mixture of main rock and pyrrhotite rejection tailings (~10 wt.% S). Tailings of this composition were deposited in the Copper Cliff Tailings Area from the late 1930's until 1994 (Stuparyk *et al.*, 1995). Since 1994, the reactive pyrrhotite tailings have been diverted for separate storage. The main rock tailings are currently deposited in the Copper Cliff Tailings Area, and now comprise 85 wt.% of all INCO tailings.

In 1993, three 10 m x 15 m field lysimeters were constructed in the Copper Cliff Tailings Area (McLaughlin and Stuparyk, 1994; Stuparyk *et al.*, 1995). The lysimeters were lined with a geomembrane to isolate the lysimeter pore-water from the surrounding groundwater flow regime. A drain was installed at the base of each lysimeter to promote downward migration of the tailings pore-water. In June 1993, the three lysimeters were filled with 200 ton samples of low sulphur, main and total tailings, respectively.

The current research project is intended to evaluate the potential of low sulphur tailings in preventing acidic drainage. The following milestones were established:

Milestone #1 - Classify low, medium and high sulphide tailings using acid-base accounting and column oxidation experiments.

Milestone #2 - Compare tailings oxidation and dissolved metal release in low, medium and high sulphide tailings field lysimeters.

Milestone #3 - Established dominant acid-neutralization reactions in low, medium and high sulphide tailings using saturated column experiments.

Milestone #1 was the subject of the first progress report written in December, 1994. Results from the field sampling campaign to July, 1995 (Milestone #2) were presented in the second progress report in December, 1995. The purpose of the present report is to provide results and discussion for the research conducted in the third year of study. This includes field data collected for the last three sampling sessions, for the completion of Milestone #2, and to report on the status of the column experiments (Milestone #3).

2. METHODS

2.1 FIELD LYSIMETERS

The field lysimeters have been monitored semi-annually since their construction in June, 1993. To date seven detailed sampling sessions have been conducted. Sampling was conducted in late spring and early fall to observe any changes in the lysimeters over the summer, when the tailings moisture content is low and sulphide oxidation is at its maximum. Each monitoring campaign included measurements of chemical and physical characteristics of the three lysimeters. Pore water, pore gas and tailings solids were collected. Since construction, variations in grain size have been observed in the lysimeters with finer grained tailings, present on the eastern side, exhibiting a higher moisture content. Initial pore-water sampling was conducted at the west (drier) side of the lysimeters (Figure 1, location G), to compare maximum differences in sulphide oxidation between the three lysimeters. More recently the lysimeters were sampled on the west side and on the east (wetter) side (Figure 1, location S) to observe the effects of moisture content variation on tailings oxidation.

2.1.1 Chemical Properties

Cores were obtained from each lysimeter and the pore water extracted using an immiscible displacement technique described by Blowes *et al.* 1991. Each core was cut into 20-25 cm sections, usually four or five were obtained per core, and the pore water was collected and filtered (0.45 μm) for chemical analysis. Pore-water pH, Eh and alkalinity measurements were made immediately on fresh sample. Solution pH was measured using a Ross combination

pH electrode (Orion® Ross 815600) and redox with a platinum combination electrode (Orion® 96-78-00). The performance of the electrodes was verified against known calibration standards, pH buffers 4.00 and 7.00 (traceable to NBS), and ZoBell and Light solution (ZoBell, 1946; Light, 1972; Nordstrom, 1977), respectively. Alkalinity was determined by titration with 0.16 N H_2SO_4 to the bromocresol green-methyl red endpoints. Filtered samples were submitted to INCO Ltd. for ion analysis including Fe, Ni, Cu, Zn and SO_4. Samples for cation analysis were acidified to pH < 1 with concentrated HCl and analyzed by inductively coupled plasma atomic emission spectrometry (ICP-AES). Anion concentrations were determined by ion chromatography. Usually 30-60 mL were obtained from each core sub-section, however, pore water was displaced from drier core samples with an immiscible liquid.

Pore-gas O_2 and CO_2 concentrations were measured in the field using a NOVA 305 gas analyzer. Hollow probes were driven into the tailings to a known depth and the instrument attached at the surface. Sealed samples were also collected for further analysis by gas chromatography at the University of Waterloo.

2.1.2 Physical Properties

Volumetric moisture contents were measured *in situ* using a neutron probe (CPN Corp., Model 503 DR Hydro probe). In addition, cores were collected periodically for gravimetric moisture content determination. The cores were cut into 10 cm sections, weighed, and dried overnight at 110°C. The dried samples were retained for particle density and particle size analysis. Particle densities were measured with an air comparison pycnometer (Beckman Model 930). Particle size distributions were determined by sieve and hydrometer techniques.

2.1.3 Data Interpretation

The geochemical data were interpreted with the aid of the MINTEQA2 equilibrium speciation mass transfer model (Allison *et al.*, 1990). This computer code calculates mineral saturation indices and suggests mineral phases that may be controlling the pore-water evolution. MINTEQA2 modelling was conducted for all pore-water samples analyzed for pH, Eh and chemical composition.

2.2 COLUMN EXPERIMENTS

In conjunction with field studies begun in 1993, a series of column experiments are being conducted under saturated flow conditions. Three columns, packed with low sulphur tailings (0.5 wt.% S), main tailings (1 wt.% S), and total tailings (2.5 wt.% S), respectively, are being evaluated for porosity and acid neutralization capacity. The tailings material was to have been obtained from INCO's Clarabelle Mill after a second plant test to produce low sulphur tailings material. As of 1997, the test has not been conducted and so alternate arrangements were made using existing frozen core solids.

Tailings cores from two different locations in each field lysimeter were collected in 7.6 cm diameter aluminum core tubes in October, 1995. The cores were sealed and frozen until use. The bottom 30 cm of each core was cut off, the tailings removed and oven-dried overnight. Samples from each lysimeter were mixed in a 1:1 ratio and this material was used to pack the columns.

Three 9 cm diameter x 10 cm tall plexiglas columns were packed with approximately 600 cm^3 of tailings. Initial porosity was estimated by weighing the column before and after

packing. Saturation of the columns with simulated groundwater (Ca-CO_3/SO_4, P_{CO2}=1%) followed to ensure that uniform flow conditions were established before acidic water was introduced. Saturation is accomplished by repeated flushing of the tailings pore-spaces with CO_2 gas followed by a slow wetting of the solids from the bottom of the column to the top. The experimental setup is shown in Figure 2. Simulated groundwater is pumped with a peristaltic pump from a sealed reservoir up through each column and sampling cell to a waste container. All column input solutions are bubbled with a 1% CO_2, N_2 gas mixture to remove dissolved oxygen before use. The headspace in the input solution reservoir is maintained at P_{CO2}=1% using a collapsible gas-tight bag. Column flow rates are maintained near 5 mL/hour to ensure proper column saturation and to prevent channelling in the column.

Following column saturation, flow and transport parameters, such as average linear velocity, dispersivity, and porosity, of each packed column will be evaluated using chloride as a conservative tracer in the simulated groundwater. The chloride breakthrough curves will be modelled using a non-linear least-squares parameter fitting model CXTFIT.

Once the transport parameters are determined, the column input solution will be changed to a 0.1 M H_2SO_4 solution (P_{CO2}=1%) to simulate acidic pore water conditions that are generated in tailings impoundments. Each column effluent will be sampled regularly for solution pH, Eh, alkalinity and dissolved metals. Solution pH and redox will be measured under sealed conditions. Solution pH will be measured using a Ross combination pH electrode (Orion® Ross 815600) and redox with a platinum combination electrode (Orion® 96-78-00). The performance of the electrodes will be verified against known calibration standards, pH buffers 1.00, 4.00 and 7.00 (traceable to NBS), and ZoBell and Light solution (ZoBell, 1946; Light, 1972; Nordstrom, 1977),

respectively. Alkalinity will determined by titration with 0.16 N H_2SO_4 to the bromocresol green-methyl red endpoints. Filtered samples will be submitted for ion analysis including Fe, Ni, Cu, Zn and SO_4. Samples for cation analysis will be acidified to pH < 1 with concentrated HCl and analyzed by inductively coupled plasma atomic emission spectrometry (ICP-AES). Anion concentrations will be determined by ion chromatography. Usually 30 mL will be available for complete analysis.

Geochemical modelling will be conducted to interpret the column effluent data. This will include the use of the equilibrium speciation/mass transfer computer code MINTEQA2 (Allison *et al.*, 1990). This will allow for the comparison of acid neutralization capacity of the three different sulphide tailings as acidic pore water contacts them.

3. RESULTS AND DISCUSSION

3.1 FIELD LYSIMETERS

3.1.1 Physical Properties

The moisture content in the field lysimeters varies both temporally and spatially (Figures 3-6). The lowest values are measured in the upper 50 cm of each lysimeter and increase with depth. Moisture contents near the surface of the west end of the MT and TT lysimeters (Figure 6, MT-2 and TT-2) are less than half the values measured at the east end (MT-3 and TT-3). Spatial differences in shallow moisture contents were not observed in the LST lysimeter where a higher degree of saturation was measured in the upper 20 cm. The establishment and preservation of a high moisture content is advantageous to tailings management programs. Because the diffusion coefficient of O_2 in water is low, diffusion of O_2 to the grain surfaces is inhibited, so that sulphide oxidation is minimized.

Spatial variations in grain size were also observed in the three lysimeters (Figure 7). Samples removed from the lysimeters are sand-silt sized particles, with a larger proportion of sand-sized particles found on the west end of each lysimeter (Figure 1, location G). This is consistent with the method of tailings deposition where, similar to a spigotting procedure, the tailings were deposited from the west side of the study area. The coarser grains settled closer to the spigotting point and the finer grain sizes migrated distally to the east end of the lysimeters.

Differences in grain size may account for the differences in moisture content observed within the MT and TT lysimeters. There is a larger proportion of silt- and clay-sized particles at the east end of the MT and TT lysimeters where higher moisture contents are measured. The

grain-size distribution in the LST lysimeter is similar for samples collected at the east and west end. This similarity may account for the more uniform moisture contents measured.

3.1.2 Oxygen

Pore-gas sampling was usually limited to the driest (west) side of the lysimeters (Figure 1) in order to attain measurements as deep as possible in each lysimeter before saturation of the pore spaces. Pore-gas O_2 concentrations are shown in Figures 8-10 for the sampling sessions and have remained relatively constant over time. Oxygen depletion, due to sulphide oxidation, occurred rapidly near the surface of the MT and TT lysimeters, as early as four months after the start of the experiment in 1993 (Figure 8). Pore-gas oxygen concentrations decline from atmospheric concentration (20.9 vol.% O_2) to nondetect levels (< 0.1 vol.%) within the upper 20 cm of the TT lysimeter and within the upper 50 cm of the MT lysimeter. Unlike the higher sulphide content cells, the LST lysimeter exhibited a relatively uniform pore-gas oxygen concentration with depth, near the atmospheric value. Depth penetration was often limited in the LST gas sampling to the upper 30 cm due to the high degree of saturation of the pore spaces.

A semi-solid hard pan, formed due to mineral precipitation reactions, is observed at the depth where the pore-gas O_2 concentration approaches zero in the MT and TT lysimeters. This hard pan may prevent diffusion of O_2 deeper into the lysimeters which inhibits further tailings oxidation. Recent gas sampling in October, 1996 (Figure 10) indicates a similar O_2 diffusion profile is present on the east side of the TT lysimeter and a hard pan is now forming near 40 cm.

3.1.3 Pore-water Geochemistry

Evidence of sulphide oxidation was found in monitoring the pore-water composition of the lysimeters over time (Figures 11-40). The important indicator parameters monitored include low pH and alkalinity, and elevated SO_4, Fe and metal concentrations. Oxidation in the MT lysimeter is observed within the first four months of operation. Although sulphide oxidation occurs to a greater extent in the TT lysimeter, acidic conditions are not seen until one year after tailings deposition. The changes in MT and TT pore-water concentration over time far exceed pore-water changes observed in the LST lysimeter, which has remained near the initial condition for more than three years.

October, 1993 (t = 4 months)

Mill discharge is present below 60 cm in all lysimeters as indicated by near-neutral pH (pH 7-8), Eh ~ 250 mV, low concentrations of dissolved Fe and other metals, SO_4 near 2,000 mg/L and alkalinity around 100 mg/L as $CaCO_3$ (Figures 11-13). Uniform pore-water geochemistry was observed in the LST lysimeter at all depths (Figure 13). Slight increases in dissolved Ni and Mn concentrations were observed in the LST lysimeter at 73 cm, however, the elevated concentrations were not seen at later times. Within one summer of operation, corresponding to one period of peak oxidation, the MT pore water is acidic (pH = 4.7) at the shallowest measuring point and increases to neutral pH at depth (Figure 12). The lower pH near the surface of the MT and TT lysimeters is accompanied by high Ni and Mn concentrations (< 15 mg/L Ni and < 5 mg/L Mn). The Ni and Mn concentrations measured at greater depths are similar to background concentrations.

Geochemical modelling with MINTEQA2 (Allison *et al.*, 1990) indicates that the pore water is undersaturated with respect to the pH buffering minerals calcite [$CaCO_3$] and dolomite [$CaMg(CO_3)_2$] in the upper 40 cm of the MT and TT lysimeters and near saturation at depth (Table 1). The pore water throughout the LST lysimeter is consistently saturated with respect to calcite and dolomite. In each lysimeter, the pore water is undersaturated with respect to siderite [$FeCO_3$], at equilibrium with respect to gypsum [$CaSO_4 \cdot 2H_2O$] and supersaturated with respect to amorphous aluminum hydroxide [am $Al(OH)_3$].

July, 1995 (t = 25 months)

Within 17 months of operation and two periods of peak oxidation, significant differences in oxidation are observed between the three lysimeters (Figures 17-19). The differences are more pronounced after 25 months (Figures 20-22). Pore-water pH values remain near pH 7 in the LST lysimeter, but have declined to pH < 4 in the shallow MT and TT zone. Acidic pH conditions are present to greater depths in the MT lysimeter than the TT lysimeter, possibly due to deeper penetration of O_2 into the subsurface.

Oxidation of the high sulphide tailings (TT) has resulted in significant release of SO_4 and Fe to the shallow pore-water zone (Figure 20). Pore-water SO_4 concentrations increased from 2,000 mg/L in October, 1993 to 19,000 mg/L in July, 1995, and Fe increased from initial values near 1 mg/L to 1,500 mg/L. Elevated heavy metal concentrations, including 50 mg/L Zn, 60 mg/L Mn, 700 mg/L Cu, and 1,900 mg/L Ni were observed at the shallowest location in the TT lysimeter at 13 cm. Although acidic conditions are present at greater depths in the MT lysimeter, SO_4, Fe and Ni concentrations remained lower (< 2,000 mg/L SO_4, < 4 mg/L Fe,

< 10 mg/L Ni) (Figure 21). High dissolved metal and SO_4 inputs to the MT pore water were not observed until three months later (October, 1995), after the third oxidation period.

After 25 months, the pore-water geochemistry in the LST lysimeter, remains relatively unchanged (Figure 22). Pore-water pH remains near neutral, SO_4 concentrations are uniform near 1,500 mg/L SO_4, dissolved metal concentrations remain low (< 4 mg/L Fe, < 3 mg/L Ni) and measurable alkalinity is present throughout.

MINTEQA2 (Allison *et al.*, 1990) modelling of the July, 1995 data (Table 4) suggests that, with the exception of the shallowest sample at 16 cm, the pore water in the LST lysimeter is near saturation with respect to calcite and dolomite, and undersaturated with respect to siderite. At 16 cm the pore water is undersaturated with respect to calcite, dolomite and siderite suggesting depletion of carbonate minerals for acid neutralization.

With the measurement of pore-water pH values < 4 in the upper 15 cm of the MT and TT lysimeters, carbonate alkalinity is absent. Carbonate saturation indices were not calculated with MINTEQA2. At a depth of 40 cm in the MT lysimeter, the pore water is undersaturated with respect to calcite and dolomite (Table 4). The pore waters in both the MT and TT lysimeters below 70 and 40 cm, respectively, approach equilibrium with respect to calcite and dolomite suggesting that the two minerals may be dissolving in this zone. Calcite and dolomite dissolution below 40 cm in the TT lysimeter coincides with a region where the pore water is at equilibrium with respect to siderite. This observation is consistent with the hypothesis that siderite precipitation occurs as calcite and dolomite are depleted. The concentrations of Fe released from sulphide oxidation, and HCO_3^- released from carbonate dissolution have been sufficient to attain saturation with respect to this mineral through a reaction such as:

$$Fe^{2+} + HCO_3^- \rightleftharpoons FeCO_{3(s)} + H^+ \quad (4)$$

In each lysimeter, the pore water is supersaturated with respect to goethite [αFeOOH], at equilibrium with respect to gypsum, and for the first time undersaturated with respect to amorphous $Al(OH)_3$. Pore water samples taken at 15 cm in the MT and TT lysimeters, where pH ≤ 4, are now undersaturated with respect to gibbsite [$Al(OH)_3$] and return to supersaturated conditions at depth.

October, 1995 (t = 28 months)

Up until July, 1995, cores were removed at the west (drier) end of each lysimeter for pore-water sampling (Figure 1, location G). Recent studies were expanded to compare the effects of moisture content on tailings oxidation. Spatial variations in moisture content were observed in the MT and TT lysimeters (Figures 5-6) and the differences are reflected in the pore-water geochemistry measured. In October 1995, and in sampling sessions thereafter, two cores were collected from each lysimeter for pore-water extraction, one from the drier (west) end and an additional core on the wetter east end (Figure 1, locations G and S, respectively).

In October, 1995, after a summer of peak oxidation, the pore water in the drier (west) end of the MT and TT lysimeters is acidic at all depths. Pore-water pH values in the TT lysimeter increase from pH 3.7 near the surface to pH 6.3 at a depth of 1.2 m (Figure 23). Elevated dissolved SO_4 concentrations, present at only the shallowest location in July, 1995 (Figure 20), are now measured down to 90 cm (Figure 23). The acidic conditions throughout result in increased concentrations of heavy metals in the pore water including Zn, Mn, Ni, Co and Cd.

Elevated SO_4, and metal concentrations are also observed at depth in the west end of the MT lysimeter where pore-water pH ≤ 4 (Figure 25).

Unlike the TT and MT lysimeters, the pore-water pH in the LST lysimeter remains near pH 7 at both sample locations and oxidation effects are not observed after 28 months (Figures 27-28). Dissolved concentrations remain low and alkalinity is measurable. At the western sampling location (Figure 27), the lower SO_4, K, Ca and Mg concentrations near the surface of the lysimeters reflect precipitation/recharge processes.

The effect of moisture content on tailings reactivity is evident when comparing the pore-water geochemistry of the two sampling locations in the MT (Figures 25-26) and TT (Figures 23-24) lysimeters. The east (wetter) side of the MT lysimeter has pore-water pH values in excess of pH 7 at all depths (Figure 26) and redox values that are 400 mV lower than on the (drier) west side (Figure 25). The neutral pH is accompanied by lower dissolved metal and SO_4 concentrations, and measurable alkalinity throughout. Similar trends are observed at depth when comparing the sampling locations in the TT lysimeter (Figures 23-24). Oxidation is occurring, however, in the upper 35 cm of the east (wetter) end of the TT lysimeter as indicated by acidic pore-water pH, decreased alkalinity, elevated redox potential and dissolved SO_4 and metal concentrations (Figure 24).

Geochemical modelling of the October, 1995 pore-water data (Table 5) suggests that the pore water on the west side of the LST lysimeter (LST-G) is near saturation with respect to calcite and dolomite, and undersaturated with respect to siderite. On the west (drier) side of the TT lysimeter (TT-G), the pore water is undersaturated with respect to calcite, dolomite and siderite to the bottom of the lysimeter. Carbonate mineralogy is assumed to be depleted to depth

on the west (drier) side of the MT lysimeter (MT-G) due to the lack of measurable alkalinity. In all three lysimeters, and at each sample location, the pore waters are supersaturated with respect to goethite, at equilibrium with respect to gypsum, and undersaturated with respect to am $Al(OH)_3$. Pore water samples in the MT and TT lysimeters, where $pH \leq 4$, are now undersaturated with respect to gibbsite and return to supersaturated conditions at depth.

June, 1996 (t = 36 months)

In June, 1996, 36 months after deposition, a minimum value of pH 2.8 is measured in the MT lysimeter at 35 cm (Figure 31). Acidification of the MT lysimeter is accompanied by substantial increases in dissolved SO_4 and metal concentrations (11,000 mg/L SO_4, 500 mg/L Fe, 400 mg/L Cu, 1,000 mg/L Ni). Dissolved metal concentrations remain high in the TT lysimeter (6,000 mg/L SO_4, 300 mg/L Fe, 400 mg/L Cu, 300 mg/L Ni) (Figure 29), although the peak oxidation period has passed.

Extensive oxidation effects are not observed in the LST pore water after three years of study (Figure 33). Dissolved concentrations at the west end of the lysimeter (300 mg/L SO_4, < 1 mg/L Fe, < 0.1 mg/L Cu, < 1 mg/L Ni, < 0.4 mg/L Mn) are equal to or lower than initial (t = 4 months) conditions. Mill-discharge water has been displaced away from this location, and the lower SO_4 concentrations reflect precipitation/recharge processes at the surface. The pore-water pH in the LST lysimeter remains near pH 7. Similar pore-water pH values and dissolved concentrations are observed at the east end of the LST lysimeter (Figure 34). Dissolved metal concentrations at both locations in the LST lysimeter are lower than concentrations measured in the two higher sulphide lysimeters.

Unlike, the drier MT sampling location (Figure 31), pH values near pH 7.5 were measured to all depths on the wetter side of the lysimeter (Figure 32). Less extensive sulphide oxidation is also indicated by the low dissolved metal concentrations (< 7 mg/L Fe , < 3 mg/L Ni, < 0.01 mg/L Cu). Dissolved SO_4 concentrations are near 1,700 mg/L at depth and decline to 600 mg/L near the surface (17 cm) where precipitation has infiltrated into the tailings. Pore-water alkalinity is present at all depths and is four to ten times greater than values measured at the drier, more oxidized location.

Oxidation is evident at both locations in the TT lysimeter (Figures 29-30). Pore water in the wetter end of the TT lysimeter (Figure 30) is acidic to depth, with alkalinity consumed in the upper 36 cm. Dissolved concentrations are elevated with maximum values measured at depth (< 5,000 mg/L SO_4, < 1,200 mg/L Fe, < 220 mg/L Ni). Recent pore-gas measurements in October, 1996 (Figure 10) indicate O_2 diffusion down to 40 cm where a hard pan is forming.

Geochemical modelling of the June, 1996 data (Table 6) indicates that the pore water on the west side of the LST lysimeter (LST-G) is near equilibrium to undersaturated with respect to calcite, and undersaturated with respect to dolomite and siderite. At both locations in the TT lysimeter, the pore water is undersaturated with respect to calcite, dolomite and, in all but the deepest locations, siderite. Supersaturation with respect to siderite is attained at depth in the TT lysimeter, suggesting precipitation of siderite as calcite and dolomite are depleted (Equation 4). The pore water in the west (drier) end of the MT lysimeter (MT-G) is undersaturated with respect to the three calcite minerals. In all three lysimeters and at each location, the pore waters remain supersaturated with respect to goethite, at equilibrium with respect to gypsum, and undersaturated with respect to $Ni(OH)_2$. Pore-water samples in the MT and TT lysimeters where pH ≤ 4 (TT-G

at 0.17 m; TT-S at ≤ 0.36 m; MT-G at ≤ 0.35 m) are now undersaturated with respect to gibbsite and return to supersaturated conditions at depth. At these locations, the pore water is undersaturated to near saturation with respect to ferrihydrite.

October, 1996 (t = 40 months)

The pore-water geochemistry measured in the three lysimeters in October, 1996 (Figures 35-40) changed very little from the values measured in the June, 1996 sampling session (Figures 29-34). The pore-water pH in the LST lysimeter remains above pH 7 at all depths and at all locations, and dissolved SO_4 and metal concentrations are low.

MINTEQA2 (Allison *et al.*, 1990) modelling of the October, 1996 data (Table 7) suggests that the pore water on the west side of the LST lysimeter (LST-G) is near equilibrium to undersaturated with respect to calcite, and undersaturated with respect to dolomite and siderite. At both locations in the TT lysimeter, the pore water is undersaturated with respect to calcite and dolomite. Carbonate minerals are assumed to be depleted in the west (drier) end of the MT lysimeter (MT-G) due to the lack of measurable alkalinity. In all three lysimeters and at each location, the pore waters remain supersaturated with respect to goethite and at equilibrium with respect to gypsum. Pore-water samples in the MT and TT lysimeters where pH ≤ 4 remain undersaturated with respect to gibbsite.

3.2 pH BUFFERING REACTIONS

The most important pH-buffering minerals in the tailings are the carbonates minerals (Blowes and Ptacek, 1994). Calcite dissolution is the most rapid and proceeds by the general reaction

$$CaCO_{3(s)} + H^+ \rightleftharpoons Ca^{2+} + HCO_3^- \quad (5)$$

Dissolution of calcite and dolomite raises pore-water pH to near neutral (pH 6.5-7.5). At this pH, precipitation of secondary mineral phases, such as siderite, and Fe and Al hydroxides such as goethite, ferrihydrite and gibbsite, may be favoured.

Over time, the amount of acid produced by sulphide oxidation has exceeded the carbonate neutralization capacity of the main and total tailings. As carbonate minerals are depleted, pore-water pH falls until equilibrium with the most soluble hydroxide mineral is attained, usually $Al(OH)_3$ (Blowes and Ptacek, 1994). Dissolution of $Al(OH)_3$ buffers pore-water pH to between pH 4.0 and 4.3. These pH values are noted in the MT and TT lysimeters 17 months after deposition (Figures 17-18). When $Al(OH)_3$ is completely consumed, the pH declines down to pH 2.5-3.5, favouring the dissolution of iron hydroxides such as ferrihydrite or goethite. Once all the Al and Fe hydroxide minerals are depleted, pore-water pH may be further lowered down to near pH 1 where aluminosilicate dissolution can occur.

The above series of reactions are occurring in the INCO Ltd. lysimeters. Three years after deposition, a step-wise pore-water pH versus depth trend is evident in the MT and TT lysimeters (Figures 29-31). The pore water at depth is buffered near pH 6-7 indicating dissolution of carbonate minerals. Above this depth is a region where pore-water pH is near 4, suggesting

$Al(OH)_3$ dissolution in this zone. Near the surface of the lysimeters, pore-water pH declines to 3, where iron hydroxide dissolution is occurring.

MINTEQA2 simulations (Allison *et al.*, 1990) also suggest that the above reactions are occurring (Tables 1-7). A summary of the June, 1996 mineral saturation indices for the TT lysimeter (Table 8) suggests depletion of the following minerals from the bottom of the lysimeter to the top:

calcite, dolomite > siderite > gibbsite > ferrihydrite

Similar results are seen in the MT lysimeter (Table 6, MT-G), although the pore water in the LST lysimeter is still supersaturated with respect to gibbsite at all depths.

Table 8: Status of pore water in the TT lysimeter with respect to the pH-buffering minerals (TT-G, June, 1996). under = undersaturated; super = supersaturated

Depth (m)	**pH**	**$CaCO_3$ $CaMg(CO_3)_2$**	**$FeCO_3$ Siderite**	**$Al(OH)_3$ Gibbsite**	**$Fe(OH)_3$ Ferrihydrite**
0.17	3.12	carbonate alkalinity = 0		under	near saturation
0.44	4.54	under	under	near saturation	supersaturated
0.7-1	5.8-6.3	under	under	super	super
1.26	6.66	under	near saturation	super	super

3.3 COLUMN RESULTS

To date, the columns are packed and are presently being saturated with simulated groundwater. With flow rates maintained near 5 mL/hour, and an estimated porosity of 30 volume % (Table 9), one pore volume of input solution will take one to two days to pass through each column. Several pore volumes must pass through each column to ensure that uniform flow is established. This will be followed by an input spiked with chloride to determine

the individual flow and transport parameters for each column. The final solution will be changed to 0.1 M H_2SO_4, where detailed and regular sampling of the pore water-geochemistry will occur.

Table 9. Column experiment data.

Column Packing	Tailings Mass (g)	Tailings Volume (cm^3)	Particle Density (g/cm^3)	Estimated Porosity
Total Tailings	1205	604	2.98	0.33
Main Tailings	1239	612	2.98	0.32
Low Sulphur Tailings	1119	615	2.96	0.38

Although acidic input solution is not yet flowing through the columns, the results obtained from the field lysimeters may be used to predict the results. Ultimately, the pH of the effluent water will approach that of the H_2SO_4 input, however, the effluent pH is expected to be controlled by dissolution of mineral phases present in the tailings. This is suggested by other field studies (Blowes and Ptacek, 1994) and column experiments (Jurjovec *et al.*, 1995), and by the geochemical data obtained in this study.

Acidic input solution will flow through the unoxidized tailings in the columns and react with the pH-buffering minerals of interest including carbonate, hydroxide and oxyhydroxide, and aluminosilicate minerals. The acidic pore water will be neutralized through the dissolution of these minerals, and during the dissolution process, the pore-water pH will be maintained within a certain range. Once a pH-buffering mineral is depleted, the pore-water pH is expected to decline until equilibrium with the next buffering mineral is attained. Unlike the field lysimeter, where peak acid generation has probably occurred, the columns will be continually fed with acid solution until the pH-buffering minerals are consumed and effluent pH drops to < 2.

The duration of the column experiments is uncertain. Previous column experiments using tailings from a gold mine impoundment, were conducted for more than 80 pore volumes before solution pH declined to pH < 2 (Jurjovec *et al.*, 1995). The carbonate content was high (8 wt.%) and existed predominantly as siderite. This is in contrast to the INCO tailings where the principal carbonate mineral identified in the Copper Cliff tailings has been dolomite (Jambor, 1994; Coggans *et al.*, 1996), and concentrations are low.

4. CONCLUSIONS

After more than three years of field study under natural weathering conditions, the pore-water pH in the low sulphur tailings lysimeter (~0.5 wt.% S) has remained near neutral. The concentrations of dissolved constituents are similar to values measured at startup, and are now two to three orders of magnitude lower than concentrations developed in the MT and TT lysimeters over time.

In the MT (~1 wt.% S) and TT (~2.5 wt.% S) lysimeters the pore water is acidic and now contains elevated concentrations of dissolved SO_4, Fe and heavy metals. The MT lysimeter exhibited the first effects of tailings oxidation within four months of tailings deposition. Factors such as moisture content and tailings grain size affect the overall rate of oxidation, acidification and the extent of metal loading to the pore water. Maintaining a high degree of moisture saturation at the surface of tailings ponds prevents O_2 penetration to unoxidized sulphide grains in the subsurface and minimizes oxidation effects.

Column experiments are underway to evaluate the acid neutralization capacity of the three tailings materials. Results from the field lysimeters suggest that the tailings pore-water may be buffered to a series of pH values as certain minerals in the tailings are dissolved:

carbonates, pH 6.5-7.5 > gibbsite, pH 4-4.3 > ferrihydrite, pH 2.5-3.5

Once a given mineral is depleted, pore-water pH declines until the next buffering mineral is favoured to dissolve.

The low sulphur tailings have potential as an alternative mining waste. When compared to tailings materials that are currently deposited, and considering factors such as sulphur content,

grain size distribution and moisture content, the material is relatively inert to oxidation. Low sulphur tailings may be useful as a filling material in waste rock dams or as a cap covering more reactive sulphide tailings, although further study with field testing is essential.

5. ACKNOWLEDGEMENTS

Funding for this project was provided by INCO Ltd. through the MEND program. We thank the University of Waterloo crew T.A. Al, J.G. Bain, D. Brown, H. Chau, K.J. DeVos, H. McCready, M.C. Moncur, C.S. Ross, and M.D. Wunderly who assisted at various stages in the field study. The cooperation of numerous INCO personnel during the pore-water extraction exercises is appreciated.

6. REFERENCES

Allison, J.D., Brown, D.S. and Novo-Gradac, K.J. 1990. MINTEQA2/PRODEFA2, a geochemical assessment model for environmental systems: User's manual. (Environmental Research Laboratory, Office of Research and Development, U.S. EPA, Athens, GA).

Blowes, D.W. and Ptacek, C.J. 1994. "Acid-neutralization mechanisms in inactive mine tailings" In: MAC Short Course Handbook on Environmental Geochemistry of Sulfide Mine-wastes, J.L. Jambor and D.W. Blowes (Eds.), Volume 22, p. 271-292. May, 1994, Waterloo, ON.

Blowes, D.W., Reardon, E.J., Jambor, J.L. and Cherry, J.A. 1991. "The formation and potential importance of cemented layers in inactive sulfide mine tailings". Geochim. Cosmochim. Acta, Volume 55, pp. 965-978.

Coggans, C.J. 1992. Hydrogeology and geochemistry of the INCO Ltd., Copper Cliff, Ontario, mine tailings impoundments. (M.Sc. thesis, University of Waterloo, Waterloo, ON), 159 p.

Coggans, C.J., Blowes, D.W., Robertson, W.D. and Jambor, J.L. 1996. "The hydrogeochemistry of a nickel-mine tailings impoundment - Copper Cliff, Ontario". Reviews in Economic Geology, In press.

Jambor, J.L. 1994. Mineralogical study of tailings from the Copper Cliff impoundments, Sudbury, Ontario. (Internal Report, University of Waterloo, Waterloo, ON), 61 p.

Jurjovec, J., Blowes, D.W. and Ptacek, C.J. 1995. "Acid neutralization in mill tailings and the effect of natrojarosite addition" In: Proceedings of Sudbury '95 - Mining and the Environment, T.P. Hynes and M.C. Blanchette (Eds.), Volume 1, pp. 29-38. May 28 - June 1, 1995, Sudbury, ON.

Light, T.S. 1972. "Standard solution for redox potential measurements". Anal. Chem., Volume 44, Number 6, pp. 1038-1039.

McGregor, R.G. 1990. A mineralogical and geochemical study of area 'A' at the INCO Copper Cliff tailings compound. (B.Sc. Thesis, University of Waterloo, Waterloo, ON), 92 p.

McLaughlin, J. and Stuparyk, R. 1994. "Evaluation of low sulphur rock tailings production at INCO's Clarabelle Mill". In: Proceedings of the Innovations in Mineral Processing Conference, T. Yalcin (Ed.), pp. 129-145, June 6-8, 1994, Laurentian University, Sudbury, ON.

Nordstrom, D.K. 1977. "Thermochemical redox equilibria of ZoBell's solution". Geochim. Cosmochim. Acta, Volume 41, pp. 1835-1841.

Puro, M.J., Kipkie, W.B., Knapp, R.A., McDonald, T.J. and Stuparyk, R.A. 1995. "Inco's Copper Cliff Tailings Area". In: Proceedings of Sudbury '95 - Mining and the Environment, T.P. Hynes and M.C. Blanchette (Eds.), Volume 1, pp. 181-191. May 28 - June 1, 1995, Sudbury, ON.

Shaw, S.C. 1996. Comparative mineralogical study of base metal mine tailings, with various sulfide contents, subjected to laboratory column oxidation and field lysimeter tests, Copper Cliff, Ontario. (M.Sc. Thesis, The University of British Columbia, Vancouver, B.C.), 220 p.

Stuparyk, R.A., Kipkie, W.B., Kerr, A.N. and Blowes, D.W. 1995. "Production and evaluation of low sulphur tailings at INCO's Clarabelle Mill". In: Proceedings of Sudbury '95 - Mining and the Environment, T.P. Hynes and M.C. Blanchette (Eds.), Volume 1, pp. 159-169. May 28 - June 1, 1995, Sudbury, ON.

ZoBell, C.E. 1946. "Studies on redox potential of marine sediments". Bull. Am. Petrol. Geologists, Volume 30, pp. 477-509.

IN - TP Test Pit Saturation Indices
Oct. 1993

TT

	Depth (m)	CALCITE	DOLOMITE	SIDERITE(D)	GOETHITE	FERRIHYD.	NI(OH)2	GYPSUM	ALOH3(A)	GIBBSITE(C)
1.10 M	0.145	-0.003	-1.006	-3.336	6.596	0.886	-0.467	-0.036	0.574	3.31
1.20 M	0.435	0.378	0.031	-0.197	6.641	0.931	-1.393	-0.034	0.48	3.216
1.30 M	0.725	0.293	0.594				-0.869	-0.014	0.223	2.959
1.41 M	1.015	0.696	1.016	-1.845	8.666	2.956	-2.209	-0.004	0.128	2.864
1.42 M	1.015	0.676	1.069	-2.647	7.87	2.159	-1.842	0.017	0.122	2.858

MT

	Depth (m)	CALCITE	DOLOMITE	SIDERITE(D)	GOETHITE	FERRIHYD.	NI(OH)2	GYPSUM	ALOH3(A)	GIBBSITE(C)
2.20 M	0.36	-0.351	-0.741	-3.731	7.192	1.482	-0.664	-0.034	0.569	3.306
2.30 M	0.60	0.351	0.829	-4.156	6.903	1.192	-0.402	-0.042	0.129	2.865
2.40 M	0.84	0.462	0.947	-2.662	7.481	1.77	-0.829	0.011	0.174	2.911
2.51 M	1.08	0.336	-0.741	-1.101	7.112	1.402	-2.38	-0.042	0.443	3.179
2.52 M	1.08	0.335	-0.641	-1.175	7.037	1.327	-2.63	-0.042	0.448	3.184

LST

	Depth (m)	CALCITE	DOLOMITE	SIDERITE(D)	GOETHITE	FERRIHYD.	NI(OH)2	GYPSUM	ALOH3(A)	GIBBSITE(C)
3.10 M	0.145	0.437	0.455	-3.926	8.895	3.185	-1.218	-0.019	0.205	2.941
3.20 M	0.435	0.486	0.594	-4.88	8.312	2.602	-1.144	-0.019	0.095	2.831
3.30 M	0.725	0.48	0.637	-5.096	7.862	2.152	-0.636	-0.036	0.239	2.976
3.40 M	1.015	0.344	0.224	-4.539	7.891	2.181	-2.12	-0.027	0.473	3.21

Table 1. Saturation index values for selected phases, October, 1993.

IN - TP Test Pits Saturation Indices
June 1994

TT

	Depth (m)	CALCITE	DOLOMITE	SIDERITE(D)	GOETHITE	FERRIHYD.	NI(OH)2	GYPSUM	ALOH3(A)	GIBBSITE(C)
1.10 M	0.125				6.538	0.828	-1.79	-0.048	1.224	3.961
1.31 M	0.625	0.292	-0.146	-2.037	8.18	2.47		-0.028	0.494	3.23
1.32 M	0.625	0.291	-0.223	-2.499	7.716	2.005		-0.053	0.467	3.203
1.40 M	0.875	0.21	-0.044	-2.001	8.459	2.749		-0.02	0.416	3.153
1.51 M	1.125	0.609	0.741	-1.066	8.083	2.373		-0.026	0.24	2.976
1.52 M	1.125	0.61	0.738	-1.191	7.959	2.248		-0.022	0.228	2.964

MT

	Depth (m)	CALCITE	DOLOMITE	SIDERITE(D)	GOETHITE	FERRIHYD.	NI(OH)2	GYPSUM	ALOH3(A)	GIBBSITE(C)
2.10 M	0.125	-0.052	-1.139	-1.8	7.653	1.943	-1.254	0.001	0.644	3.38
2.30 M	0.625	0.712	0.625	-2.231	7.892	2.182	-0.813	-0.011	0.173	2.91
2.41 M	0.875	-0.132	-1.372	-0.169	7.105	1.395	-2.182	0.127	1.1	3.837
2.42 M	0.875	-0.14	-1.391	-1.983	5.284	-0.426	-2.42	0.109	1.08	3.816
2.51 M	1.125	0.138	-0.922	0.393	7.157	1.447	-2.706	-0.171	0.9	3.636
2.52 M	1.125	0.128	-0.962	0.26	7.02	1.309		-0.198	0.863	3.599

LST

	Depth (m)	CALCITE	DOLOMITE	SIDERITE(D)	GOETHITE	FERRIHYD.	NI(OH)2	GYPSUM	ALOH3(A)	GIBBSITE(C)
3.10 M	0.2575	0.09	-1.118	-3.05	8.318	2.608	-1.462	-0.092	0.632	3.368
3.21 M	0.5225	0.696	0.928	-2.47	8.611	2.901	-2.144	-0.027	0.465	3.202
3.22 M	0.5225	0.698	0.921	-2.542	8.538	2.827	-2.53	-0.04	0.461	3.197
3.31 M	0.7875	0.64	0.93	-1.893	8.616	2.906		-0.026	0.321	3.057
3.32 M	0.7875	0.641	0.92	-2.001	8.508	2.798		-0.026	0.362	3.098
3.40 M	1.0525				7.661	1.95		-0.015	0.31	3.046
3.51 M	1.3175	0.332	0.359	-3.324	7.938	2.227		-0.016	0.486	3.222
3.52 M	1.3175	0.341	0.372					-0.004	0.5	3.237

Table 2. Saturation index values for selected phases, June, 1994.

IN - TP Test Pit Saturation Indices
Nov. 1994

TT

	Depth (m)	CALCITE	DOLOMITE	SIDERITE(D)	GOETHITE	FERRIHYD.	NI(OH)2	GYPSUM
1.10 M	0.13				4.197	-1.513	-5.033	-0.054
1.21 M	0.39	-0.202	-0.518	1.084	8.032	2.321	-0.596	-0.067
1.22 M	0.39	-0.129	-0.447	0.894	7.822	2.112	-0.645	-0.016
1.31 M	0.65	0.665	1.283	0.334	8.346	2.635	-2.939	-0.036
1.32 M	0.65	0.667	1.259	0.409	8.42	2.709		-0.044
1.41 M	0.91	1.061	1.51	0.196	9.144	3.433		-0.012
1.42 M	0.91	1.041	1.623	-1.313	7.638	1.928		0.003
1.51 M	1.17	0.913	1.284	0.64	8.673	2.963		-0.026
1.52 M	1.17	0.912	1.249	0.166	8.197	2.487		-0.029

MT

	Depth (m)	CALCITE	DOLOMITE	SIDERITE(D)	GOETHITE	FERRIHYD.	NI(OH)2	GYPSUM
2.20 M	0.425				3.836	-1.874	-7.148	-0.015
2.30 M	0.675	0.987	0.96				-0.716	-0.007
2.40 M	0.925	0.716	0.365	-1.24	6.556	0.846	-1.652	-0.012

LST

	Depth (m)	CALCITE	DOLOMITE	SIDERITE(D)	GOETHITE	FERRIHYD.	NI(OH)2	GYPSUM
3.10 M	0.12	0.754	0.759	-3.367	8.289	2.579	-0.965	-0.039
3.20 M	0.36	0.726	0.762	0.176	8.865	3.154	-1.824	-0.045
3.31 M	0.6	0.339	0.274	-2.732	7.589	1.878	-2.553	-0.046
3.32 M	0.6	0.338	0.274				-2.837	-0.046
3.40 M	0.84	0.611	0.775	-4.071	6.982	1.271	-0.98	-0.056
3.50 M	1.08	0.789	0.941	-0.811	9.249	3.539	-1.406	-0.005

Table 3. Saturation index values for selected phases, November, 1994.

IN-TP **July 1995 Saturation Indices**

Sample	Depth (m)	calcite	dolomite	siderite (d)	goethite	ferrihydrite	ni(oh)2	gypsum	aloh3(a)	gibbsite (c)
TT-C1	0.13	*******	********	********	3.53	-2.256	-6.981	0.167	-5.664	-2.947
TT-C2	0.40	0.598	0.499	0.453	6.432	0.648	-1.019	0.054	-0.163	2.554
TT-C3	0.66	0.778	1.201	-0.253	7.92	2.137	-1.808	0.044	-0.446	2.272
TT-C4-1	0.92	0.97	1.526	1.356	6.67	0.887	-2.191	0.056	-0.485	2.232
TT-C4-2	0.92	0.98	1.485	1.522	6.838	1.055	-2.823	0.065	-0.47	2.248
TT-C5	1.20	0.712	0.795	1.03	6.752	0.969	-2.29	-0.062	-0.416	2.301

Sample	Depth (m)	calcite	dolomite	siderite (d)	goethite	ferrihydrite	ni(oh)2	gypsum	aloh3(a)	gibbsite (c)
MT-C1	0.14	*******	********	********	1.382	-4.437	-7.235	0.06	-5.004	-2.296
MT-C2	0.42	-0.536	-1.926	-1.35	3.917	-1.903	-3.747	0.064	0.211	2.92
MT-C3	0.70	1.417	1.85	-4.222	7.05	1.23	-2.233	0.086	-0.83	1.878
MT-C4-1	0.98	1.023	1.237	-0.79	8.674	2.855	-2.955	0.032	-0.651	2.057
MT-C4-2	0.98	1.018	1.218	********	********	********	-2.566	0.032	-0.651	2.057
MT-C5	1.26	0.716	0.469	0.009	6.165	0.346	-3.039	0.102	-0.276	2.433

Sample	Depth (m)	calcite	dolomite	siderite (d)	goethite	ferrihydrite	ni(oh)2	gypsum	aloh3(a)	gibbsite (c)
LST-C1	0.16	-0.025	-1.298	-0.556	8.348	2.492	-2.046	0.044	-0.017	2.683
LST-C2-1	0.48	0.967	0.74	-2.229	7.708	1.853	-2.017	0.035	-0.725	1.974
LST-C2-2	0.48	0.971	0.726	-2.372	7.565	1.71	-2.012	0.041	-0.723	1.976
LST-C3-1	0.80	0.446	-0.179	-0.713	4.856	-0.999	-3.278	0.025	-0.145	2.554
LST-C3-2	0.80	0.444	-0.193	-0.64	4.929	-0.927	-3.448	0.024	-0.138	2.562
LST-C4-1	1.13	0.825	0.581	0.148	6.155	0.3	-3.328	0.044	-0.419	2.28
LST-C4-2	1.13	0.835	0.612	-0.81	5.198	-0.658	-3.361	0.067	-0.467	2.232
LST-C5-1	1.46	0.609	-0.091	0.092	8.198	2.342	-2.788	-0.036	0.178	2.877
LST-C5-2	1.46	0.636	-0.065	-2.308	5.799	-0.057	-3.123	-0.005	-0.383	2.316

Table 4. Saturation index values for selected phases, July, 1995.

IN-TP **October 1995 Saturation Indices**

Sample	Depth (m)	calcite	dolomite	siderite (d)	goethite	ferrihydrite	ni(oh)2	gypsum	aloh3(a)	gibbsite (c)
TT-G1	0.13	********	********	********	5.309	-0.475	-6.012	-0.053	-3.327	-0.61
TT-G2	0.39	********	********	********	4.682	-1.104	-5.586	0.192	-4.503	-1.786
TT-G3	0.65	-3.902	-7.048	-2.214	7.522	1.737	-3.689	0.123	-2.657	0.061
TT-G4	0.90	-3.657	-6.639	-2.04	7.556	1.771	-3.566	0.136	-3.058	-0.341
TT-G5	1.17	-1.946	-4.221	-0.094	7.608	1.825	-1.476	-0.158	0.448	3.166
TT-S1	0.11	********	********	********	4.697	-1.087	-5.967	0.012	-3.804	-1.086
TT-S2	0.34	-3.494	-7.196	-2.144	4.366	-1.417	-4.68	-0.178	-2.268	0.449
TT-S3-1	0.56	0.48	0.51	1.174	6.372	0.588	-2.771	0.096	-0.284	2.433
TT-S3-2	0.56	0.49	0.527	1.16	6.358	0.574	-2.967	0.114	-0.29	2.427
TT-S4-1	0.78	-0.462	-1.09	0.924	6.323	0.54	-2.861	0.029	0.111	2.828
TT-S4-2	0.78	-0.473	-1.104	0.936	6.333	0.55	-3.246	0.008	0.073	2.791
TT-S5-1	1.03	0.422	0.475	0.678	6.463	0.679	-2.882	-0.031	-0.303	2.414
TT-S5-2	1.03	0.424	0.46	0.776	6.561	0.778	-2.831	-0.025	-0.284	2.433

Sample	Depth (m)	calcite	dolomite	siderite (d)	goethite	ferrihydrite	ni(oh)2	gypsum	aloh3(a)	gibbsite (c)
MT-G4	0.70	********	********	********	4.41	-1.374	-4.975	-0.026	-4.511	-1.793
MT-G5-1	0.90	********	********	********	4.775	-1.008	-5.557	0.025	-4.582	-1.864
MT-G5-2	0.90	********	********	********	4.938	-0.846	-5.596	0.011	-4.591	-1.874
MT-S1-1	0.11	0.024	-1.017	-2.408	6.791	1.008	-1.204	-0.536	-0.937	1.78
MT-S1-2	0.11	0.029	-1.066	********	********	********	-1.217	-0.524	-1.076	1.642
MT-S2-1	0.34	0.636	0.847	-0.101	7.27	1.487	-0.591	-0.008	-0.868	1.85
MT-S2-2	0.34	0.638	0.73	-0.245	7.126	1.343	-0.56	-0.027	-0.849	1.869
MT-S3	0.57	0.757	1.101	0.49	6.786	1.003	-2.274	-0.011	-0.679	2.039
MT-S4	0.79	1.069	1.712	0.803	6.853	1.069	-2.688	-0.027	-0.801	1.917

Table 5. Saturation index values for selected phases, October, 1995.

IN-TP October 1995 Saturation Indices

Sample	Depth (m)	calcite	dolomite	siderite (d)	goethite	ferrihydrite	ni(oh)2	gypsum	aloh3(a)	gibbsite (c)
LST-G1-1	0.11	0.175	-0.707	-3.45	7.33	1.547	-1.821	-0.969	-1.408	1.31
LST-G1-2	0.11	0.07	-0.949	********	********	********	-2.099	-1.304	-1.647	1.07
LST-G2-1	0.33	0.122	-0.593	-1.257	9.204	3.42	-0.333	-0.119	0.324	3.041
LST-G2-2	0.33	0.225	-0.451	-3.089	7.307	1.524	-0.966	-0.062	-0.536	2.181
LST-G3-1	0.56	0.334	-0.283	-3.25	7.343	1.559	-1.123	0.037	-0.632	2.086
LST-G3-2	0.56	0.337	-0.201	********	********	********	-1.235	0.032	-0.646	2.072
LST-G4-1	0.78	0.427	-0.185	********	********	********	-1.384	-0.021	-0.625	2.093
LST-G4-2	0.78	0.453	-0.123	********	********	********	-1.368	0.044	-0.651	2.067
LST-G5	0.99	0.674	0.239	********	********	********	-1.062	-0.259	-0.903	1.814
LST-S1	0.13	-0.152	-1.5	-5.337	7.244	1.461	-1.58	-0.009	-0.583	2.135
LST-S2	0.40	-0.085	-1.016	-5.8	7.85	2.066	-1.305	0.019	-0.4	2.318
LST-S3	0.66	0.493	0.263	-3.956	8.262	2.478	0.337	-0.004	-0.924	1.794
LST-S4	0.93	0.49	0.191	-6.06	7.497	1.713	-0.208	0.007	-0.807	1.911
LST-S5-1	1.20	1.114	1.426	-2.679	7.757	1.974	-1.964	0.058	-0.826	1.892
LST-S5-2	1.20	1.119	1.409	-2.564	7.871	2.088	-2.126	0.057	-0.842	1.875

Table 5. Continued.

IN-TP **June 1996 Saturation Indices**

Sample	Depth (m)	calcite	dolomite	siderite (d)	goethite	ferrihydrite	ni(oh)2	gypsum	aloh3(a)	gibbsite (c)
TT-G1	0.17	*******	********	********	3.863	-1.957	-7.35	-0.041	-5.075	-2.366
TT-G2	0.44	-4.516	-8.987	-2.572	6.174	0.355	-4.913	-0.782	-1.968	0.74
TT-G3	0.71	-2.318	-4.811	-3.26	7.073	1.253	-2.192	-0.763	-0.625	2.084
TT-G4	0.99	-1.42	-3.423	-2.523	6.953	1.134	-1.711	-0.995	-0.514	2.194
TT-G5-1	1.26	-0.967	-2.626	0.485	8.852	3.033	-1.922	-1.009	-0.55	2.159
TT-G5-2	1.26	-0.948	-2.608	0.097	8.47	2.65	-1.719	-0.993	-0.422	2.286
TT-S1	0.12	*******	********	********	5.457	-0.326	-5.515	-0.099	-2.896	-0.179
TT-S2-1	0.36	*******	********	********	4.6	-1.184	-6.199	-0.092	-5.392	-2.675
TT-S2-2	0.36	*******	********	********	4.595	-1.189	-6.15	-0.004	-5.464	-2.747
TT-S3	0.60	-2.138	-4.492	-0.295	7.077	1.294	-1.493	-0.025	0.377	3.095
TT-S4	0.84	-1.725	-3.302	0.456	6.633	0.849	-1.621	0.033	0.163	2.88
TT-S5	1.08	-1.486	-2.831	0.608	6.846	1.062	-1.535	0.018	0.093	2.81

Sample	Depth (m)	calcite	dolomite	siderite (d)	goethite	ferrihydrite	ni(oh)2	gypsum	aloh3(a)	gibbsite (c)
MT-G1	0.12	*******	********	********	3.916	-1.832	-6.523	0.103	-5.046	-2.319
MT-G2	0.35	*******	********	********	3.976	-1.772	-7.534	0.158	-6.136	-3.409
MT-G3	0.58	-2.783	-6.043	-1.16	6.758	1.011	-2.994	-0.028	-0.01	2.716
MT-G4-1	0.81	-3.436	-7.578	-2.079	5.985	0.238	-5.645	-0.024	-2.519	0.208
MT-G4-2P	0.81	-3.461	-7.519	-2.018	6.056	0.309	-5.65	-0.015	-2.334	0.393
MT-G5	1.04	-2.894	-6.333	-1.107	6.153	0.406	-4.645	-0.016	-2.175	0.552
MT-S1	0.17	0.33	-0.521	-1.712	7.781	2.034	-1.559	-0.507	-0.74	1.987
MT-S2	0.50	0.488	0.127	-0.67	6.843	1.096	-1.258	-0.035	-0.584	2.143
MT-S3-1	0.84	0.667	0.889	0.458	6.409	0.662	-2.423	-0.032	-0.603	2.124
MT-S3-2	0.84	0.665	0.877	0.464	6.415	0.668	-2.469	-0.031	-0.678	2.049

Table 6. Saturation index values for selected phases, June, 1996.

IN-TP June 1996 Saturation Indices

Sample	Depth (m)	calcite	dolomite	siderite (d)	goethite	ferrihydrite	ni(oh)2	gypsum	aloh3(a)	gibbsite (c)
LST-G1	0.13	-0.051	-1.055	-6.836	7.323	1.576	-1.154	-0.942	-1.662	1.065
LST-G2	0.39	-0.126	-1.541	-3.557	7.209	1.462	-2.345	-1.163	-1.422	1.305
LST-G3	0.65	0.276	-0.631	-3.485	8.089	2.342	-2.011	-0.874	-1.196	1.531
LST-G4	0.91	-1.412	-3.952	-1.704	6.321	0.574	-3.94	-1.361	-0.209	2.518
LST-G5	1.18	0.121	-1.038	********	********	********	-1.812	-1.086	-1.105	1.622
LST-S1	0.14	-0.253	-1.859	-2.564	8.773	3.026	-1.613	-0.523	-0.837	1.89
LST-S2-1	0.42	0.543	-0.344	-2.088	7.966	2.22	-1.724	-1.313	-1.538	1.188
LST-S2-2	0.42	0.538	-0.511	-2.413	7.642	1.896	-1.52	-1.307	-1.676	1.051
LST-S3	0.69	0.976	0.301	-1.979	8.348	2.602	-1.186	-0.051	-1.002	1.725
LST-S4-1	0.97	0.712	-0.535	-1.295	7.645	1.899	-1.998	-0.04	-0.821	1.906
LST-S4-2	0.97	0.711	-0.555	-1.062	7.879	2.132	-2.077	-0.041	-0.806	1.921
LST-S5-1	1.24	0.737	0.098	0.052	7.189	1.442	-2.204	-0.03	-0.853	1.873
LST-S5-2	1.24	0.735	0.015	0.03	7.165	1.418	-2.256	-0.036	-0.853	1.874

Table 6. Continued.

IN-TP **Oct 1996 Saturation Indices**

Sample	Depth (m)	calcite	dolomite	siderite (d)	goethite	ferrihydrite	ni(oh)2	gypsum	aloh3(a)	gibbsite (c)
TT-G1	0.16	*******	********	********	3.998	-1.668	-7.551	-0.204	-5.153	-2.405
TT-G2	0.50	*******	********	********	5.415	-0.251	-5.534	-0.254	-3.699	-0.951
TT-G3-1	0.84	-1.475	-3.093	0.425	8.767	3.101	-1.442	-0.396	-0.023	2.724
TT-G3-2	0.84	-1.397	-2.996	0.268	8.605	2.939	-1.375	-0.316	0.327	3.075
TT-G4-1	1.17	-2.341	-4.802	-0.452	8.547	2.881	-2.386	-0.214	-0.046	2.702
TT-G4-2	1.17	-2.318	-4.778	-0.503	8.494	2.828	-2.313	-0.192	0.137	2.884
TT-S1	0.16	*******	********	********	4.943	-0.663	-5.85	-0.502	-4.394	-1.631
TT-S2	0.47	-2.659	-5.464	-1.906	7.432	1.825	-2.778	-0.214	-1.52	1.243
TT-S3-1	0.78	-1.064	-2.493	0.197	8.918	3.312	-1.942	0.008	0.085	2.848
TT-S3-2	0.78	-1.055	-2.461	0.148	8.863	3.257	-2.072	0.013	0.023	2.786
TT-S4-1	1.08	-0.346	-1.473	0.451	9.882	4.276	-1.054	0.023	-0.129	2.634
TT-S4-2	1.08	-0.327	-1.447	0.234	9.662	4.056	-1.021	0.036	-0.055	2.708
Sample	**Depth (m)**	**calcite**	**dolomite**	**siderite (d)**	**goethite**	**ferrihydrite**	**ni(oh)2**	**gypsum**	**aloh3(a)**	**gibbsite (c)**
MT-G1	0.11	*******	********	********	3.201	-2.488	-7.921	0.03	-5.853	-3.111
MT-G2	0.34	*******	********	********	3.394	-2.295	-7.936	-0.547	-6.144	-3.402
MT-G3	0.56	*******	********	********	4.922	-0.767	-5.839	0.128	-2.97	-0.228
MT-G4-1	0.79	*******	********	********	5.38	-0.308	-5.595	-0.467	-2.536	0.206
MT-G4-2	0.79	*******	********	********	5.345	-0.344	-5.587	-0.371	-2.483	0.259
MT-S1-1	0.18	0.213	-0.111	-4.543	8.884	3.255	-0.282	-0.21	-0.381	2.376
MT-S1-2	0.18	0.173	-0.354	-4.925	8.475	2.847	-0.489	-0.351	-0.772	1.985
MT-S2-1	0.53	0.551	0.701	-3.854	9.242	3.613	-1.221	-0.011	-0.805	1.952
MT-S2-2	0.53	0.556	0.687	-4.884	8.213	2.584	-1.106	-0.005	-0.808	1.949
MT-S3-11	0.89	0.184	0.158	0.169	9.389	3.76	-2.4	-0.001	-0.311	2.446
MT-S3-22	0.89	0.189	0.146	0.155	9.374	3.745	-2.773	0.003	-0.337	2.42

Table 7. Saturation index values for selected phases, October, 1996.

IN-TP **Oct 1996 Saturation Indices**

Sample	Depth (m)	calcite	dolomite	siderite (d)	goethite	ferrihydrite	ni(oh)2	gypsum	aloh3(a)	gibbsite (c)
LST-G1-1	0.16	-0.008	-0.907	-2.743	8.541	2.89	-0.928	-0.009	-0.091	2.66
LST-G1-2	0.16	-0.008	-0.975	-3.273	8.007	2.356	-0.995	-0.02	-0.247	2.504
LST-G2-1	0.47	0.394	-0.116	-4.085	7.912	2.261	-0.76	-0.029	-0.608	2.144
LST-G2-2	0.47	0.384	-0.111	-4.018	7.975	2.324	-0.819	-0.046	-0.643	2.108
LST-G3-1	0.79	0.347	0.196	-4.31	8.164	2.513	-0.845	-0.066	-0.537	2.214
LST-G3-2	0.79	0.378	0.093	********	********	********	-0.902	-0.003	-0.47	2.281
LST-G4-1	1.10	0.092	-0.061	-3.591	8.847	3.196	-0.45	-0.595	-0.942	1.81
LST-G4-2	1.10	0.122	-0.006	-4.183	8.263	2.612	-0.405	-0.516	-0.78	1.971
LST-S1-1	0.14	0.55	0.218	********	********	********	-0.469	-0.052	-0.527	2.234
LST-S1-2	0.14	0.544	0.204	-3.42	7.766	2.153	-0.526	-0.079	-0.528	2.233
LST-S2-1	0.42	0.788	0.604	-3.024	8.613	2.999	-0.621	-0.012	-0.507	2.254
LST-S2-2	0.42	0.756	0.567	-3.726	7.902	2.288	-0.87	-0.039	-1.292	1.469
LST-S3-1	0.68	0.862	0.827	-0.02	8.498	2.884	-1.783	-0.002	-0.668	2.093
LST-S3-2	0.68	0.868	0.838	0.038	8.557	2.943	-1.787	0.012	-0.7	2.061
LST-S4-1	0.93	0.909	0.89	-0.588	8.492	2.879	-1.444	-0.024	-0.905	1.856
LST-S4-2	0.93	0.924	0.9	-0.719	8.362	2.748	-1.868	0	-0.975	1.786

Table 7. Continued.

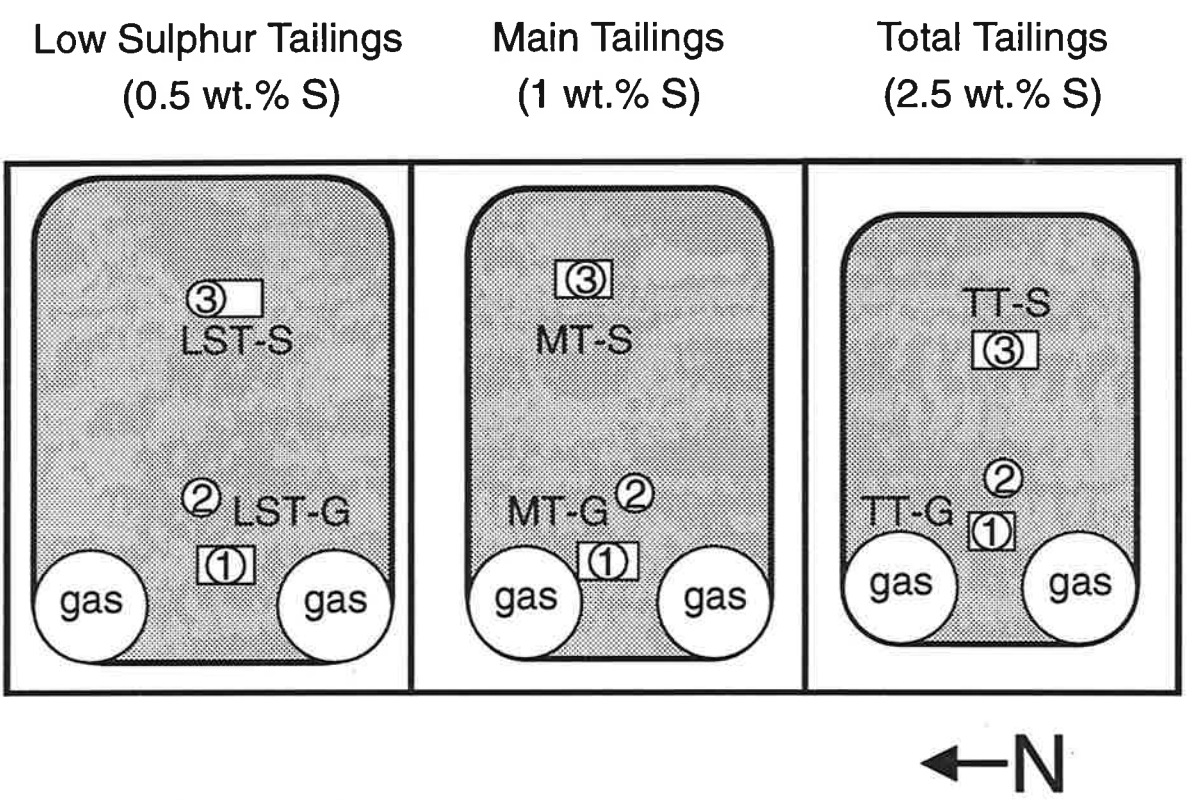

Figure 1. Plan view of the study area.

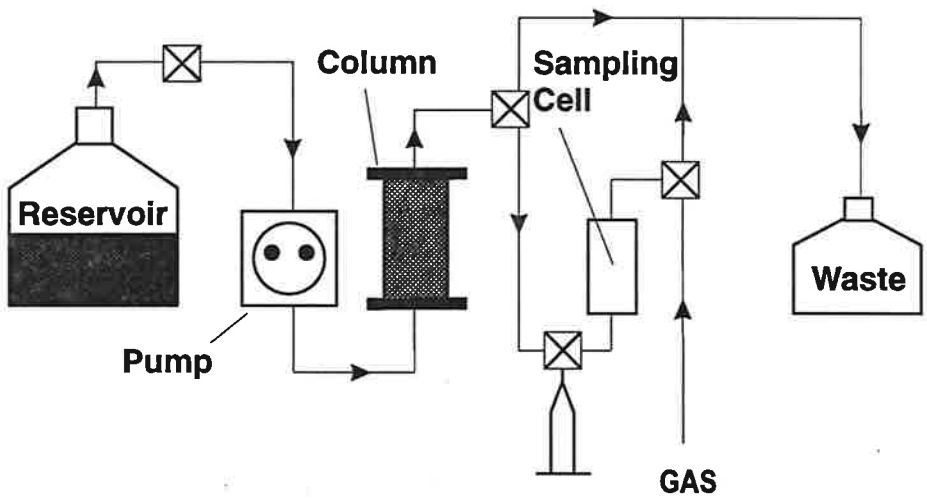

Figure 2. Schematic of saturated flow column experiments.

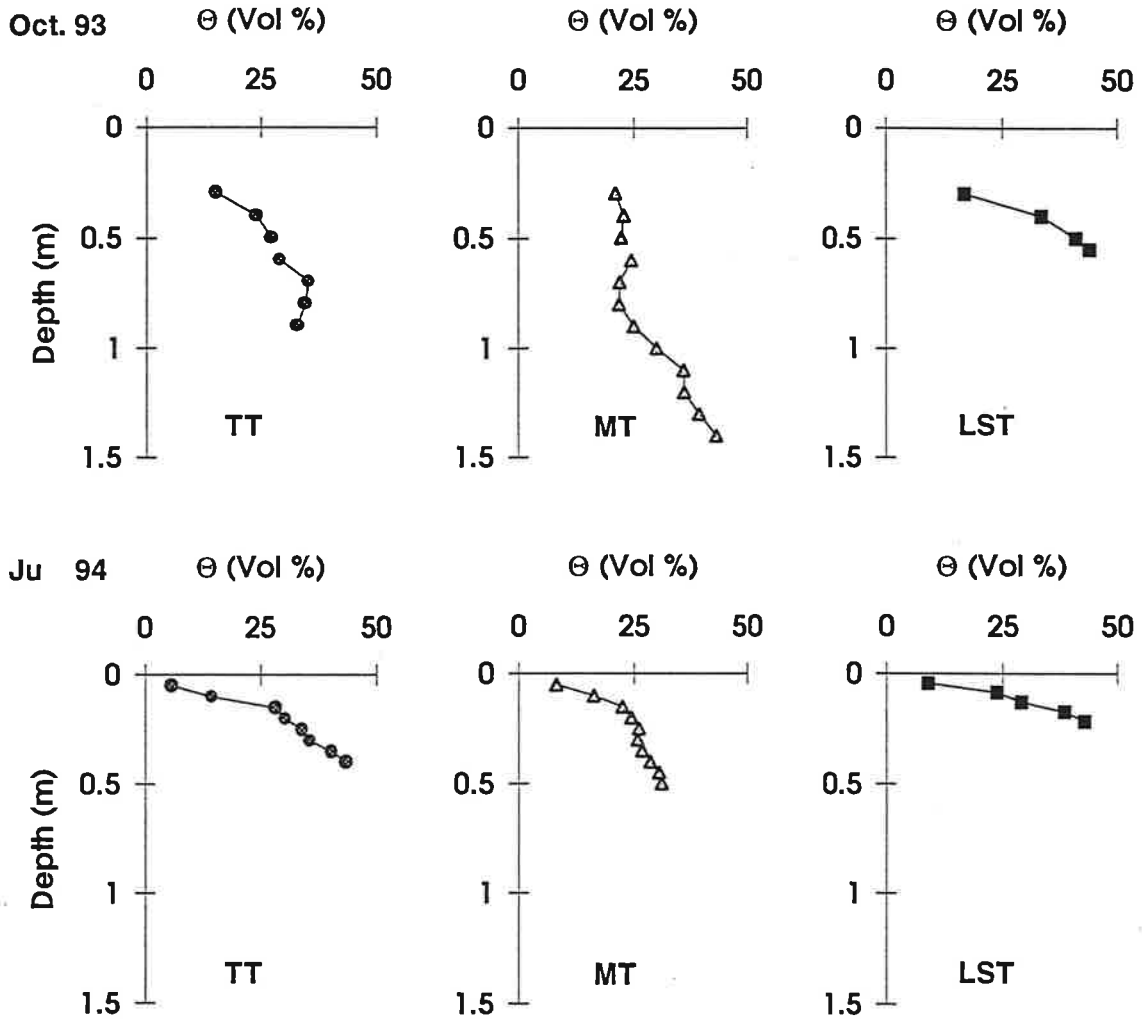

Figure 3. Moisture contents in the TT, MT and LST lysimeters measured using the neutron probe (October, 1993 and June, 1994).

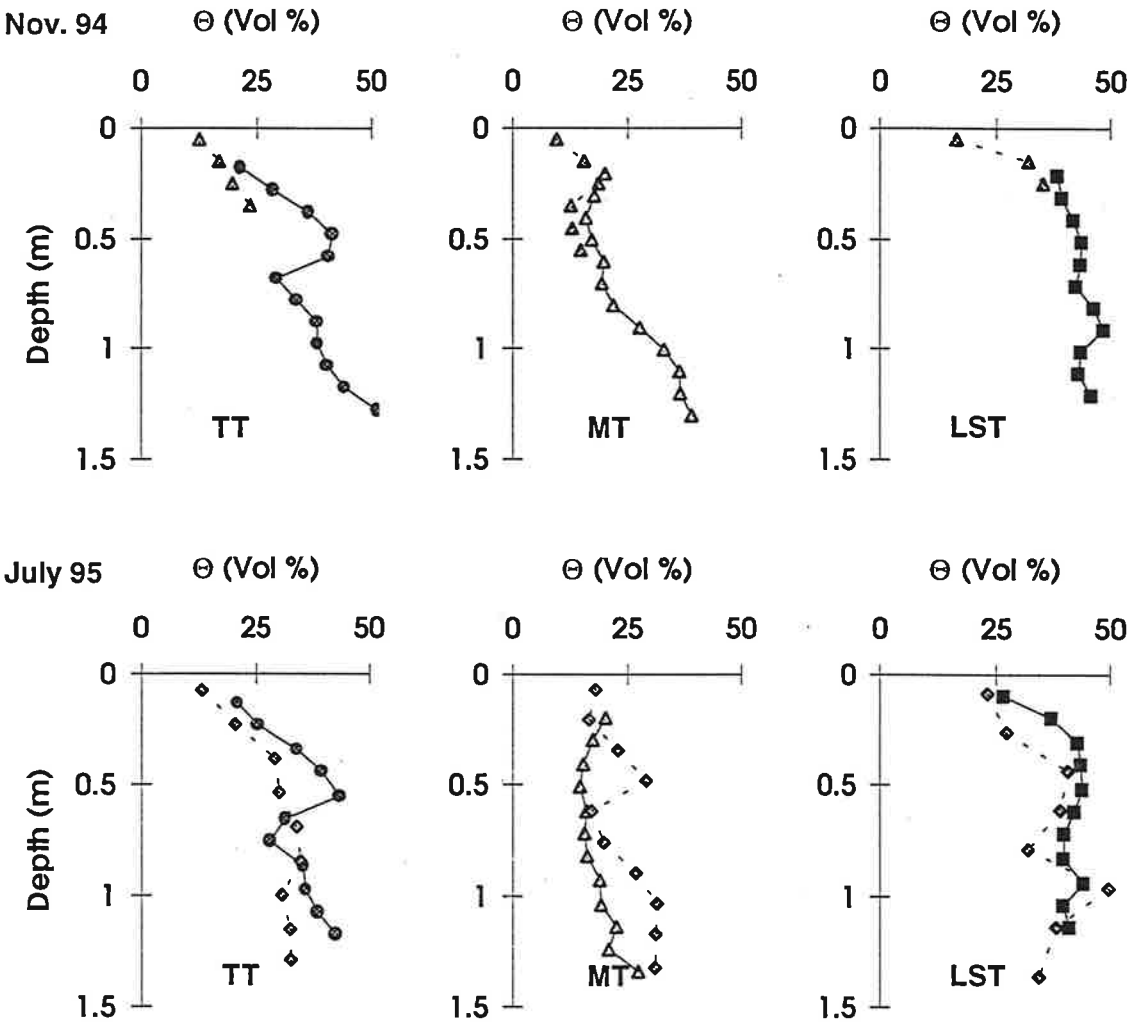

Figure 4. Moisture contents in the TT, MT and LST lysimeters (November, 1994 and July, 1995). ---- = gravimetric; —— = neutron probe

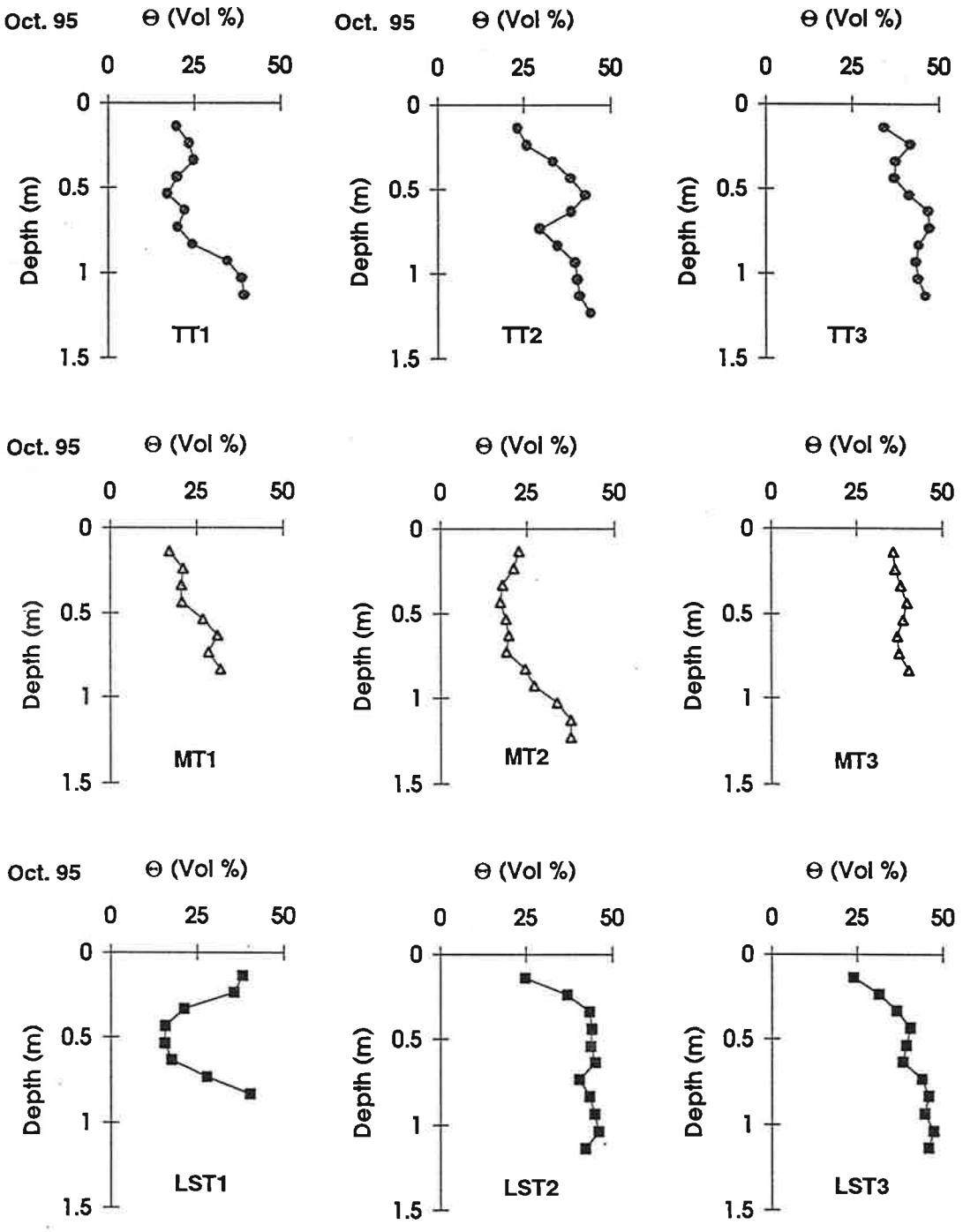

Figure 5. Moisture contents in the TT, MT and LST lysimeters measured using the neutron probe (October, 1995). Sample locations are identified in Figure 1.

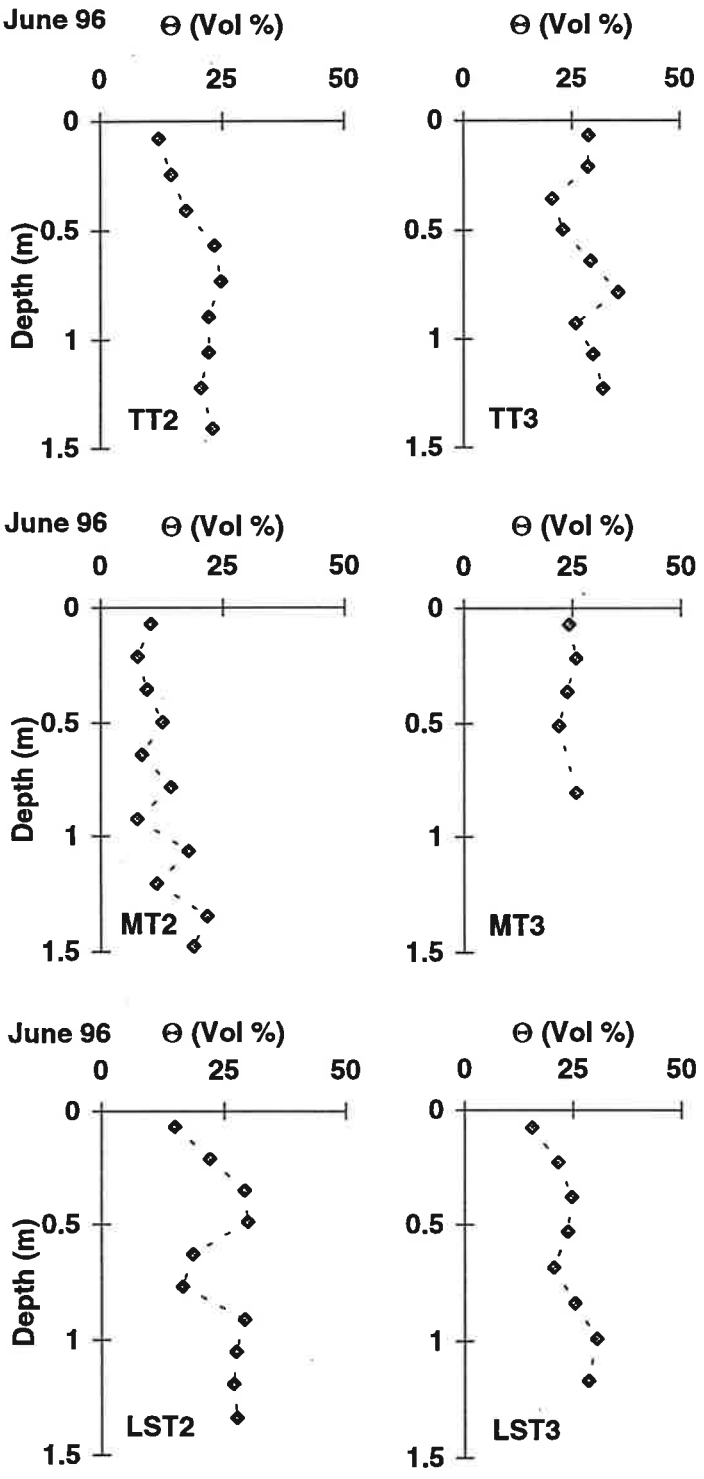

Figure 6. Gravimetric moisture contents in the TT, MT and LST lysimeters (June, 1996). Sample locations are identified in Figure 1.

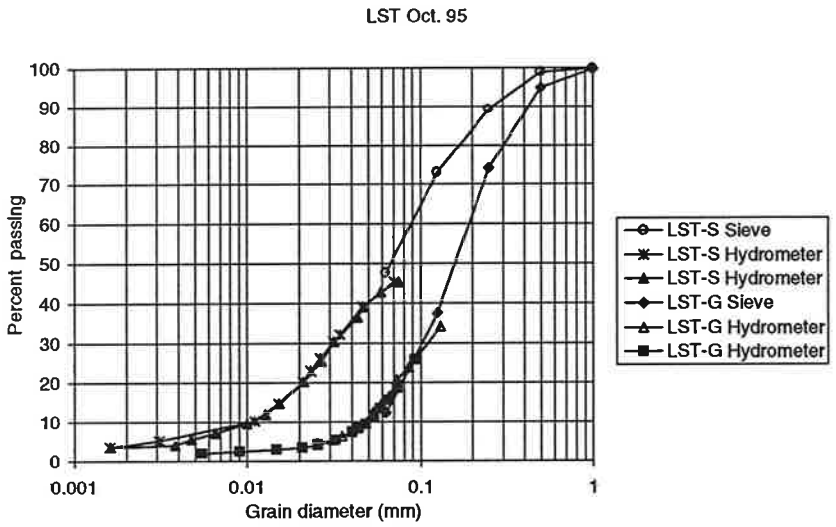

Percent	LST-S	LST-G
clay	4	1
silt	44	15
sand	52	84
(Wentworth classification)		
Hazen K (cm/s)	1.00E-04	2.40E-03

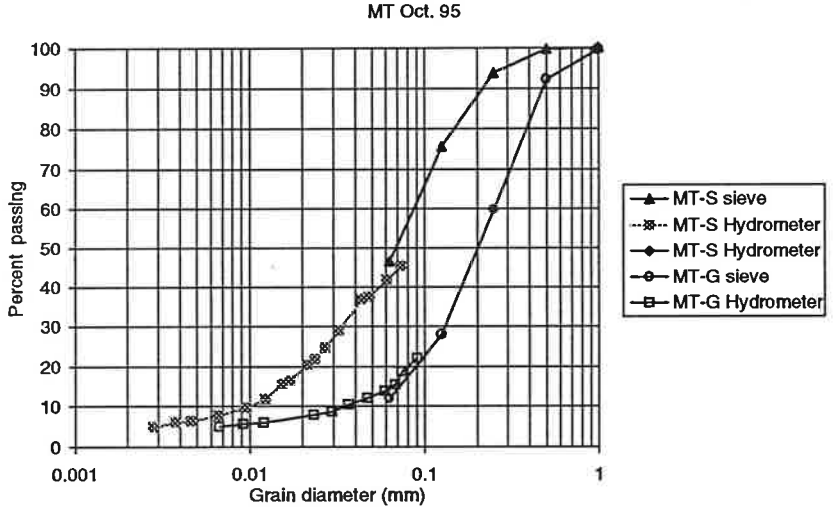

Percent	MT-S	MT-G
clay	5	3
silt	42	12
sand	53	85
Hazen K (cm/s)	1.00E-04	1.16E-03

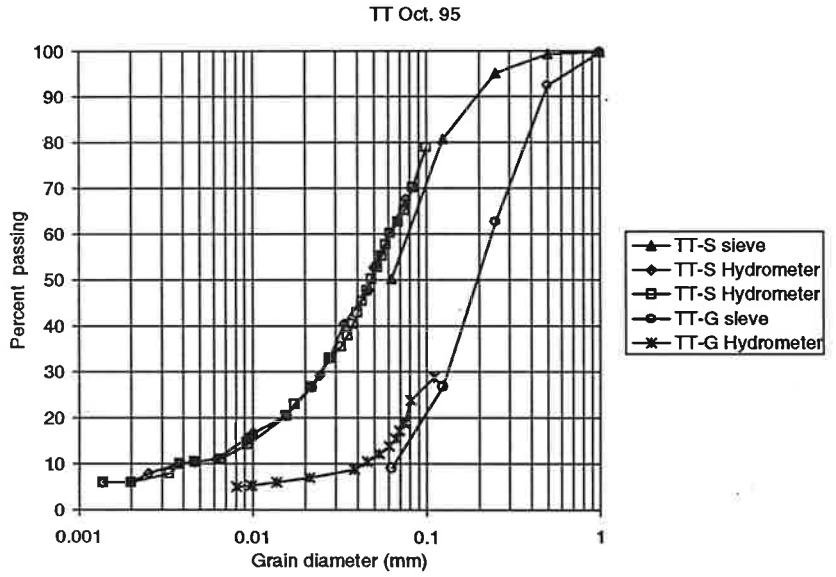

Percent	TT-S	TT-G
clay	6	3
silt	56	12
sand	38	85
Hazen K (cm/s)	2.03E-05	1.68E-03

Figure 7. Grain size curves for cores collected in October, 1995. Sample locations are identified in Figure 1. The core samples were used in the saturated column experiments.

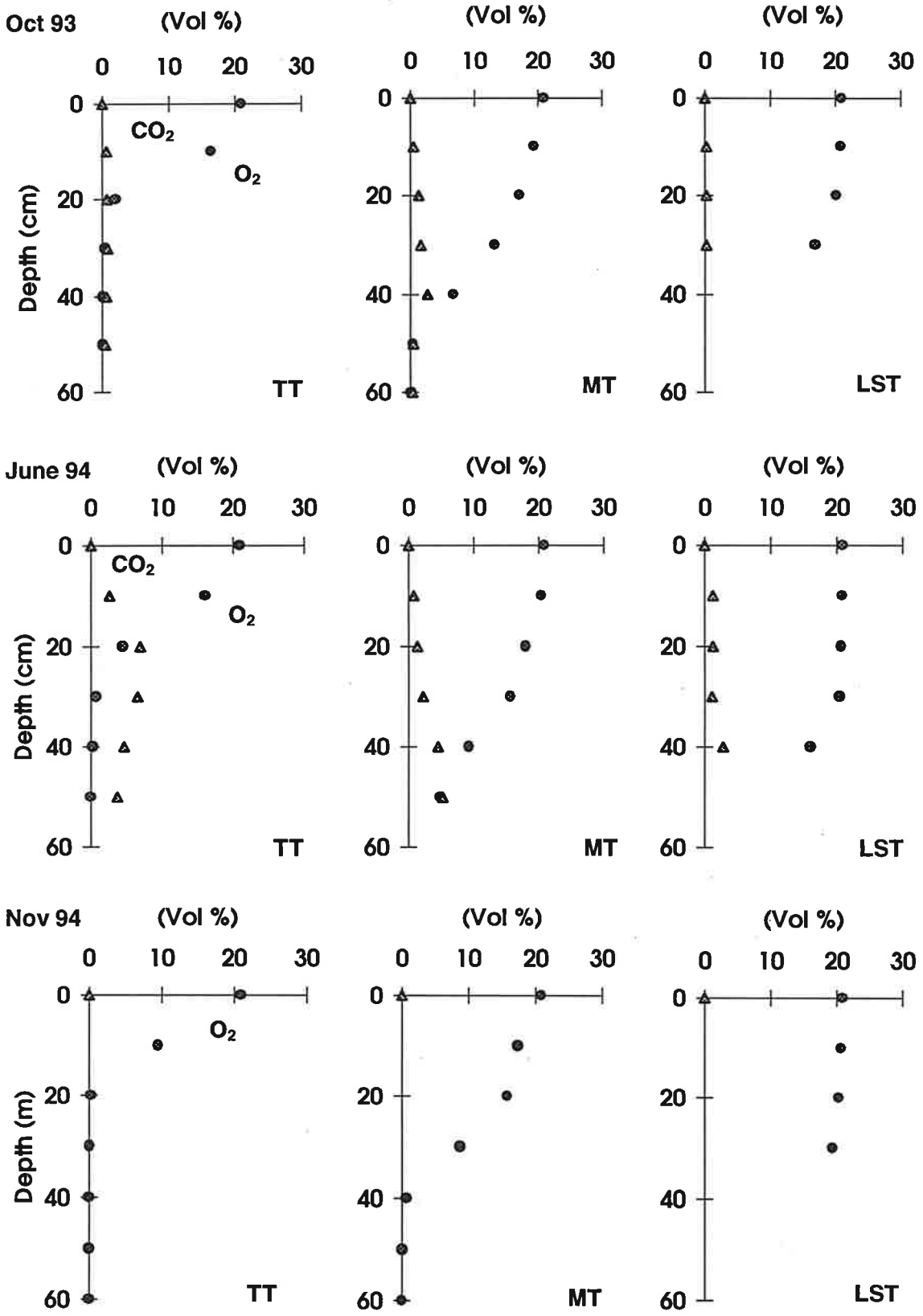

Figure 8. Pore-gas concentrations of O_2 and CO_2 in the TT, MT and LST lysimeters.

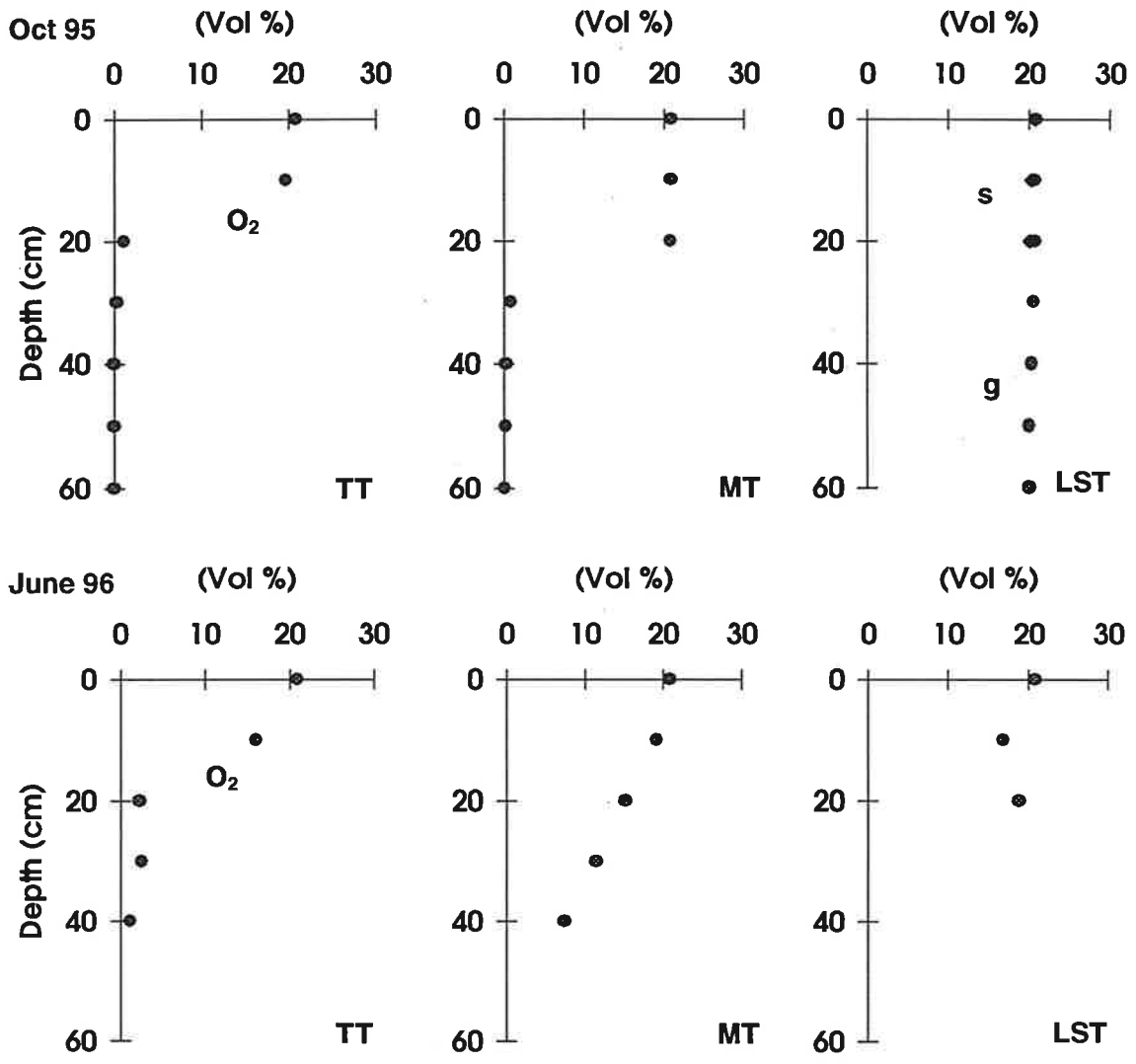

Figure 9. Pore-gas concentrations of O_2 in the TT, MT and LST lysimeters.

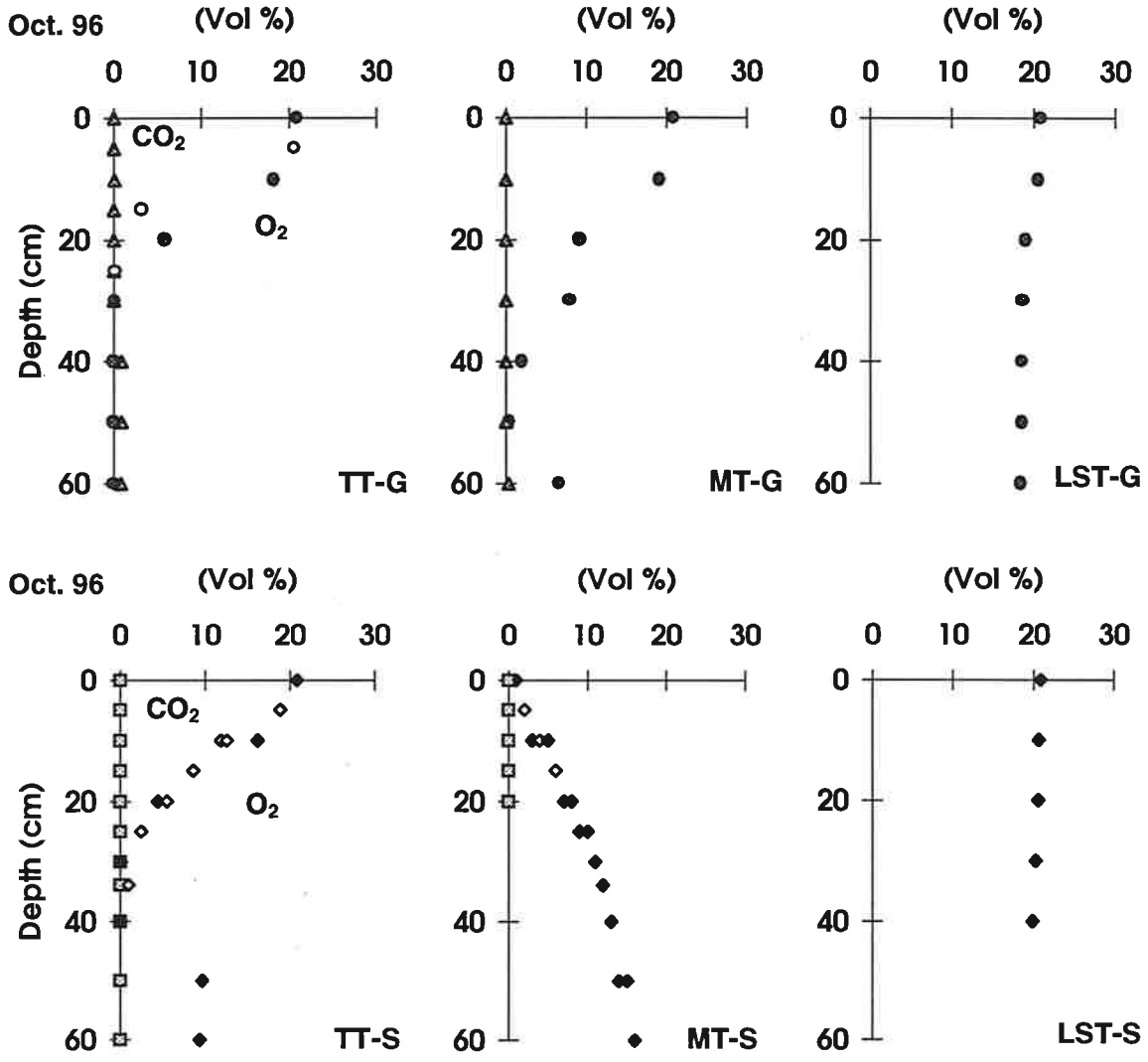

Figure 10. Pore-gas concentrations of O_2 and CO_2 in the TT, MT and LST lysimeters.

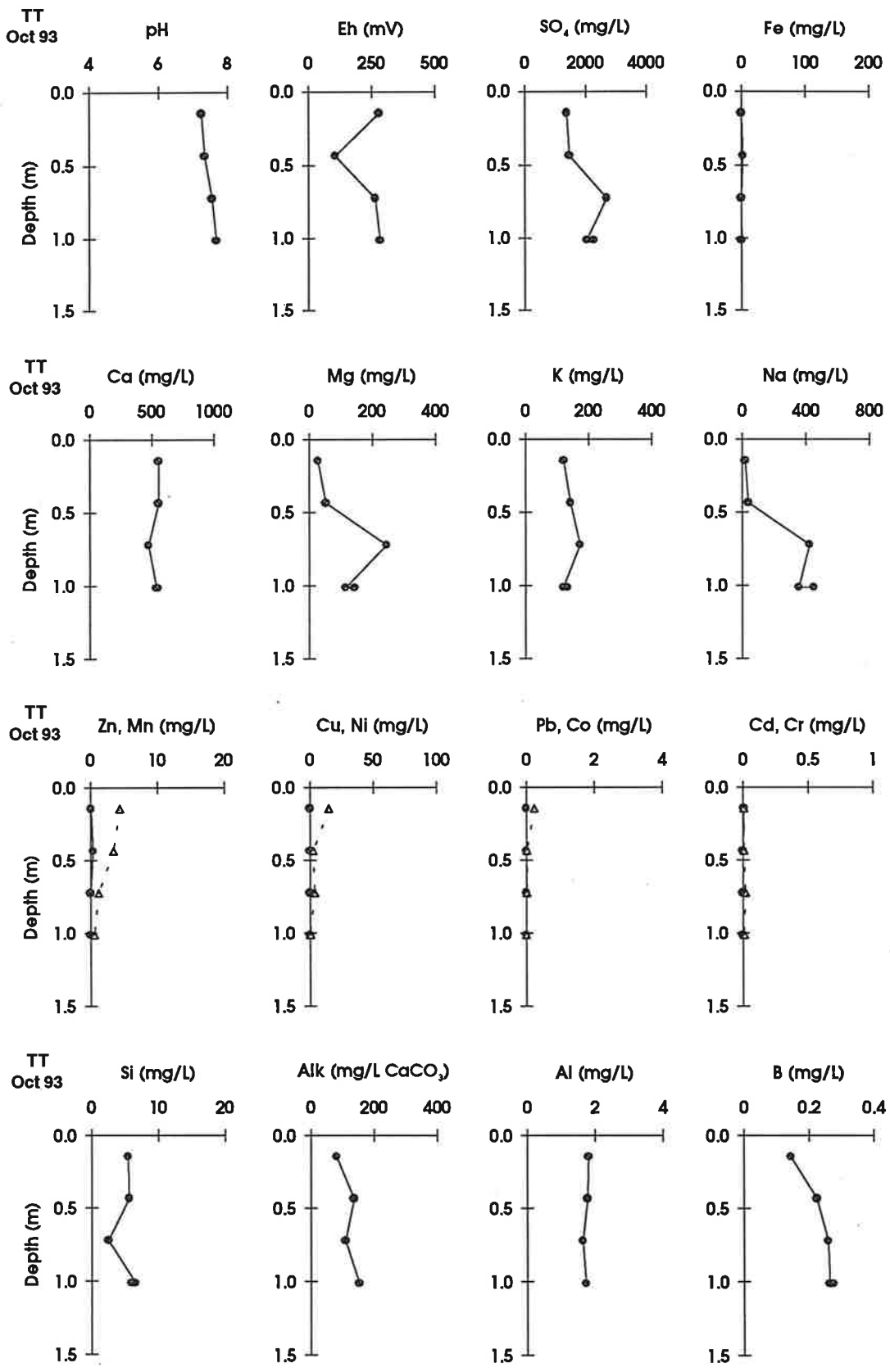

Figure 11. Pore-water geochemistry in the TT lysimeter, October, 1993. • = Zn, Cu, Pb, Cd; Δ = Mn, Ni, Co, Cr

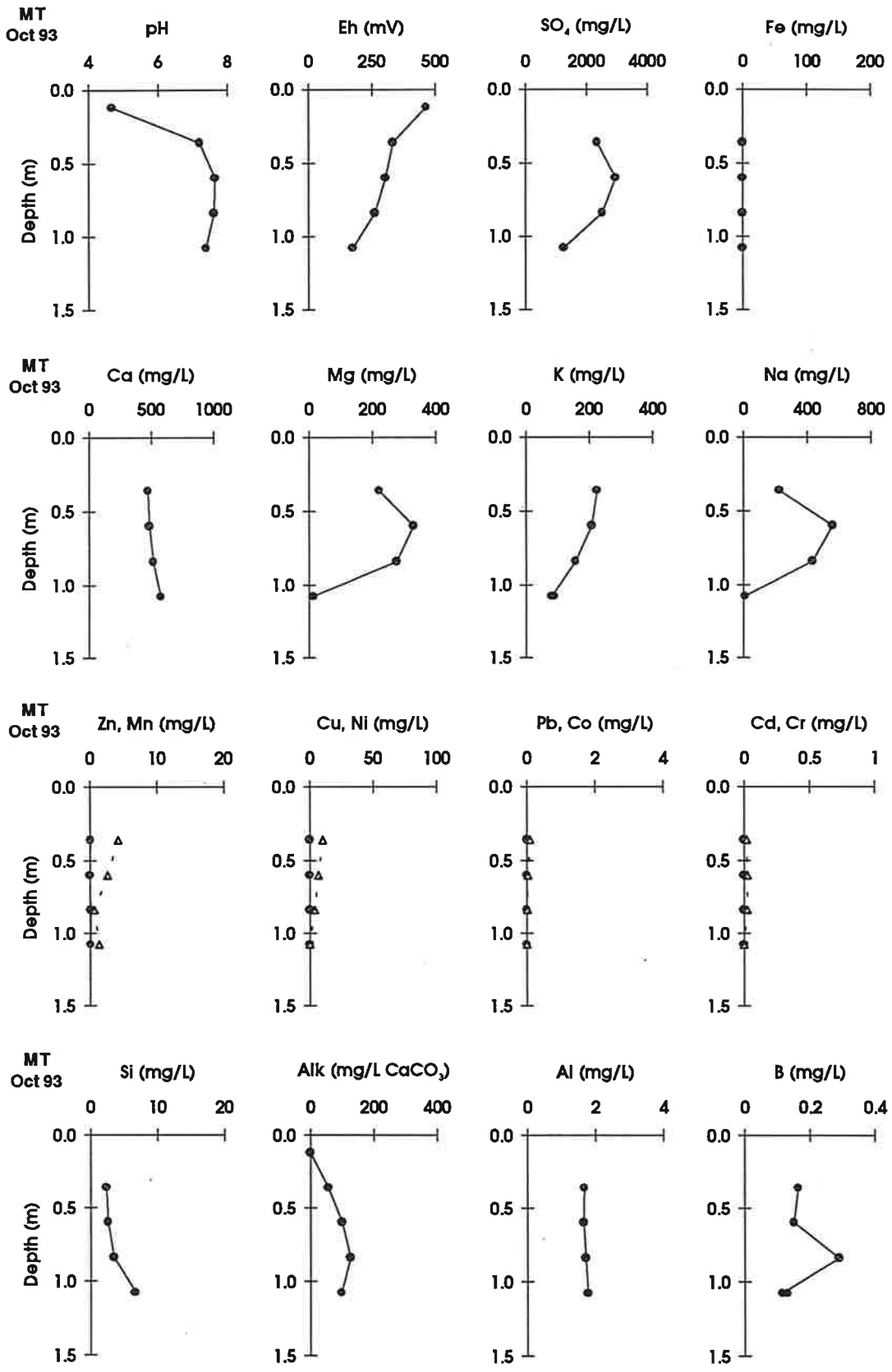

Figure 12. Pore-water geochemistry in the MT lysimeter, October, 1993. • = Zn, Cu, Pb, Cd; Δ = Mn, Ni, Co, Cr

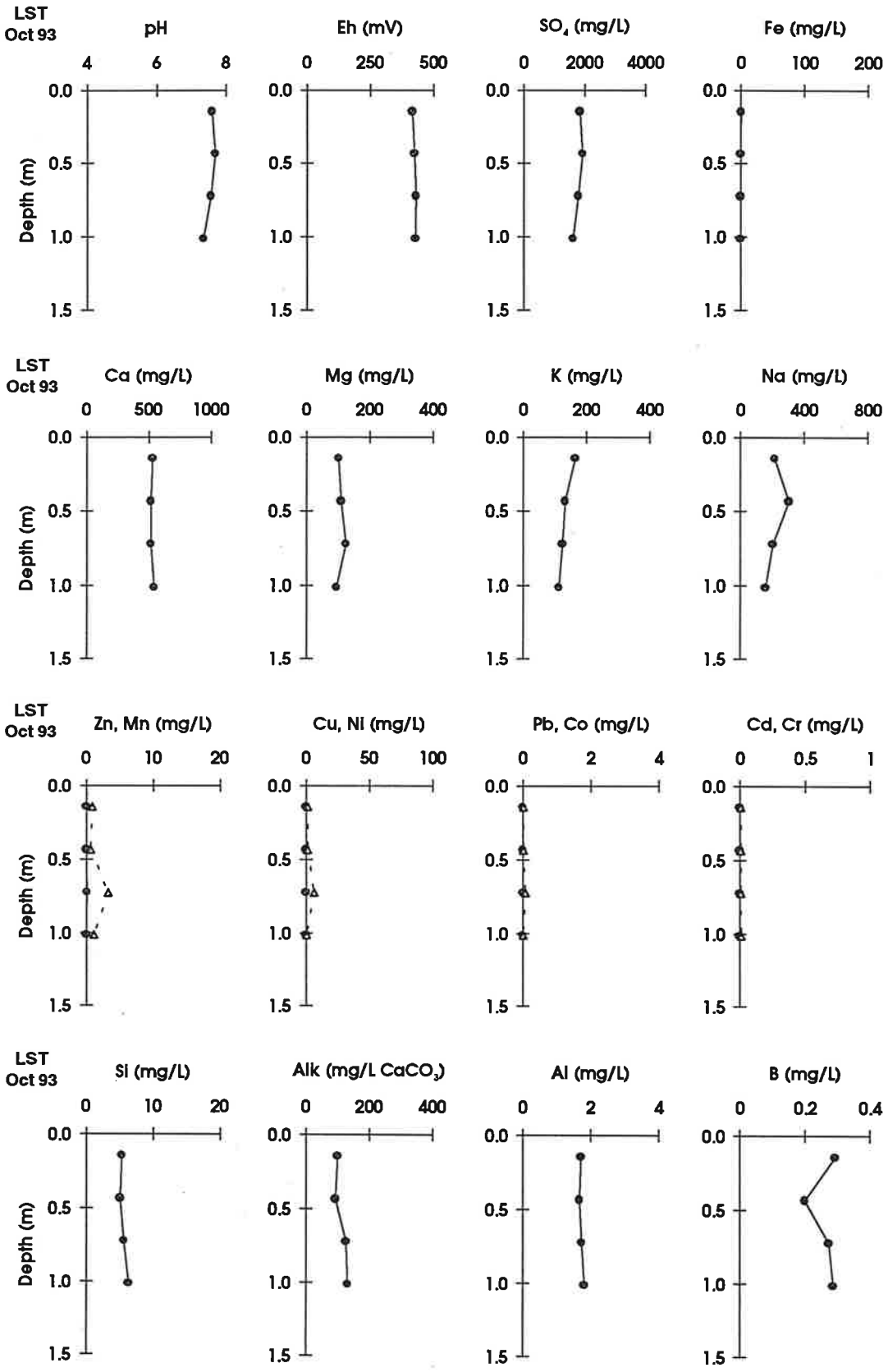

Figure 13. Pore-water geochemistry in the LST lysimeter, October, 1993. • = Zn, Cu, Pb, Cd; Δ = Mn, Ni, Co, Cr

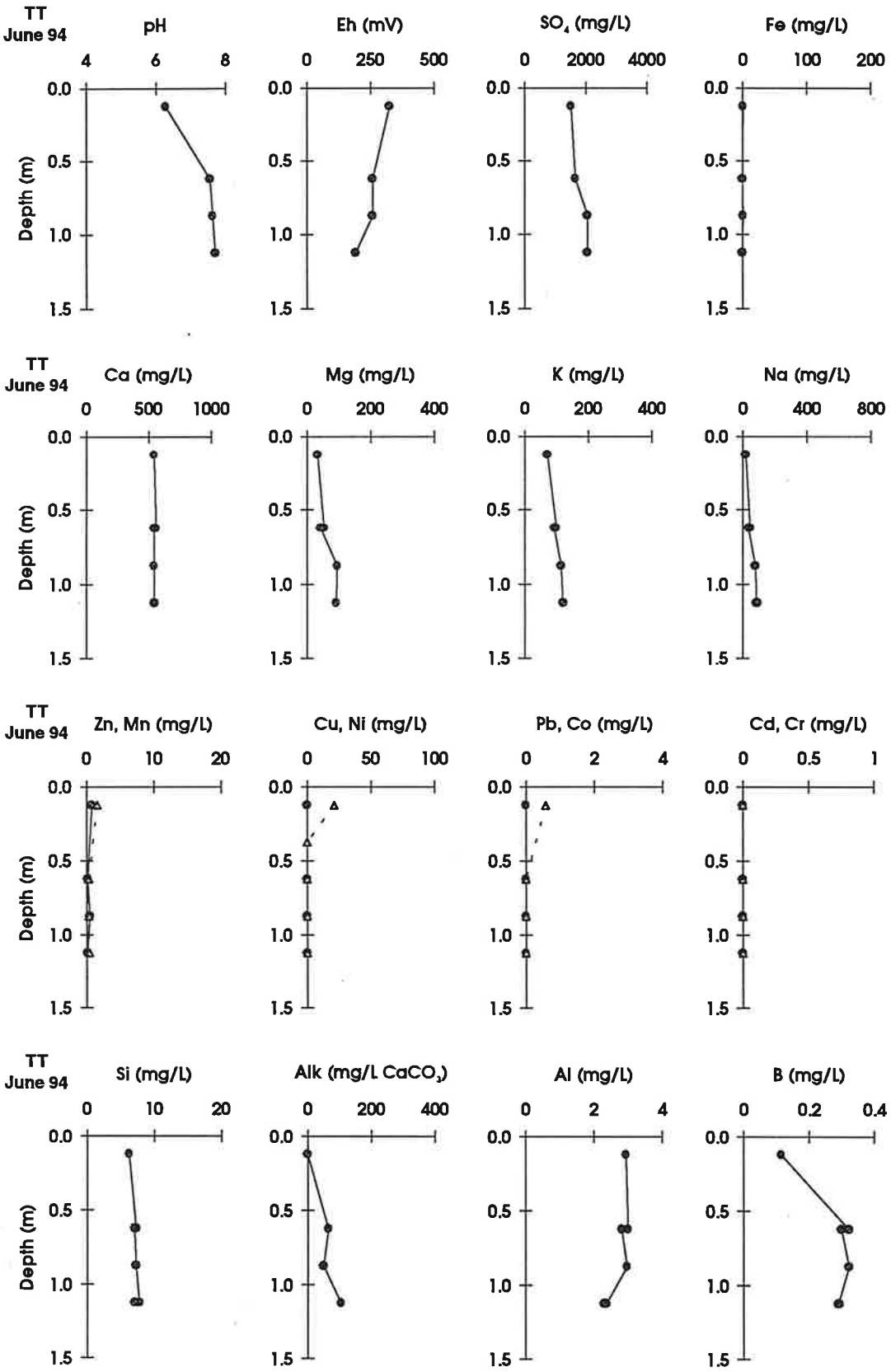

Figure 14. Pore-water geochemistry in the TT lysimeter, June, 1994. • = Zn, Cu, Pb, Cd; Δ = Mn, Ni, Co, Cr

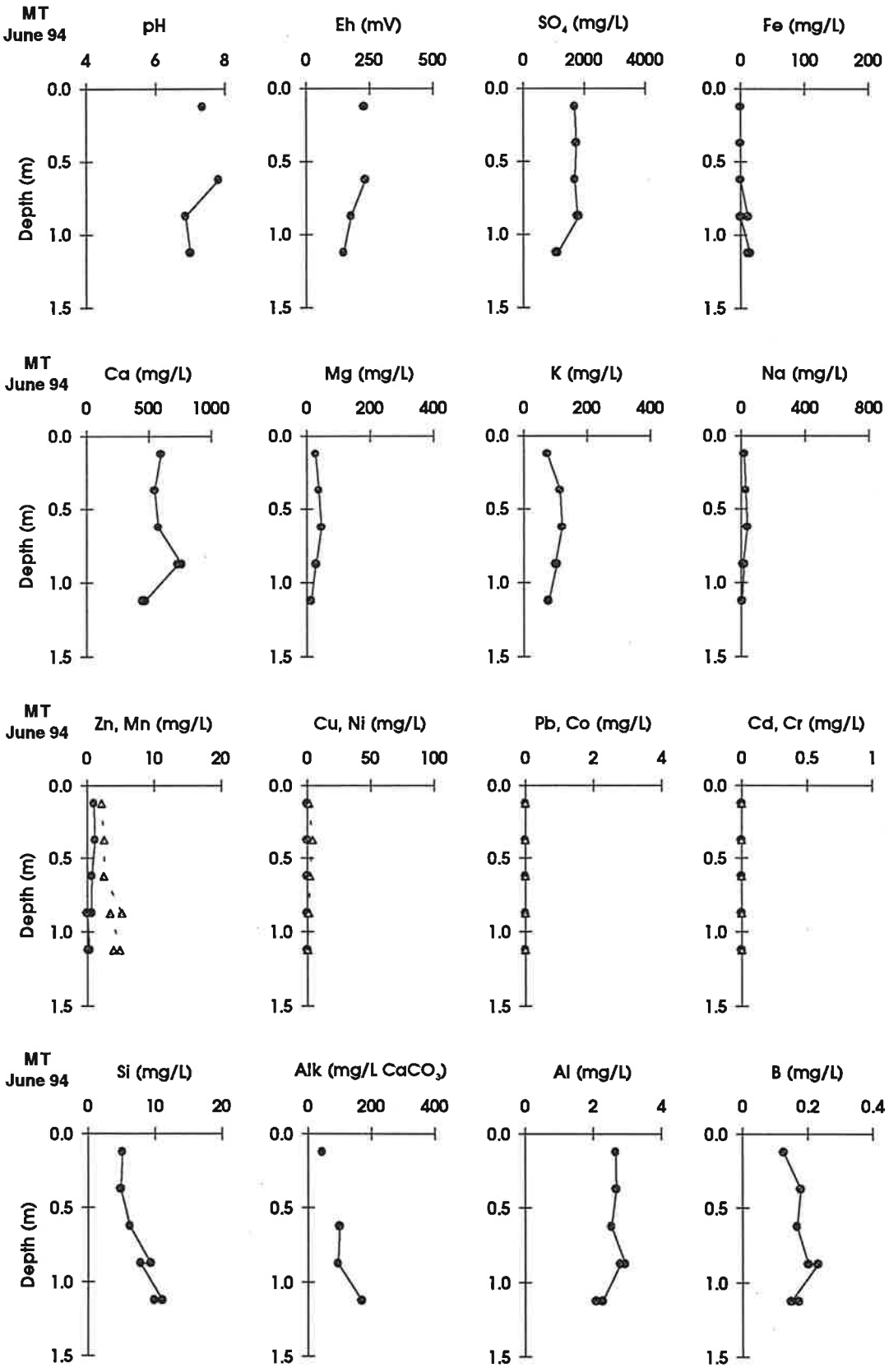

Figure 15. Pore-water geochemistry in the MT lysimeter, June, 1994. • = Zn, Cu, Pb, Cd; Δ = Mn, Ni, Co, Cr

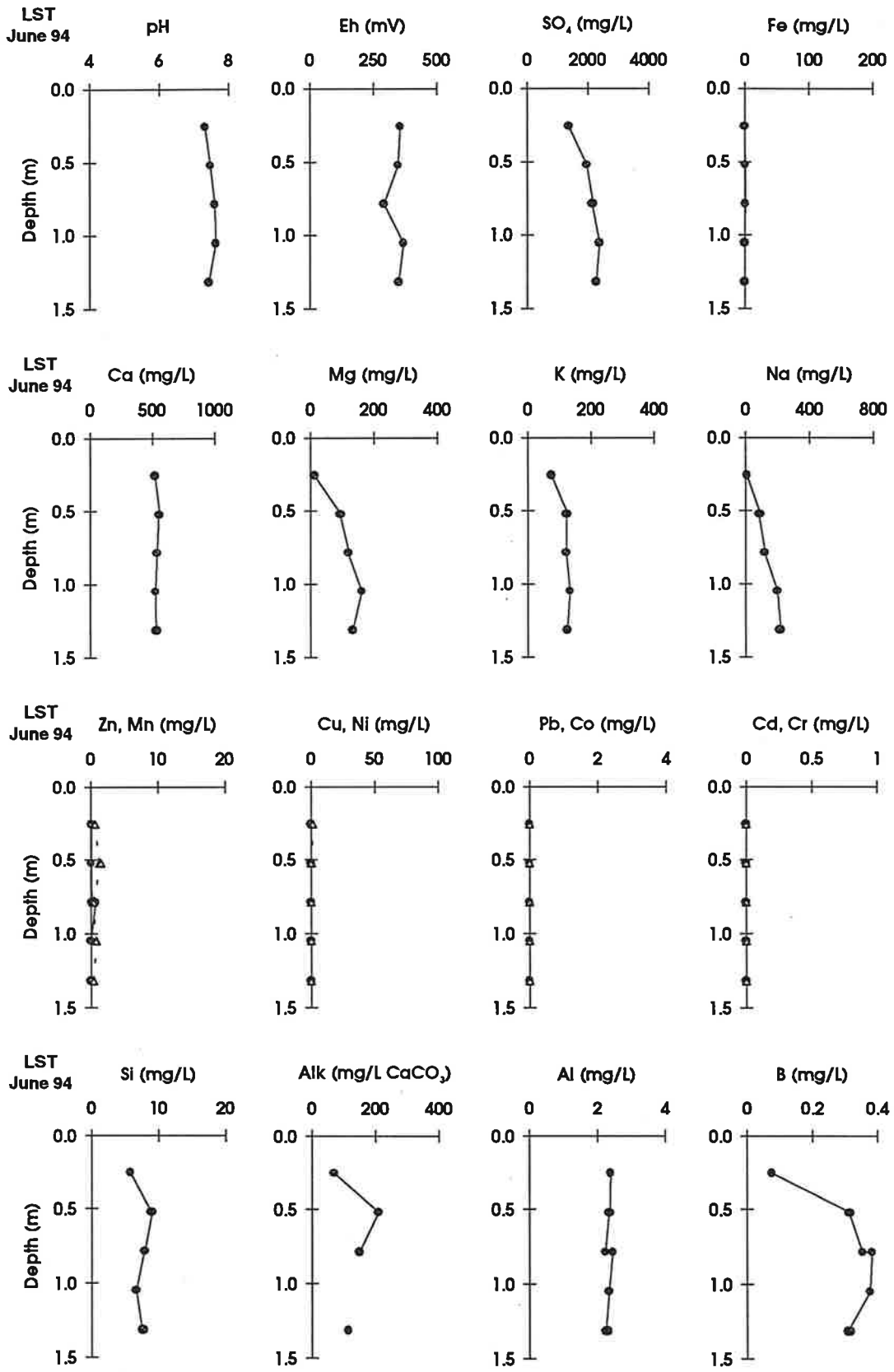

Figure 16. Pore-water geochemistry in the LST lysimeter, June, 1994. • = Zn, Cu, Pb, Cd; Δ = Mn, Ni, Co, Cr

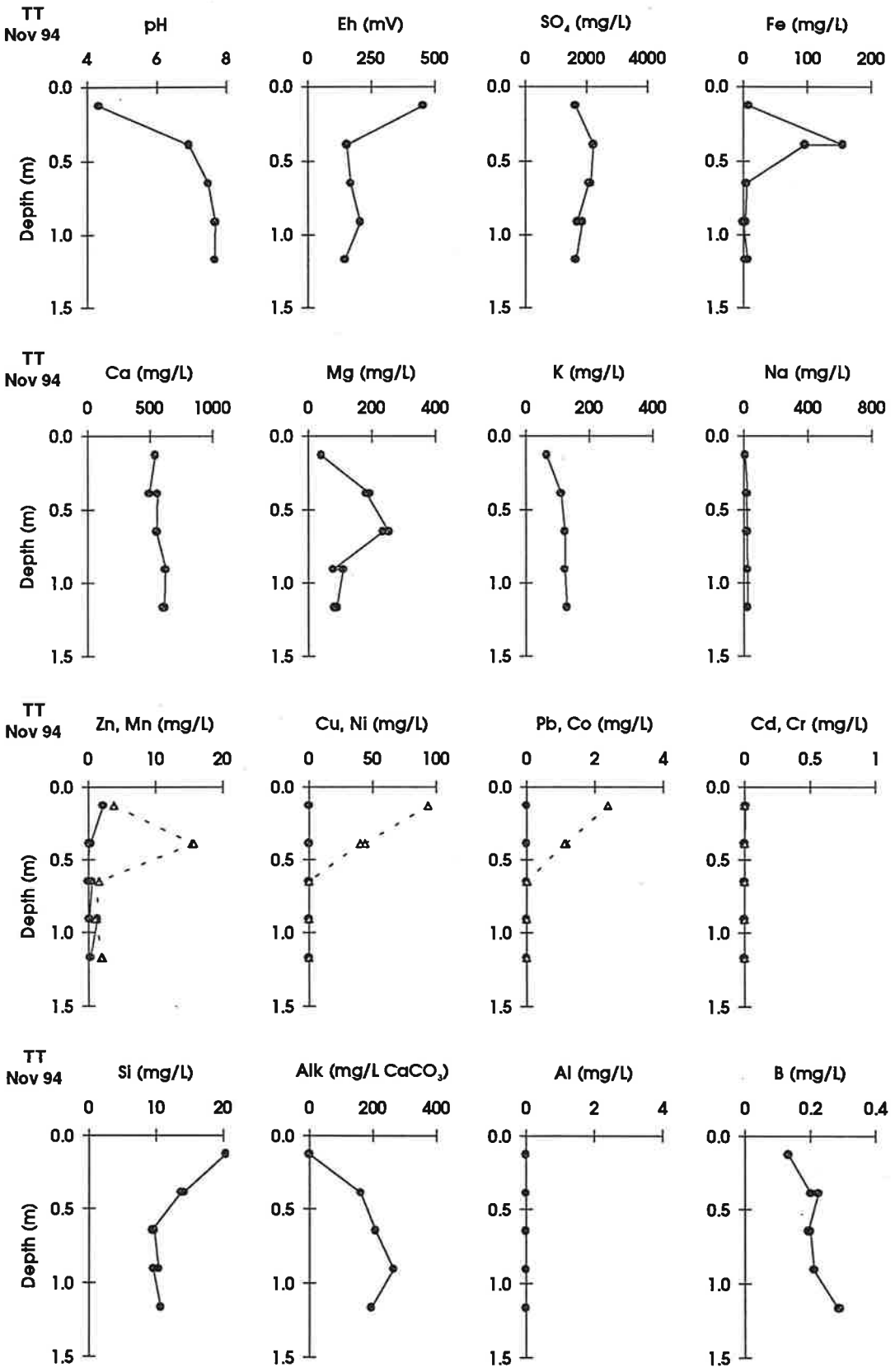

Figure 17. Pore-water geochemistry in the TT lysimeter, November, 1994. • = Zn, Cu, Pb, Cd; Δ = Mn, Ni, Co, Cr

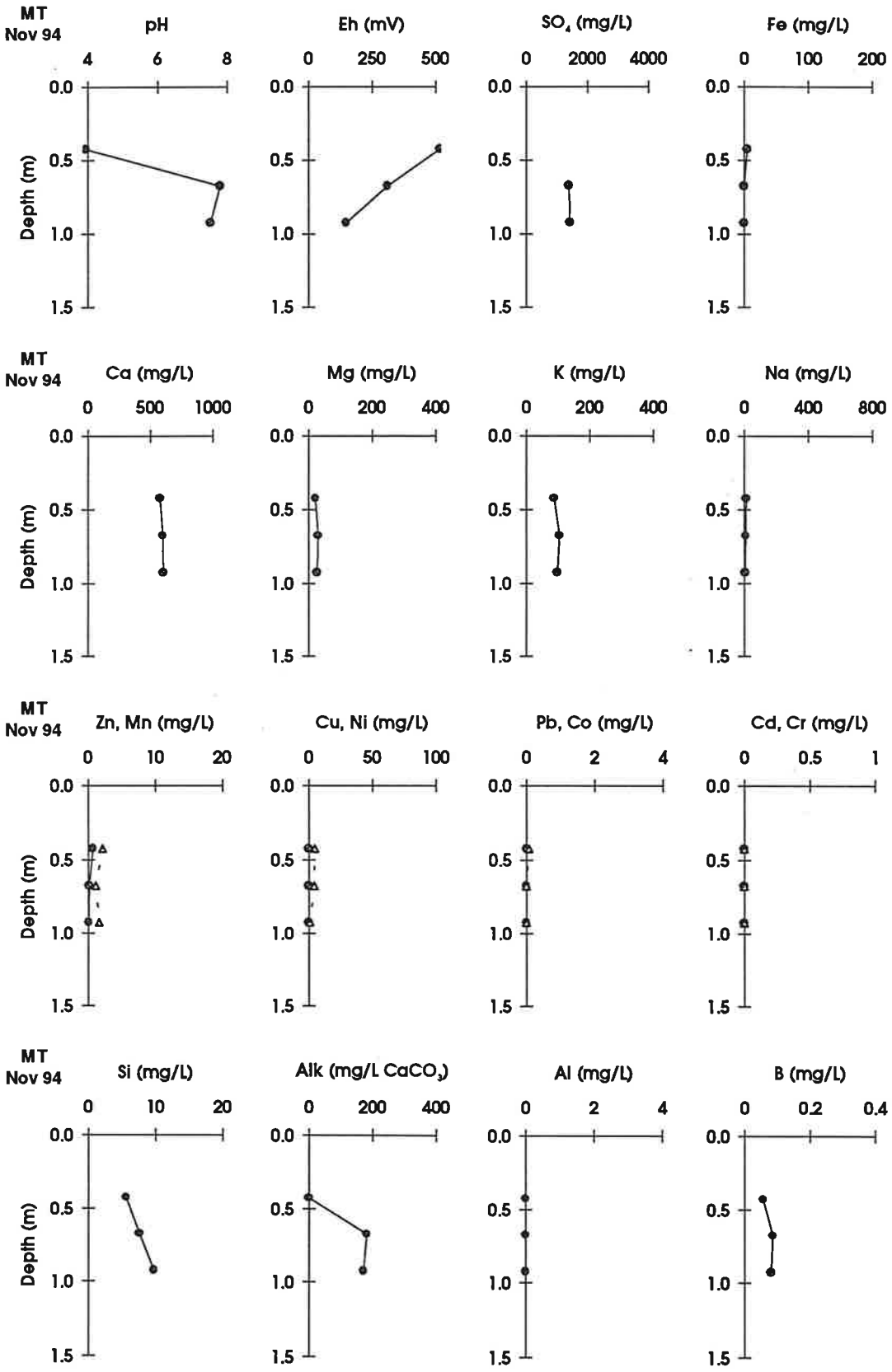

Figure 18. Pore-water geochemistry in the MT lysimeter, November, 1994. • = Zn, Cu, Pb, Cd; Δ = Mn, Ni, Co, Cr

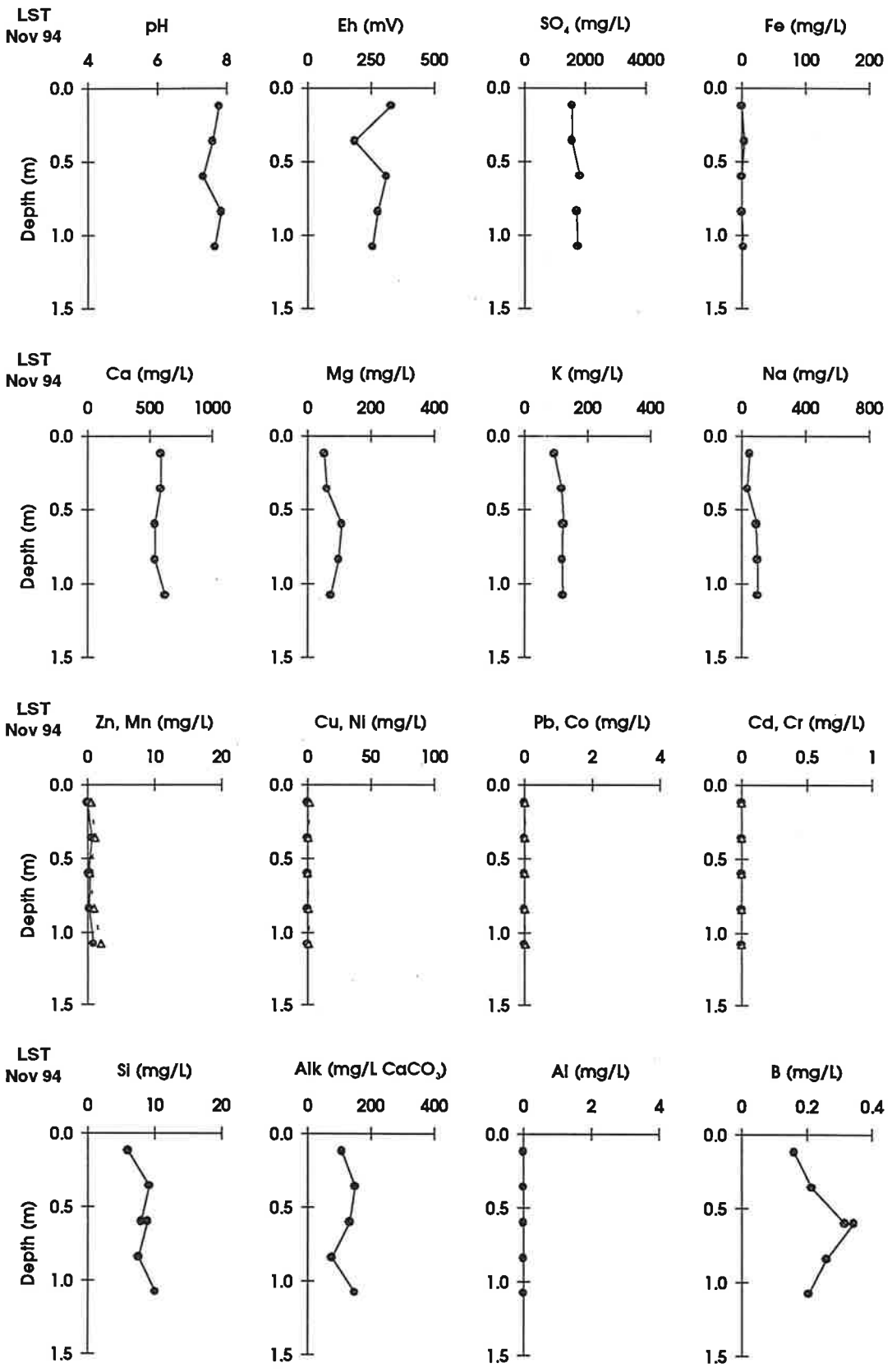

Figure 19. Pore-water geochemistry in the LST lysimeter, November, 1994. • = Zn, Cu, Pb, Cd; Δ = Mn, Ni, Co, Cr

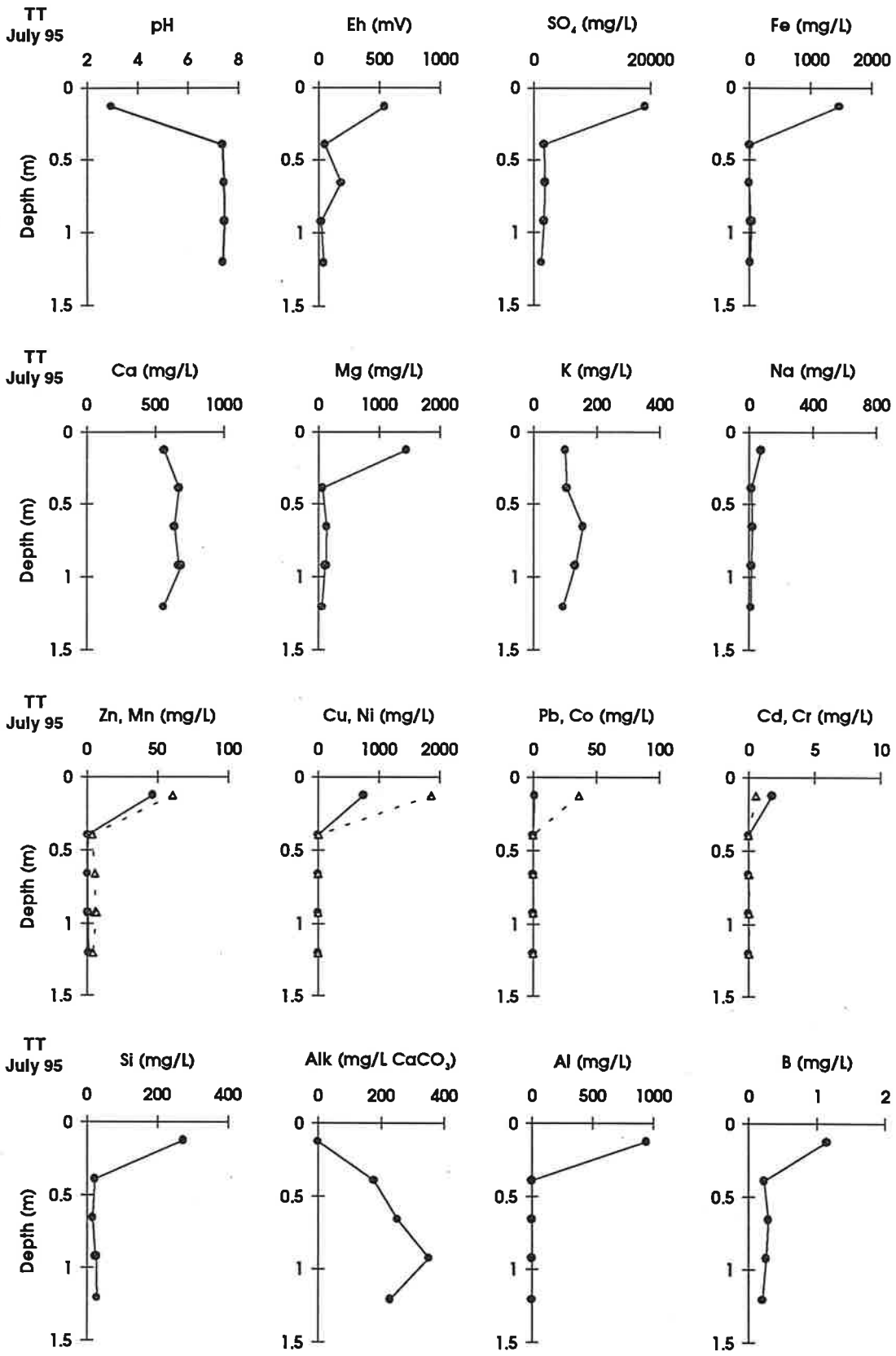

Figure 20. Pore-water geochemistry in the TT lysimeter, July, 1995. • = Zn, Cu, Pb, Cd; Δ = Mn, Ni, Co, Cr

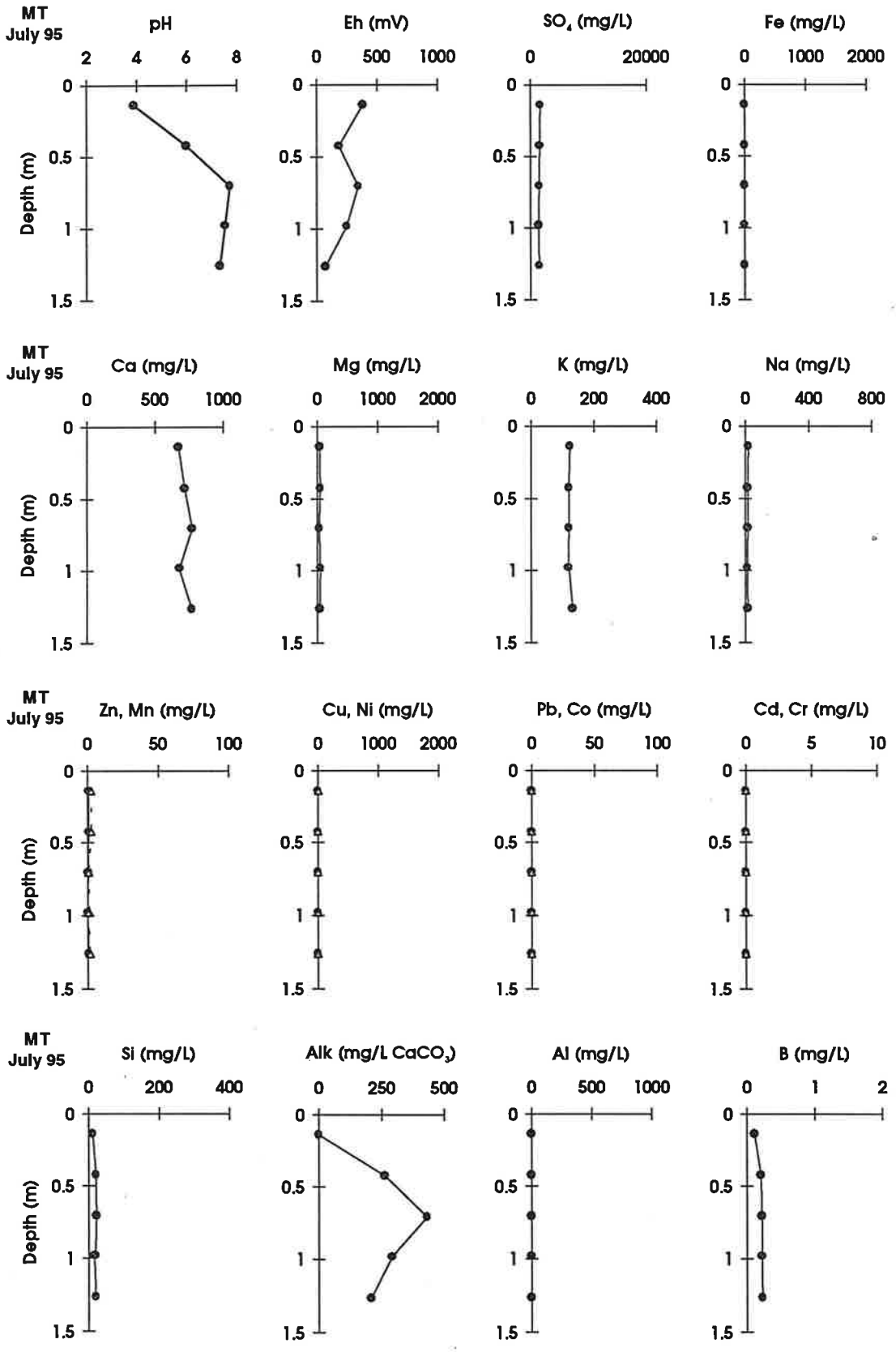

Figure 21. Pore-water geochemistry in the MT lysimeter, July, 1995. • = Zn, Cu, Pb, Cd; Δ = Mn, Ni, Co, Cr

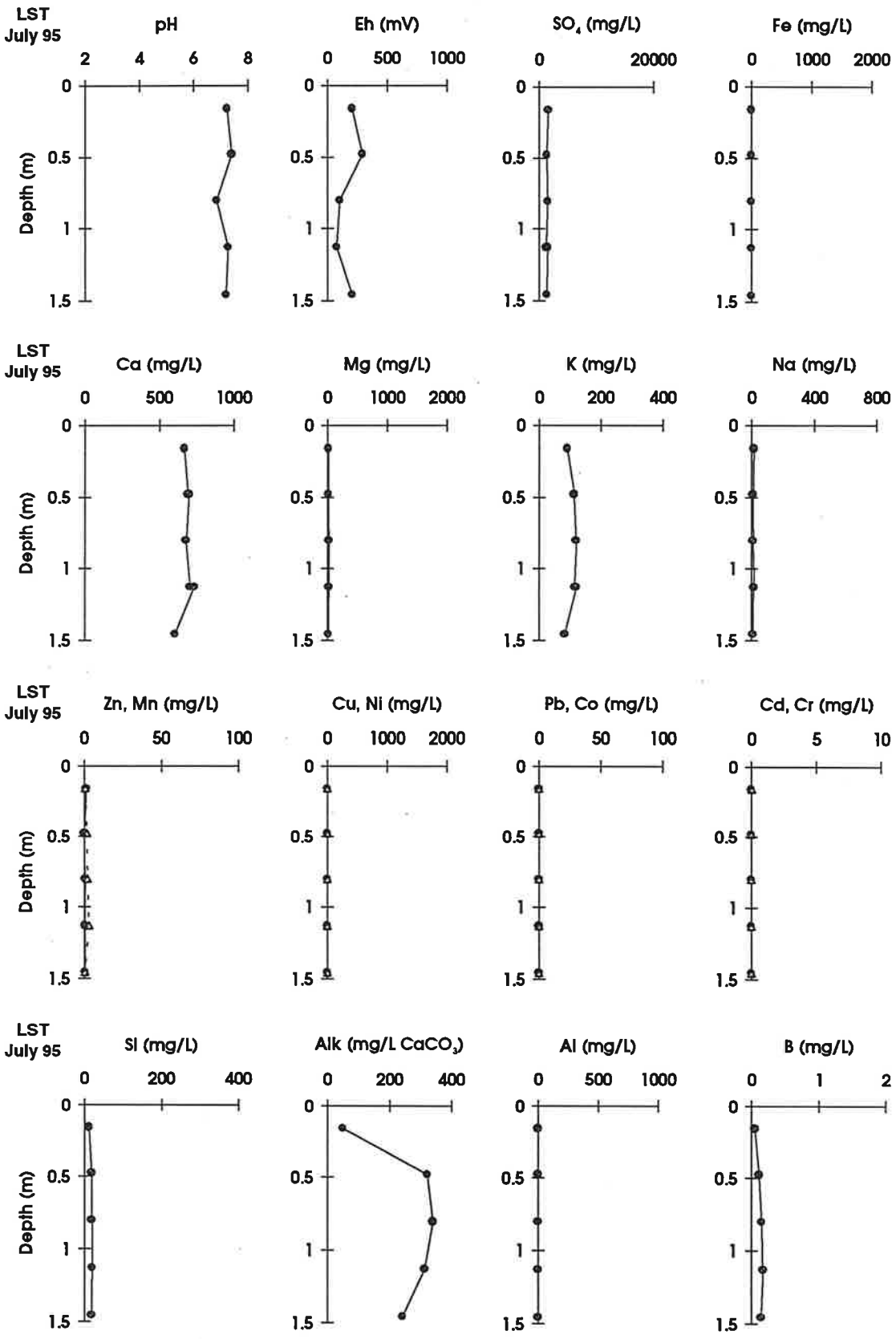

Figure 22. Pore-water geochemistry in the LST lysimeter, July, 1995. • = Zn, Cu, Pb, Cd; Δ = Mn, Ni, Co, Cr

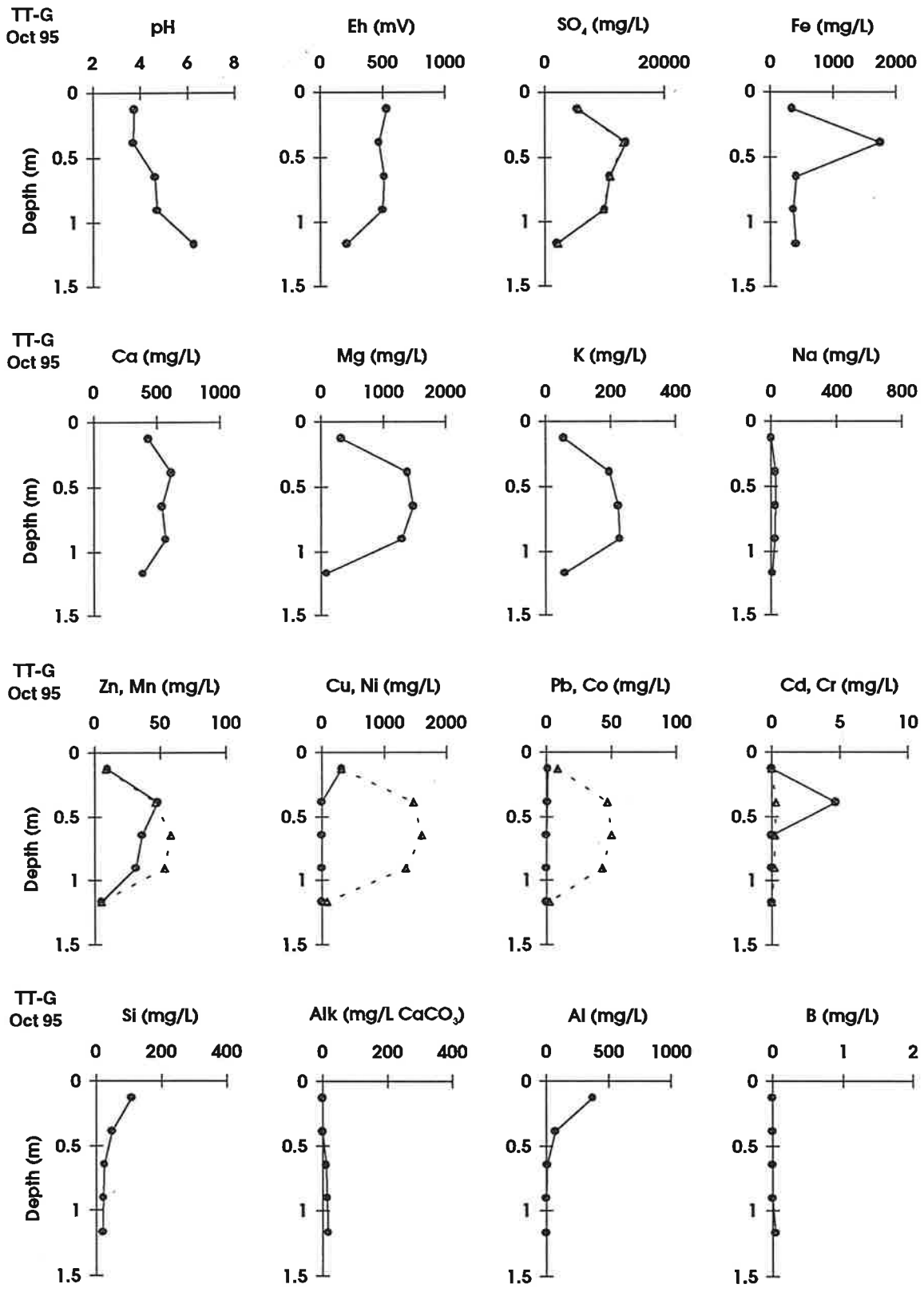

Figure 23. Pore-water geochemistry in the TT lysimeter, October, 1995. Location G is identified in Figure 1. • = Zn, Cu, Pb, Cd; Δ = Mn, Ni, Co, Cr

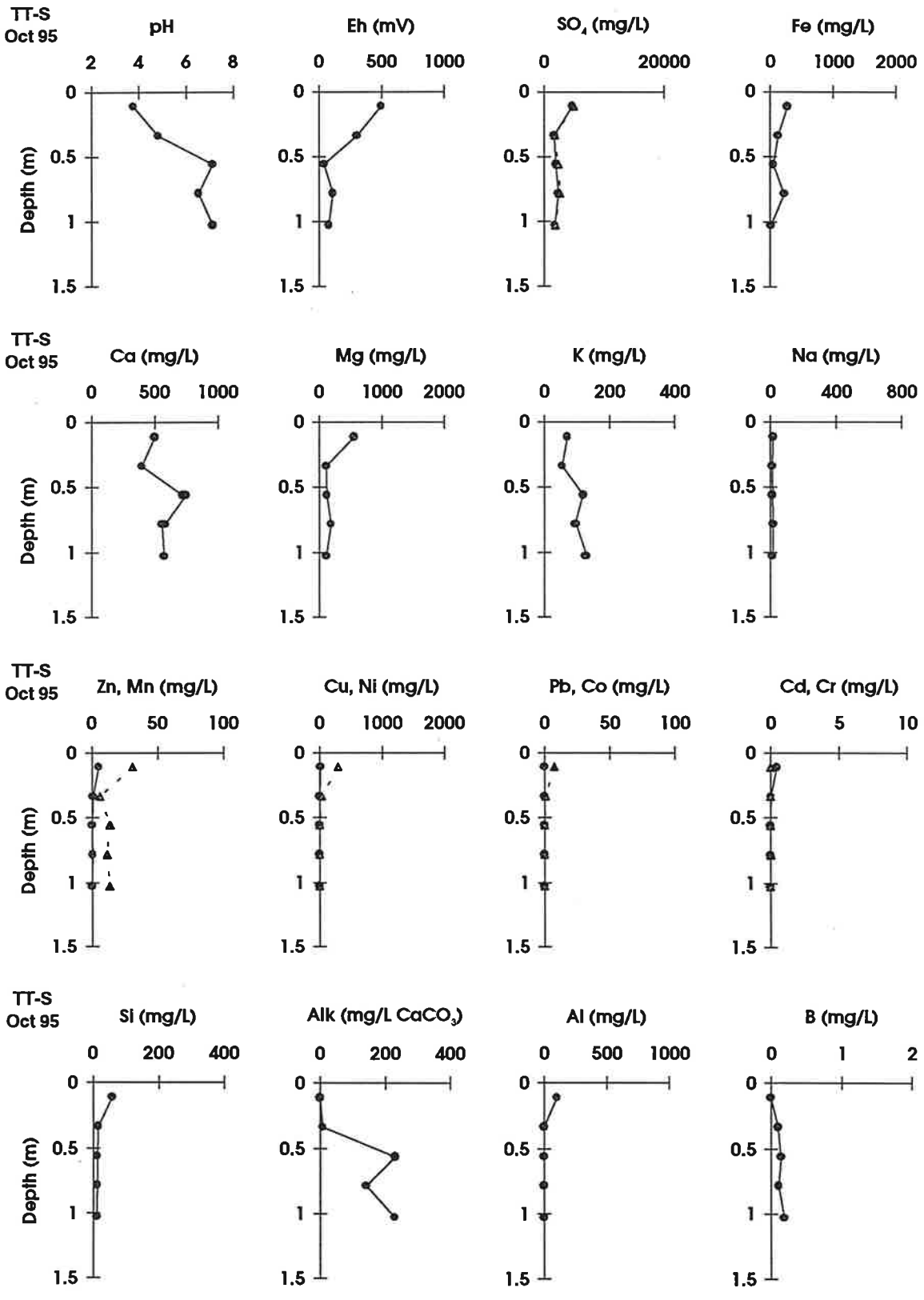

Figure 24. Pore-water geochemistry in the TT lysimeter, October, 1995. Location S is identified in Figure 1. • = Zn, Cu, Pb, Cd; Δ = Mn, Ni, Co, Cr

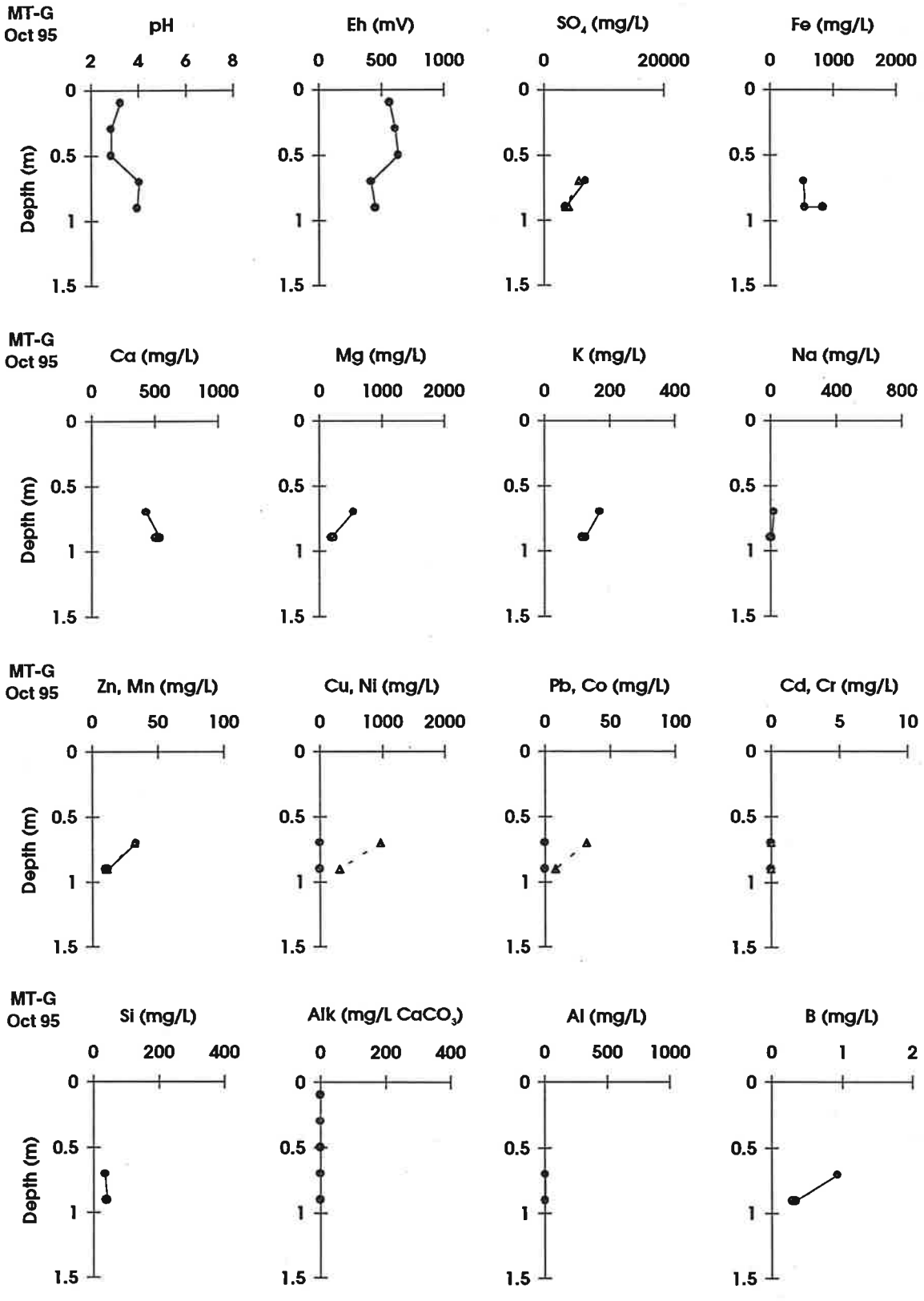

Figure 25. Pore-water geochemistry in the MT lysimeter, October, 1995. Location G is identified in Figure 1. • = Zn, Cu, Pb, Cd; Δ = Mn, Ni, Co, Cr

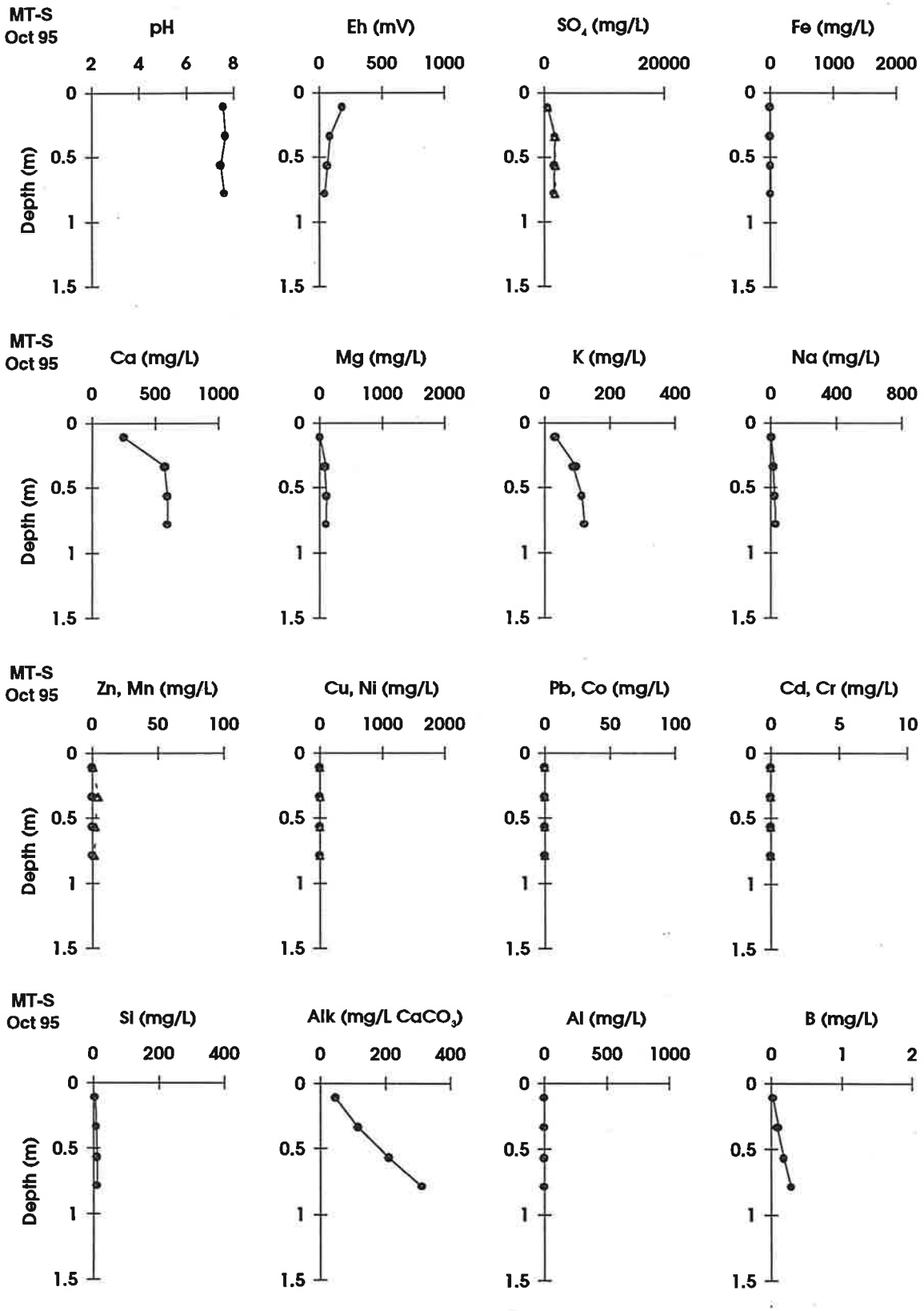

Figure 26. Pore-water geochemistry in the MT lysimeter, October, 1995. Location S is identified in Figure 1. • = Zn, Cu, Pb, Cd; Δ = Mn, Ni, Co, Cr

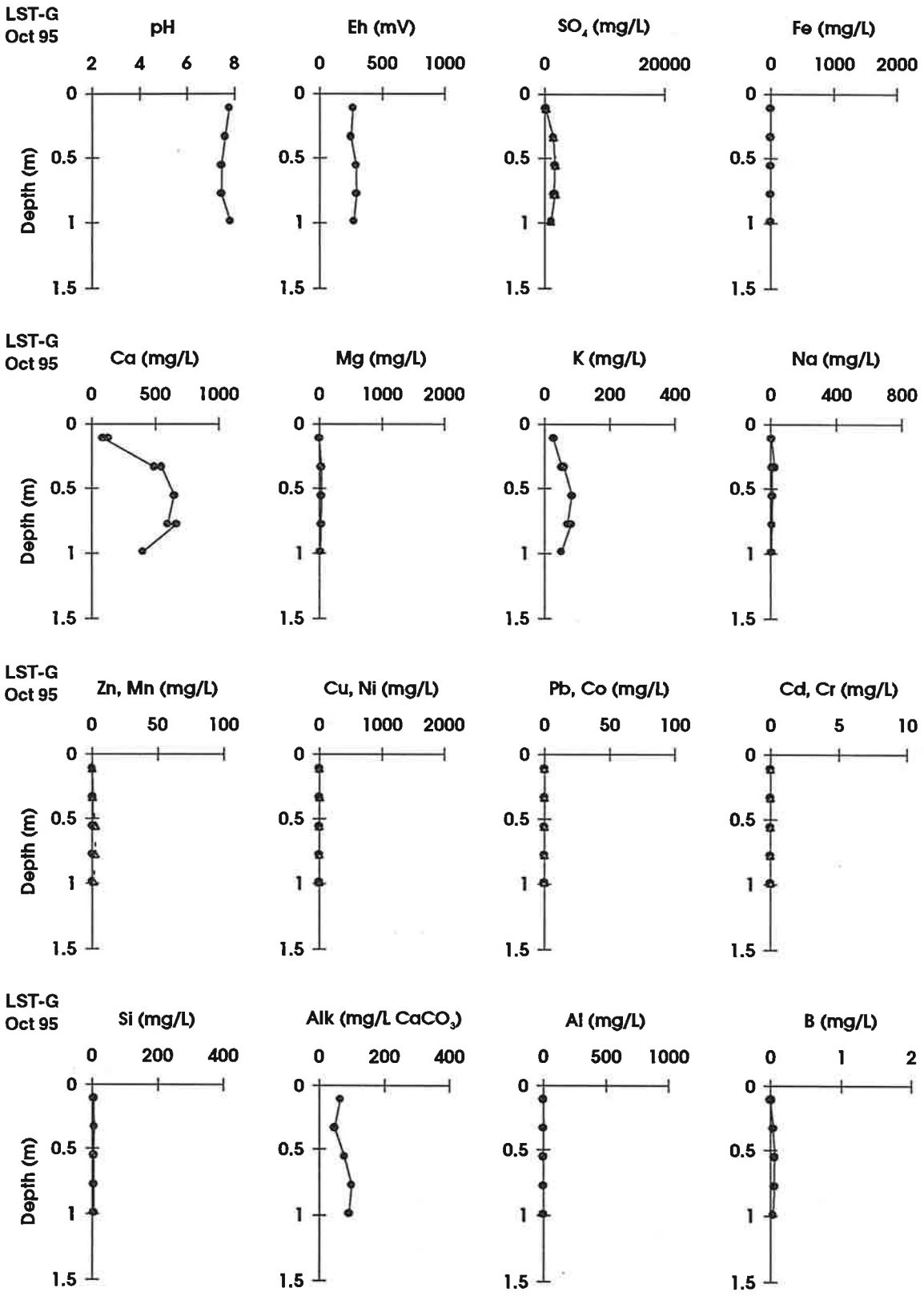

Figure 27. Pore-water geochemistry in the LST lysimeter, October, 1995. Location G is identified in Figure 1. • = Zn, Cu, Pb, Cd; Δ = Mn, Ni, Co, Cr

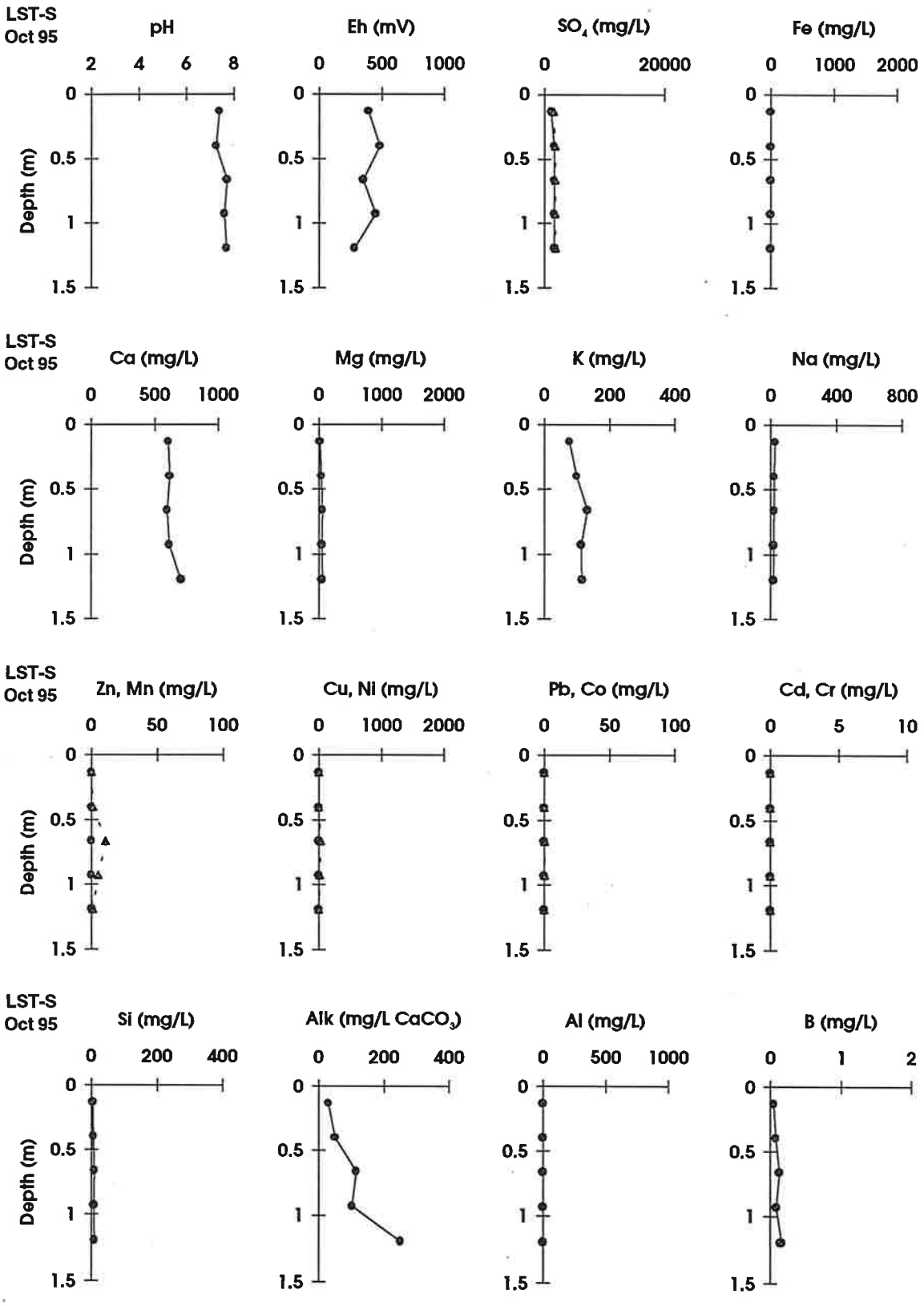

Figure 28. Pore-water geochemistry in the LST lysimeter, October, 1995. Location S is identified in Figure 1.
• = Zn, Cu, Pb, Cd; Δ = Mn, Ni, Co, Cr

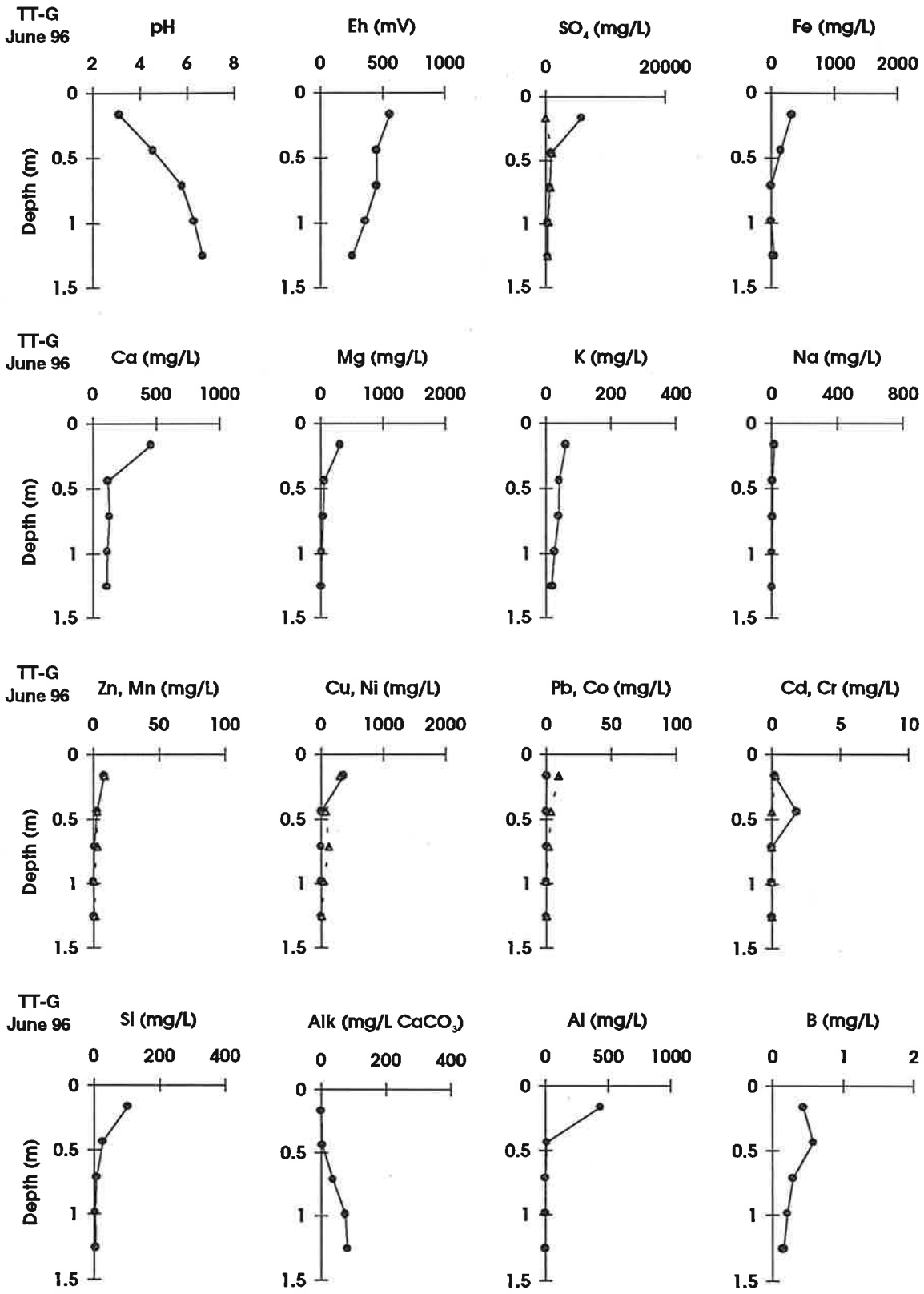

Figure 29. Pore-water geochemistry in the TT lysimeter, June, 1996. Location G is identified in Figure 1. • = Zn, Cu, Pb, Cd; Δ = Mn, Ni, Co, Cr

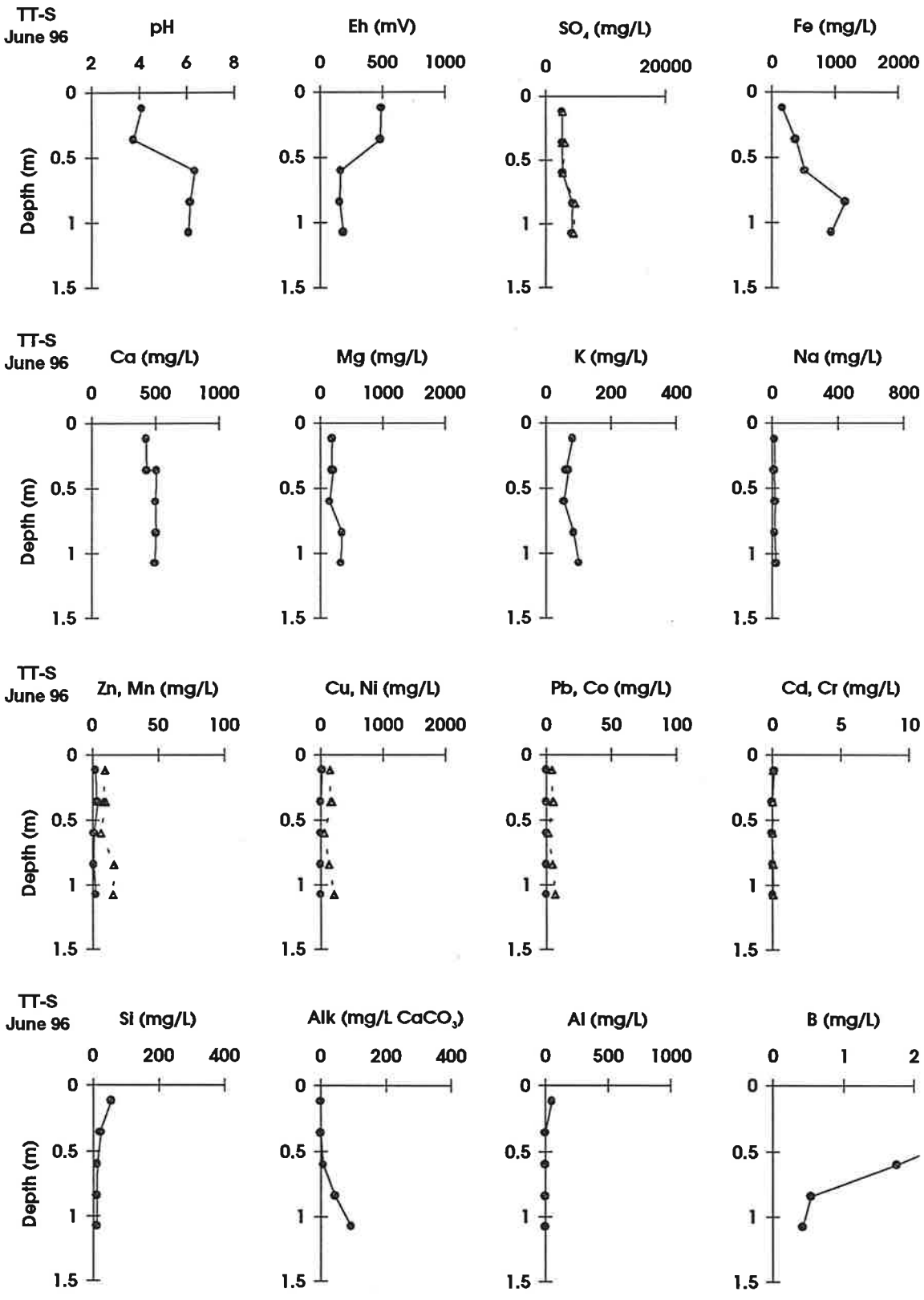

Figure 30. Pore-water geochemistry in the TT lysimeter, June, 1996. Location S is identified in Figure 1. • = Zn, Cu, Pb, Cd; Δ = Mn, Ni, Co, Cr

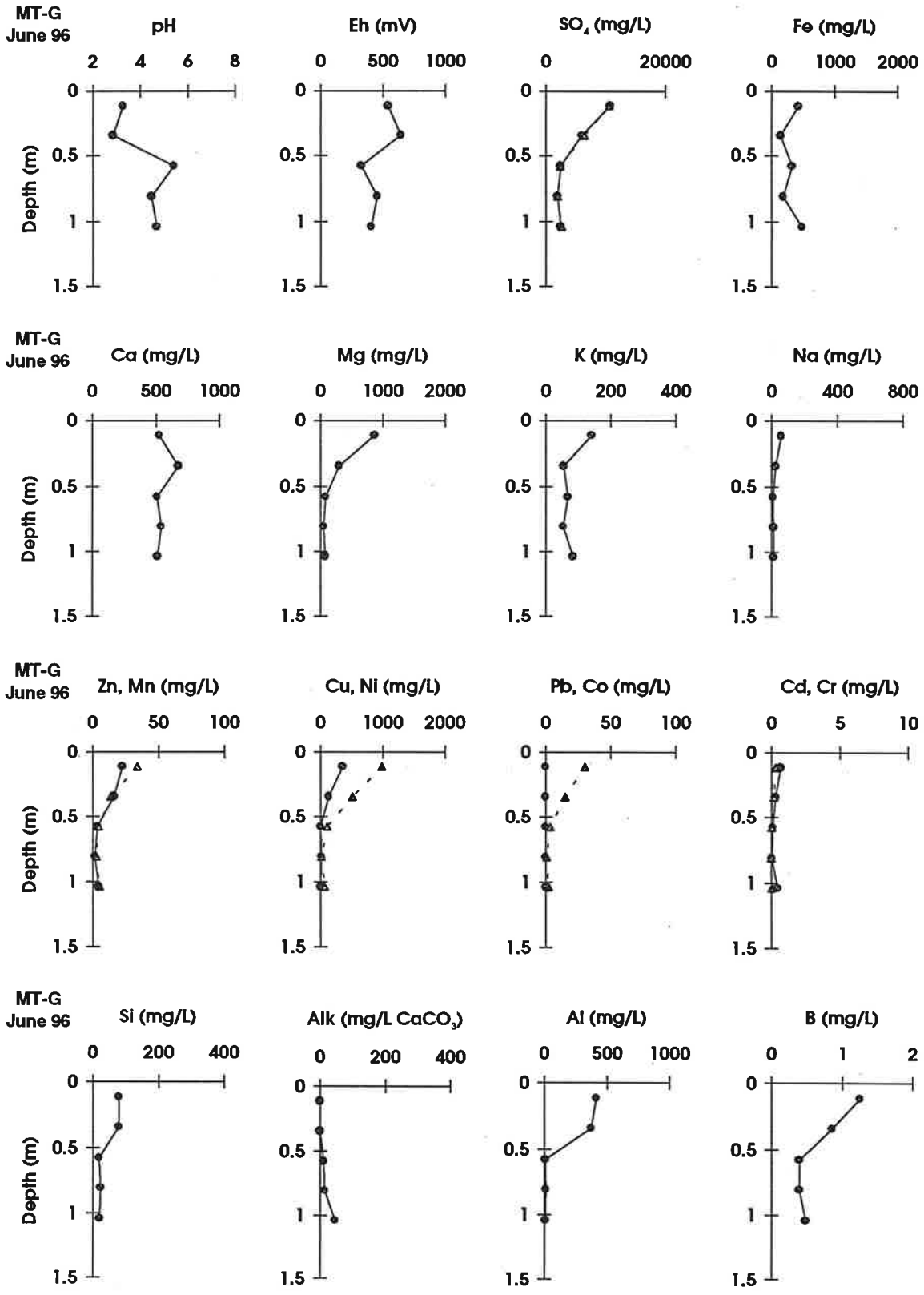

Figure 31. Pore-water geochemistry in the MT lysimeter, June, 1996. Location G is identified in Figure 1. • = Zn, Cu, Pb, Cd; Δ = Mn, Ni, Co, Cr

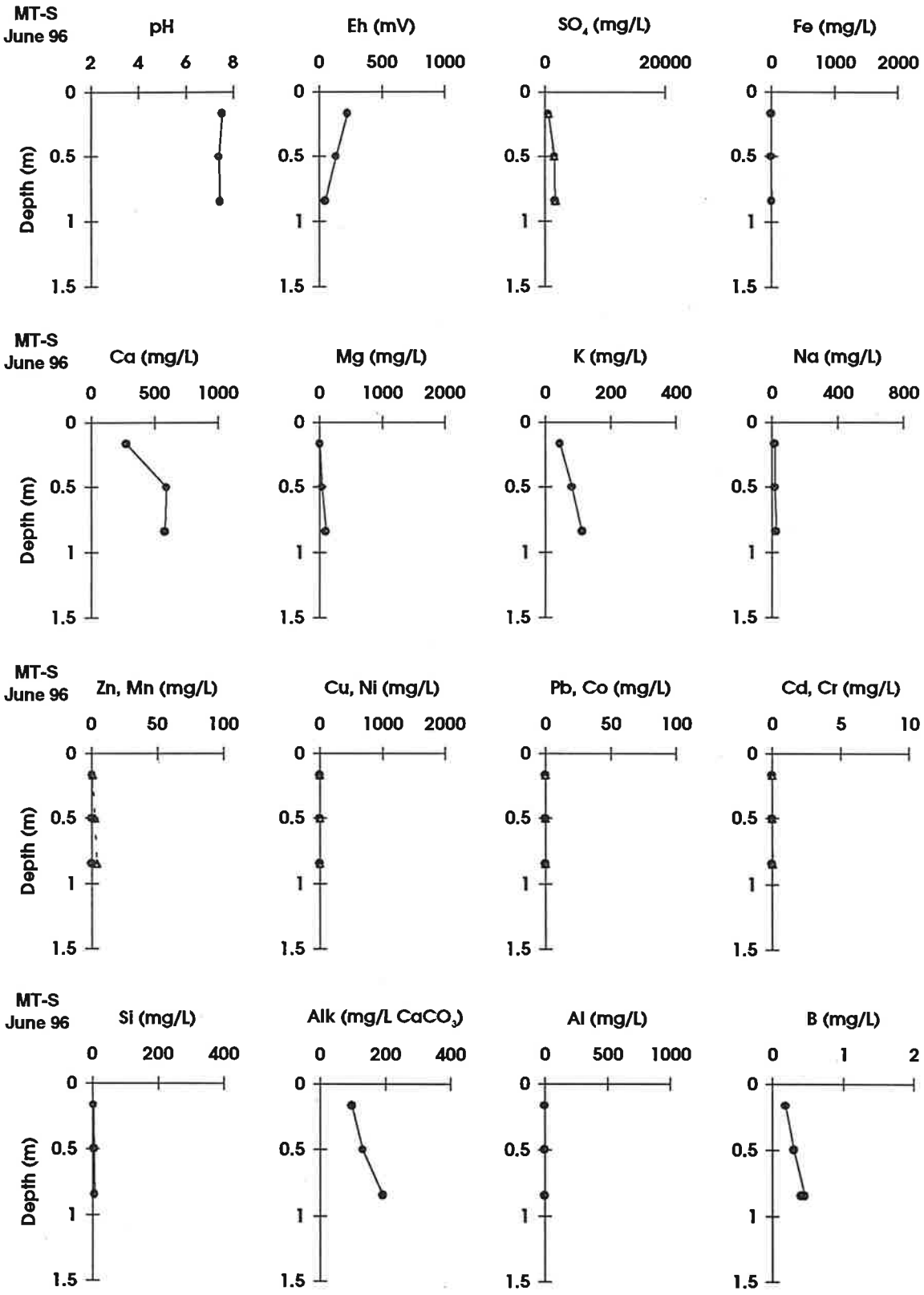

Figure 32. Pore-water geochemistry in the MT lysimeter, June, 1996. Location S is identified in Figure 1. • = Zn, Cu, Pb, Cd; Δ = Mn, Ni, Co, Cr

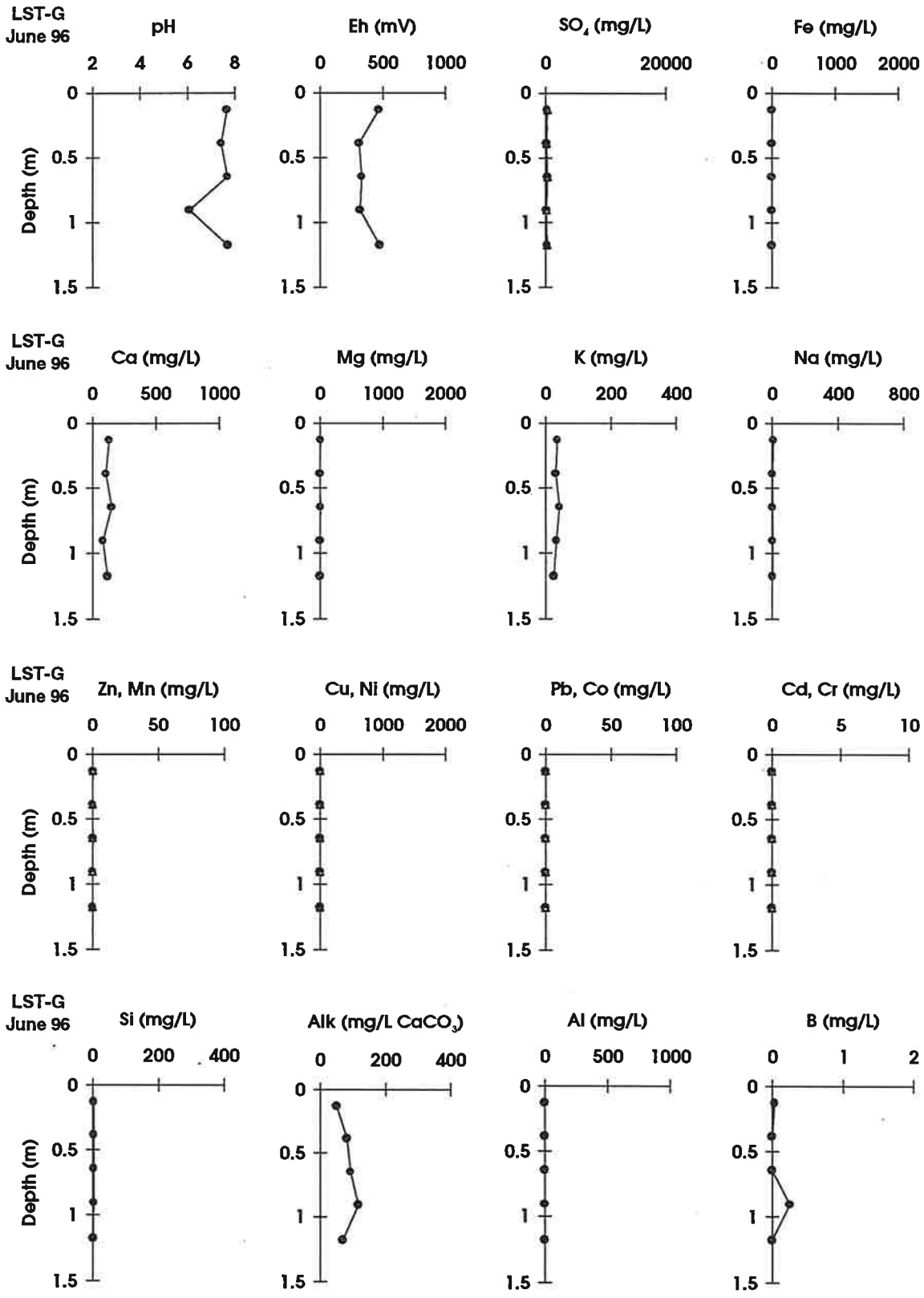

Figure 33. Pore-water geochemistry in the LST lysimeter, June, 1996. Location G is identified in Figure 1. • = Zn, Cu, Pb, Cd; Δ = Mn, Ni, Co, Cr

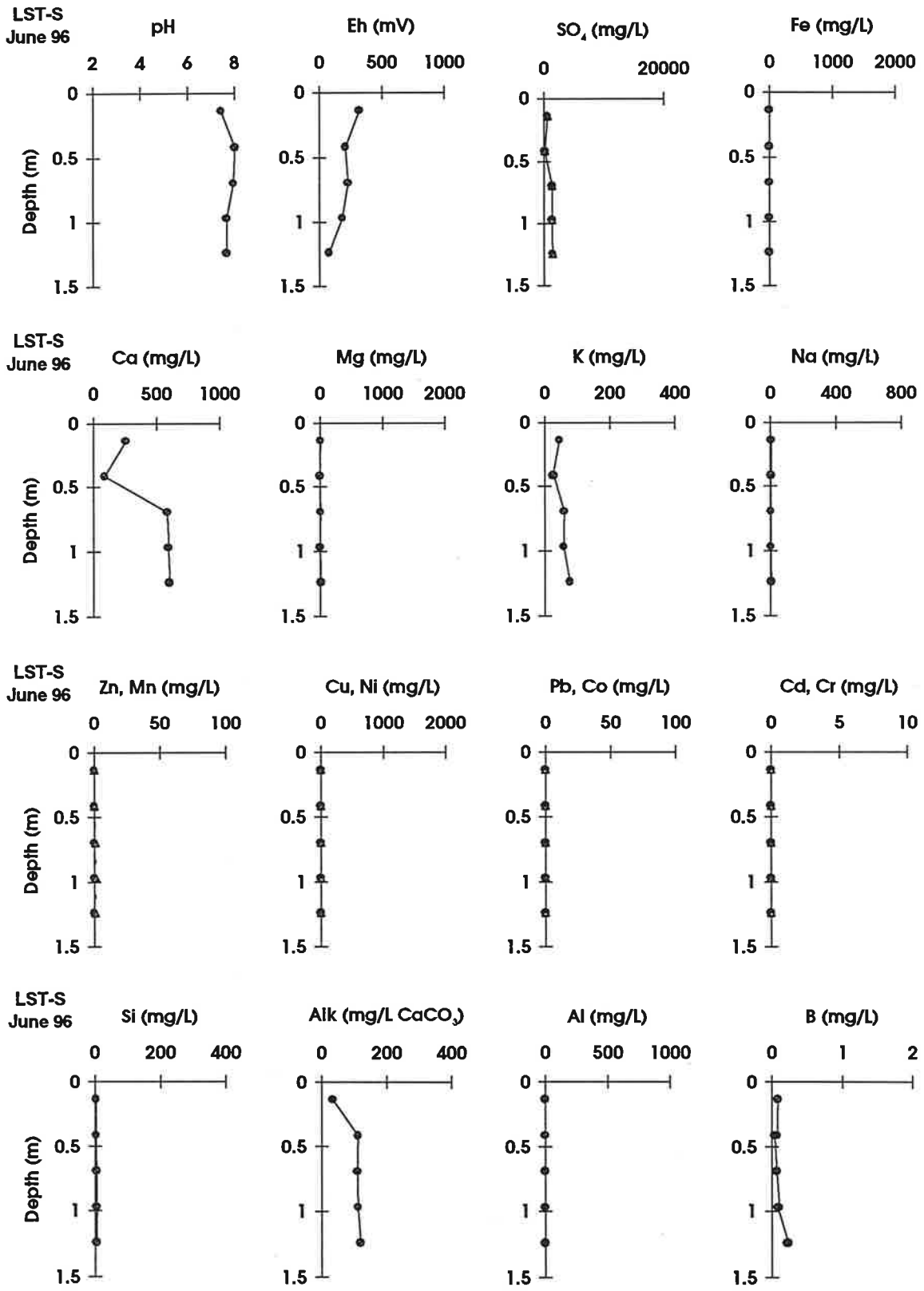

Figure 34. Pore-water geochemistry in the LST lysimeter, June, 1996. Location S is identified in Figure 1. • = Zn, Cu, Pb, Cd; Δ = Mn, Ni, Co, Cr

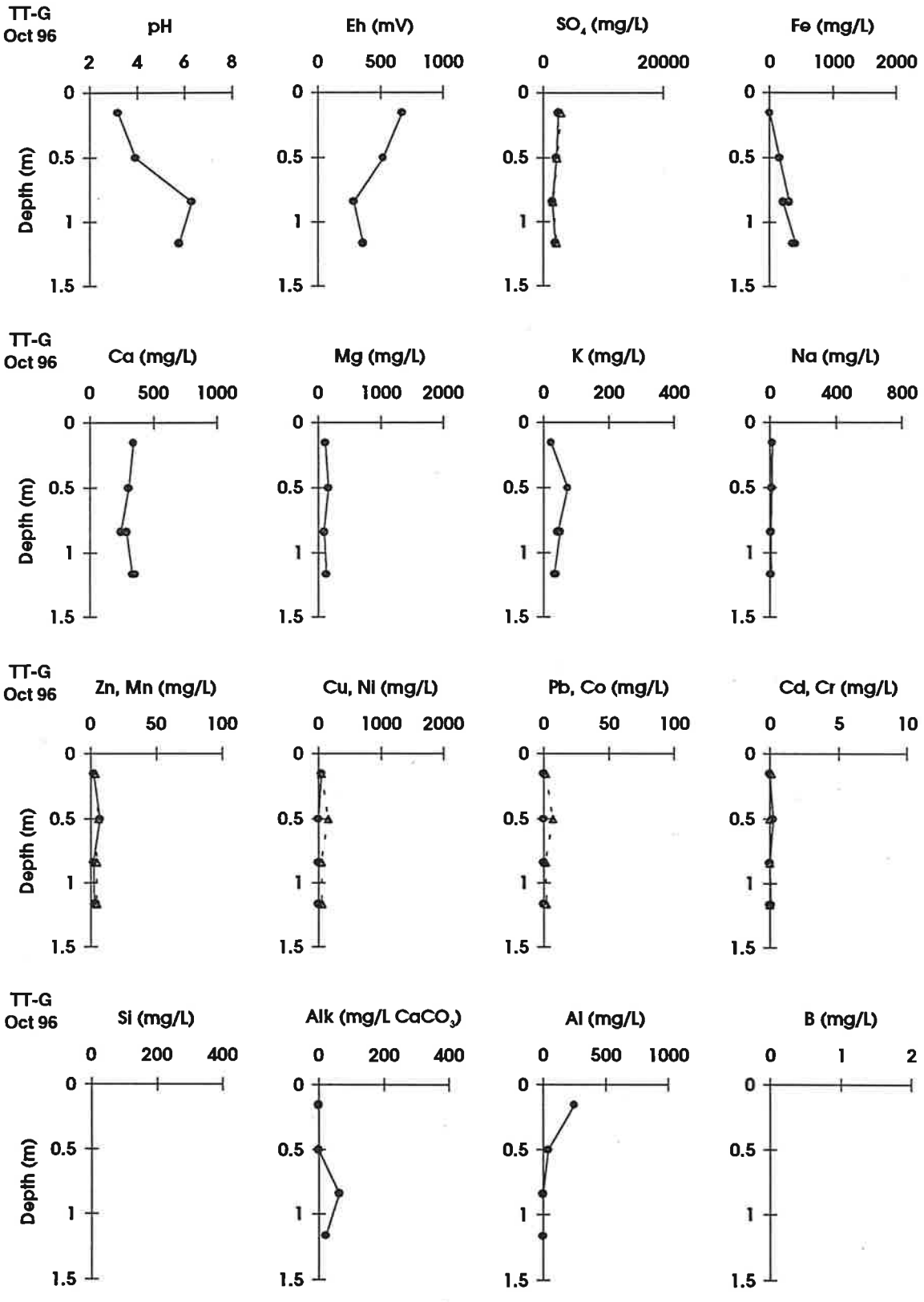

Figure 35. Pore-water geochemistry in the TT lysimeter, October, 1996. Location G is identified in Figure 1. • = Zn, Cu, Pb, Cd; Δ = Mn, Ni, Co, Cr

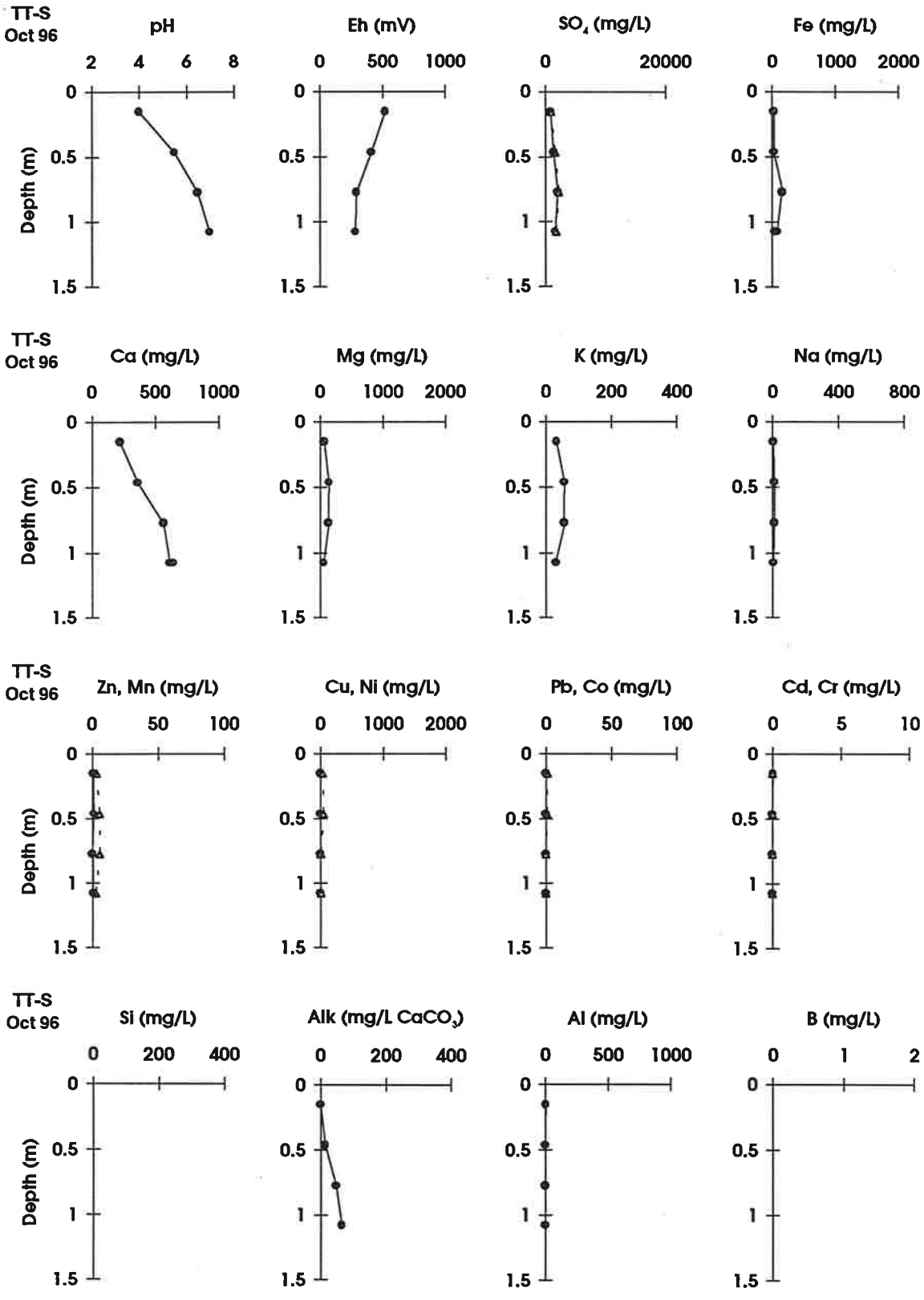

Figure 36. Pore-water geochemistry in the TT lysimeter, October, 1996. Location S is identified in Figure 1. • = Zn, Cu, Pb, Cd; Δ = Mn, Ni, Co, Cr

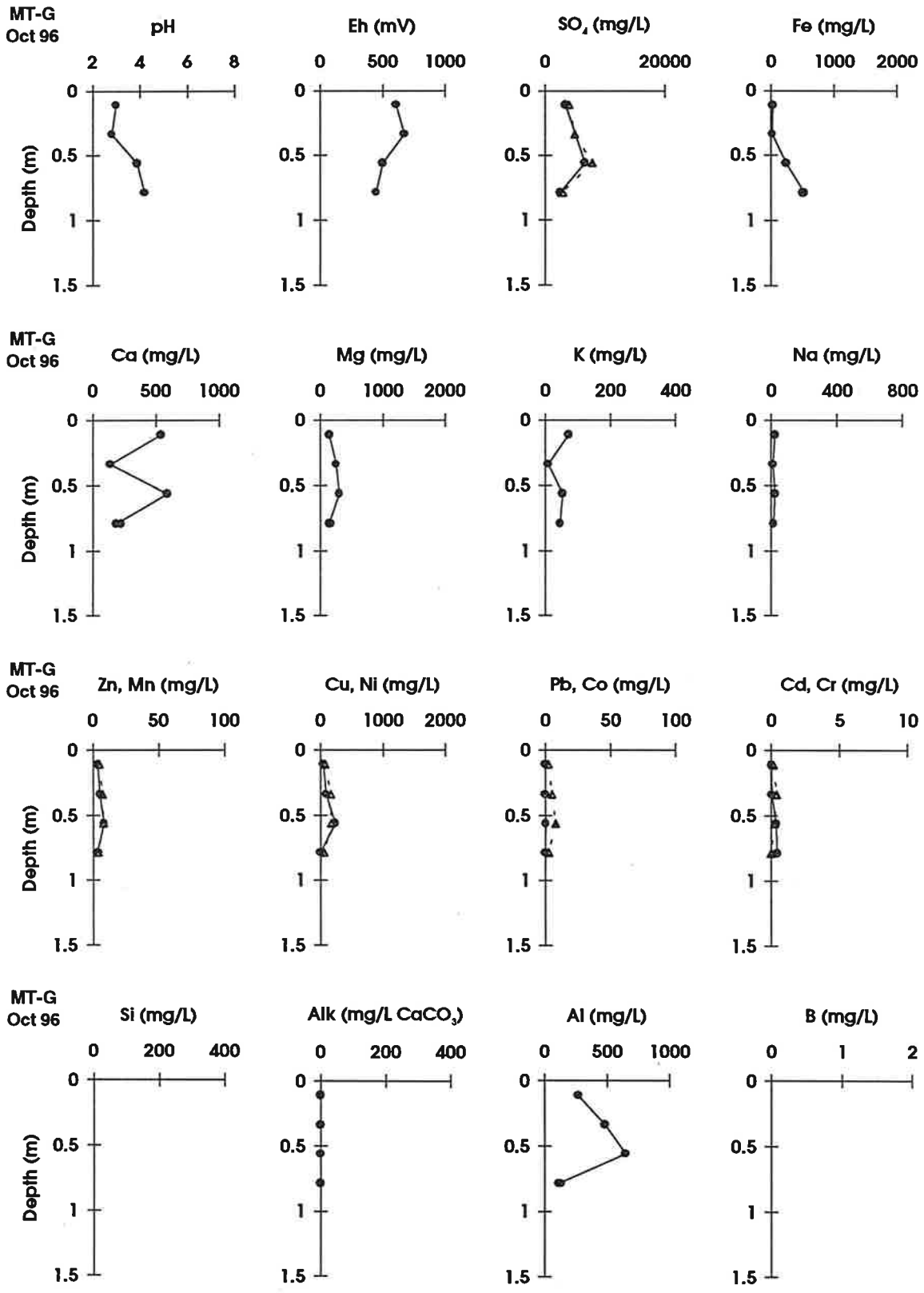

Figure 37. Pore-water geochemistry in the MT lysimeter, October, 1996. Location G is identified in Figure 1. • = Zn, Cu, Pb, Cd; Δ = Mn, Ni, Co, Cr

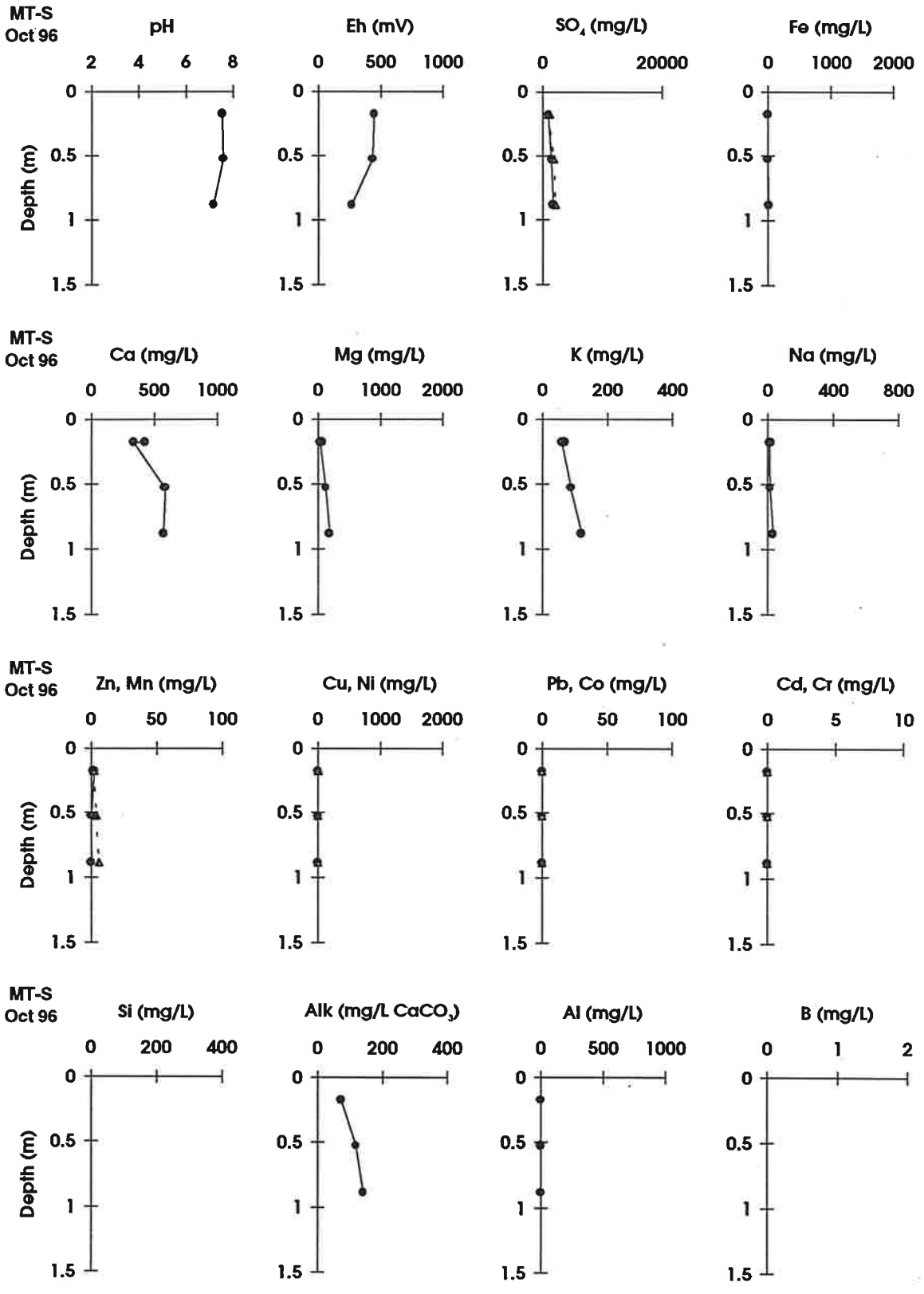

Figure 38. Pore-water geochemistry in the MT lysimeter, October, 1996. Location S is identified in Figure 1. • = Zn, Cu, Pb, Cd; Δ = Mn, Ni, Co, Cr

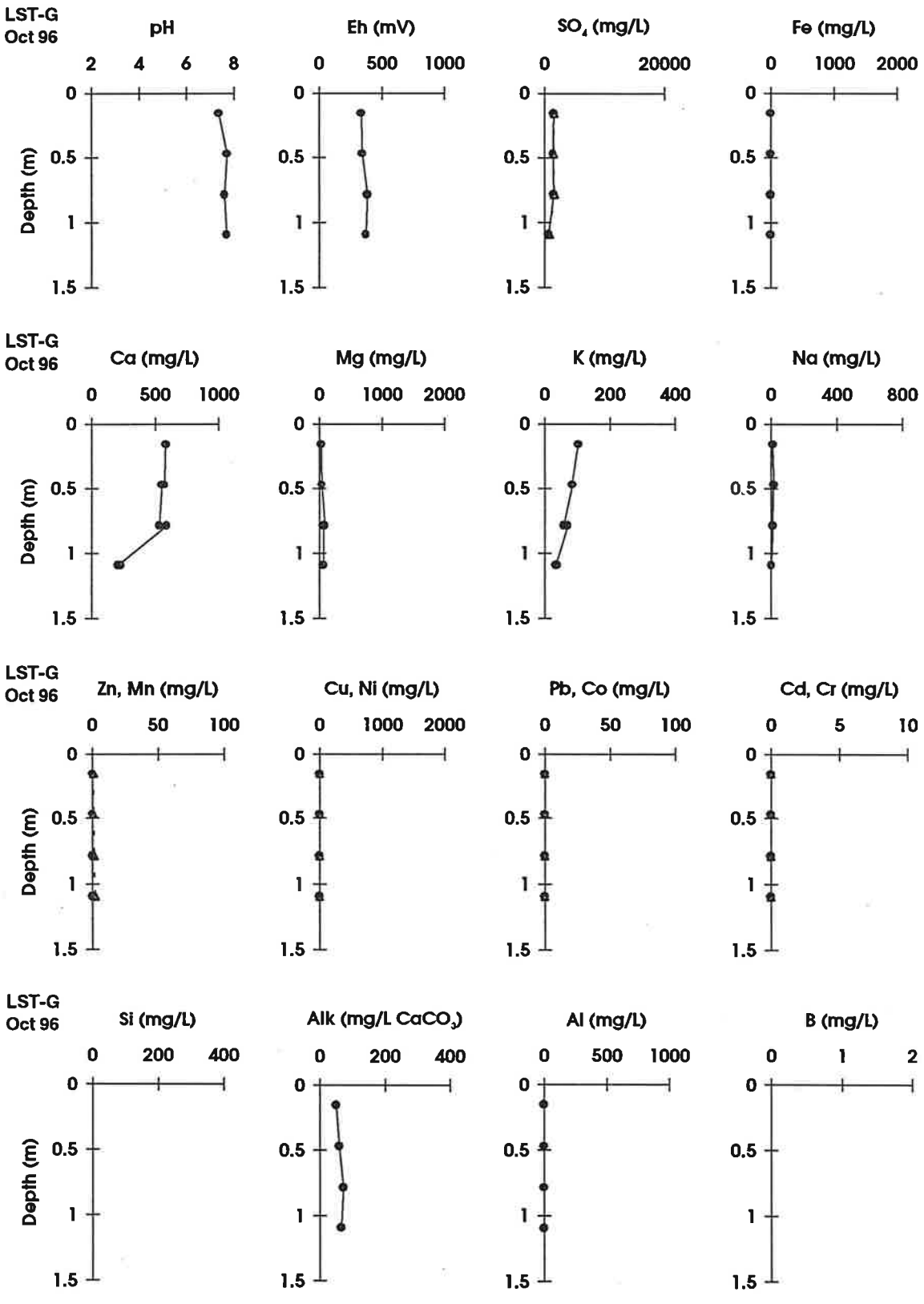

Figure 39. Pore-water geochemistry in the LST lysimeter, October, 1996. Location G is identified in Figure 1. • = Zn, Cu, Pb, Cd; Δ = Mn, Ni, Co, Cr

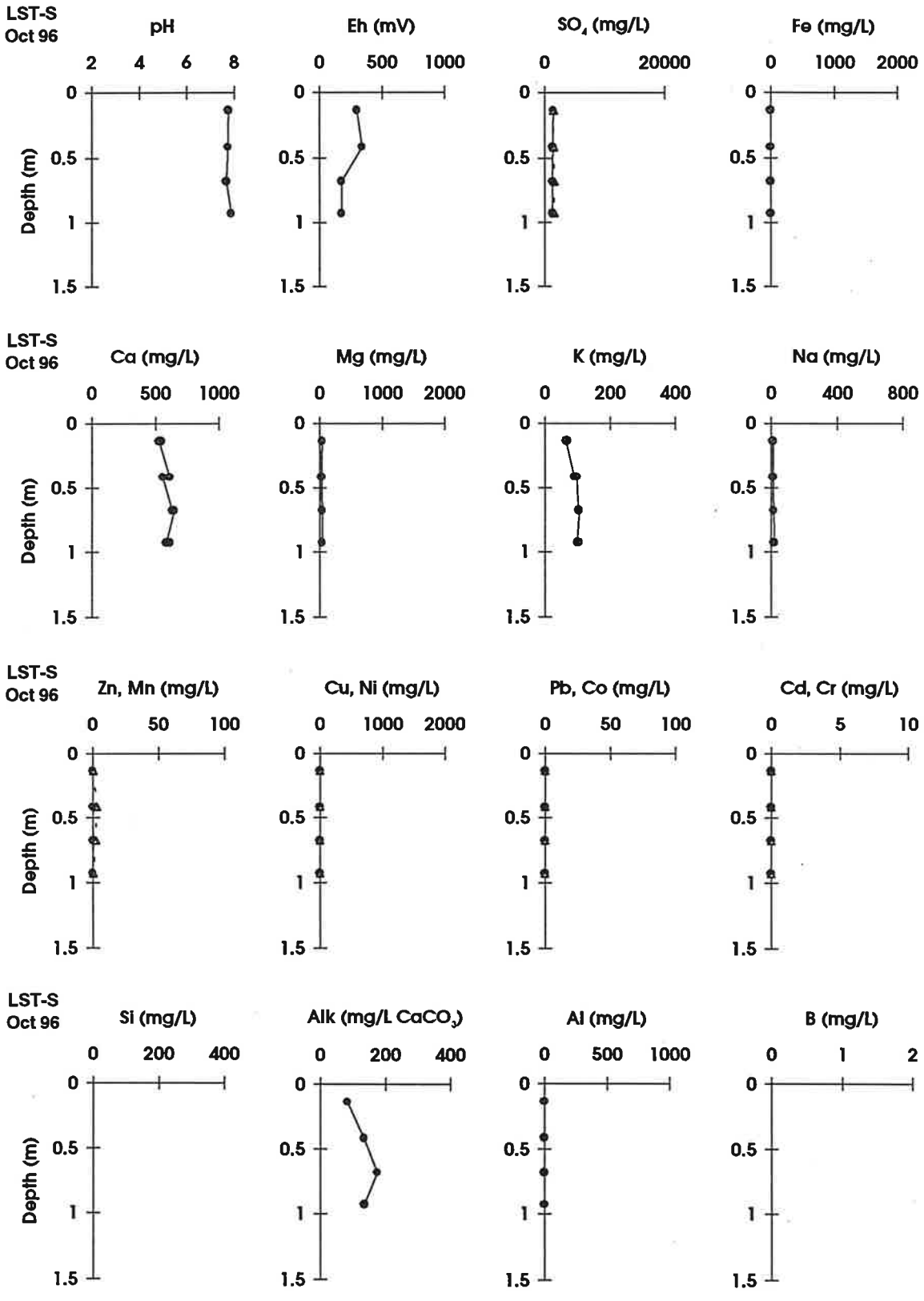

Figure 40. Pore-water geochemistry in the LST lysimeter, October, 1996. Location S is identified in Figure 1. • = Zn, Cu, Pb, Cd; Δ = Mn, Ni, Co, Cr